12-2021

A GIS-SWMM System to Evaluate Low Impact Development (LID) Feature Effectiveness on UNO's Campus

Demetria C. Christo
University of New Orleans, demetria.christo@gmail.com

A GIS-SWMM System to Evaluate Low Impact Development (LID) Feature Effectiveness on UNO's Campus

A Thesis

Submitted to the Graduate Faculty of the
University of New Orleans
in partial fulfillment of the
requirements for the degree of

Master of Science in Engineering
In
Civil Engineering

by

Demetria C. Christo

B.S. Tulane University, 2006

December 2021

ACKNOWLEDGEMENTS

I send my deepest thanks to Dr. Gianna Cothren, Dr. Guillermo Rincón, and Dr. Satish Bastola, who all invested countless mentoring hours throughout graduate school and for their guidance on this thesis. I am inspired by such a brilliant group of people who so generously share their wealth of knowledge with their pupils.

I dedicate this thesis to my family. To my son, Rhodes, who makes the pursuit of engineering a better world most motivating. To my wonderful husband, Casey Valadie, without whose care and support the logistics of graduate school would not be possible. To my mother, Dr. Kathleen Farrell, who always offers wise professional and scientific guidance. To my parents and brother, Steve, Kathleen, and Ivan, thank for your inspiration and encouragement. To Rick and Tami, my wonderful parents-in-law, who lovingly entertained the baby most weekends so I could work on graduate school.

TABLE OF CONTENTS

LIST OF TABLES

LIST OF FIGURES

LIST OF APPENDICES

ABSTRACT

The EPA's Storm Water Management Model (SWMM) includes the ability to model low impact development (LID) systems involving various types of green infrastructure (GI) for stormwater detention and infiltration.

The SWMM model requires hydrologic attribute inputs for individual subcatchments, including percent impervious surfaces, surface roughness, depression storage, and curve number. These SWMM attributes can be more accurately, consistently, and efficiently be defined in GIS by calculating the subcatchment area-weighted attribute values and importing them to SWMM. Thus, GIS becomes a valuable pre-processing input tool for SWMM-LID modeling.

The three objectives of this thesis are to 1) use GIS geoprocessing tools to calculate hydrologic attributes more accurately and consistently for 82 subcatchments, 2) use GIS to more efficiently enter attributes into the SWMM model, and 3) conduct a preliminary study to evaluate the effectiveness of low impact development (LID) features in a SWMM model of the University of New Orleans (UNO).

Keywords: GIS; SWMM; Hydrologic Attributes; Modeling LID; Roughness; Storage; Curve Number

1. INTRODUCTION

1.1 Problems with Traditional Subcatchment Hydrologic Attribute Selection and Entry

The EPA's Stormwater Management Model (SWMM) models low impact development (LID) systems for stormwater detention and infiltration. SWMM requires hydrologic attribute inputs for individual subcatchments including percent impervious surfaces, surface roughness, depression storage, and Curve Number, among others.

However, when there are a large number of subcatchments, manual attribute selection and entry for each subcatchment pose significant time and consistency challenges. For 95 subcatchments, for example, approximately 4000 subcatchment attributes total could be assigned. The GIS attribute tables in the figure below (left) illustrate the large number of attributes that can be imported into SWMM. These figures show data for only 10 of the 95 subcatchments in the SWMM model at the time of this report. Manual selection and entry of these attributes clearly this pose time and consistency challenges.

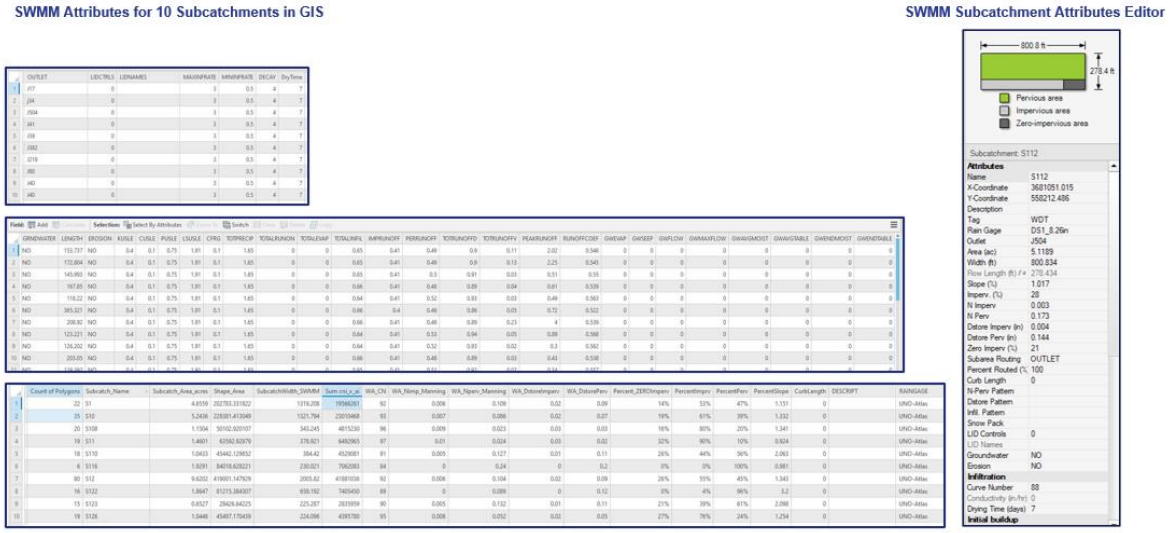

Figure 1.1. Left: GIS attribute table excerpt for 10 subcatchments. Right: SWMM subcatchment attributes editor.

Additionally, the researcher faces challenges selecting attributes representative of a whole subcatchment, especially when there are diverse surface materials such as asphalt, trees and metal roofs, each with their own attribute values. Traditionally, to select a value representative of each attribute for the whole subcatchment, the researcher might visually estimate by reviewing a map for various surface materials and subjectively "ballpark" attribute values, as illustrated in the figure below. This can be a laborious, subjective, inefficient and an inconsistent process across multiple subcatchments.

1.1.1 GIS Opportunities to Calculate Area-Weighted Subcatchment Attributes

GIS offers the opportunity to resolve the above attribute selection and entry problems. These SWMM attributes can be more consistently and efficiently defined in GIS by calculating the subcatchment area-weighted attribute values and then importing them to SWMM. Thus, GIS becomes a valuable pre-processing input tool for SWMM-LID modeling.

The figure below compares the traditional visual analysis method to define SWMM attributes representative of a whole subcatchment versus the GIS-calculated area-weighted values method.

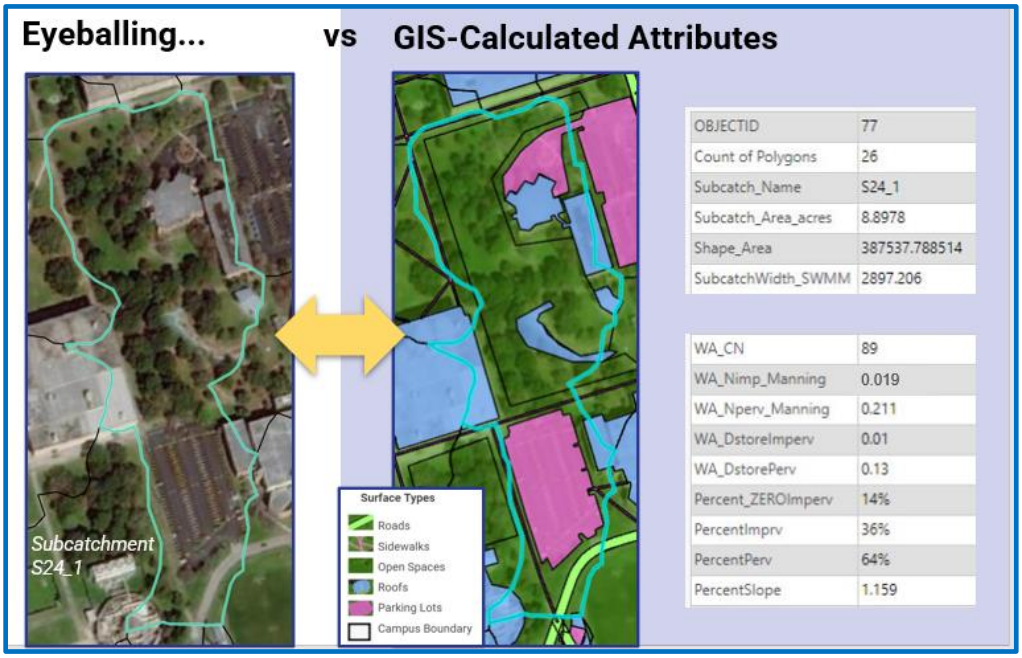

Figure 1.2. Traditional visual analysis methods versus GIS area-weighted attribute calculation method to define hydrologic attributes representative of a whole subcatchment.

1.2 Objectives

The three main objectives are to 1) use GIS geoprocessing tools to calculate hydrologic attributes for multiple subcatchments, 2) use GIS to enter attributes more consistently and efficiently into the SWMM model, and 3) apply the first two objectives as an exercise to conduct a preliminary study to evaluate the effectiveness of low impact development (LID) features in a SWMM model of the University of New Orleans (UNO).

1.3 Location Significance

The University of New (UNO), located at 2000 Lakeshore Drive, New Orleans, Louisiana, 70148, sits adjacent to the New Orleans Gentilly Resilience District. The Gentilly Resilience District is a combination of water and land management strategies to address environmental and social challenges through a $141 Million award from the US Department of Housing and Urban Development (HUD) to rebuild more resiliently following Hurricane Katrina's devastation in 2009 (City of N.O., 2018a).

UNO's "Master Plan 2020", published in 2013, suggests that at approximately 258 acres, UNO is likely the largest single entity stormwater contributor to the Gentilly Resilience District (UNO, 2013). The 2013 plan calls for a more rigorous assessment of stormwater management opportunities to reduce flooding on campus and reduce peak flow runoff impacts to the surrounding, lower-lying neighborhoods during rain events.

Figure 1.3. Left: Gentilly Resilience District map with UNO overlay (City of N.O., *Gentilly Resilience District Fact Sheet,* 2018a). Right top: campus drainage outfalls. Right bottom: flooding on campus (UNO, 2013).

In June, 2021, the UNO Master Planning Committee and design team released the "University of New Orleans Comprehensive Master Plan", which describes many future campus stormwater and green infrastructure projects, illustrated below. Even though the LIDs and SWMM model for this thesis were already under development prior to the release of this master plan, some master plan proposed LID features share the same locations and similar designs to the LIDs designed in this thesis. For example, both the design team and this thesis propose pervious pavement stormwater infrastructure on the Cove and Lafitte Village parking lots.

The SWMM model developed in this thesis can be a valuable tool in assessing the master plan's proposed LIDs in a timely, cost-effective manner. Future modelers would only need to add new "scenarios" and their LID feature attributes to this SWMM model. A technical appendix with model results does not accompany the master plan, indicating that this SWMM model may be a very timely preliminary assessment tool for the master plan's proposed campus stormwater LIDs.

Figure 1.4. Left: Proposed campus stormwater park. Right: proposed campus stormwater features (UNO Master Planning Committee, et al., 2021).

1.4 Limitations and Application

At the time of this study, this SWMM model is uncalibrated. The SWMM model built in this study is based on a University of New Orleans Civil Engineering Department SWMM model under development dated 13 September 2021. The UNO model is dynamic and is routinely updated to match field observations (Cothren, 2021; Cothren & Christo, 2021). A description of the model as received and the modifications to it are discussed later in this report.

Because this is a preliminary study with relative results, the uncalibrated model is still an effective tool to demonstrate the applicability of the GIS-attribute import to SWMM and the effectiveness of select LID features on reducing runoff Peak Flow, Mean Total Inflow, Total Inflow Volume and delayed Time to Peak on UNO's campus. Benefits of this preliminary SWMM model include a time-effective, cost-effective, and versatile way to test the impact of various LID features across campus, without needing to wait for a complete, calibrated model.

This preliminary GIS-SWMM study is a building block towards broader objectives in collaboration with the UNO research team under the direction of Dr. Gianna Cothren to 1) model the university campus drainage and runoff with ongoing site developments in real-time, 2) evaluate the effectiveness of the proposed UNO 2021 Campus Master Plan stormwater and green infrastructure, and 3) model UNO's runoff impacts on the adjacent Gentilly Resilience District.

The proposed LID features in this study are hypothetical, purely for the exercise of applying the GIS-SWMM system developed in this thesis to model evaluating LID effectiveness. Following preliminary analysis using a SWMM model, actual LID features would need to be engineered to suit the drainage capacity of the existing infrastructure and would need to be cost engineered to remain within budget constraints.

2. BACKGROUND INFORMATION

2.1 Models

2.1.1 What is ArcGIS Pro?

Geographic Information Systems (GIS) "is a spatial system that creates, manages, analyzes and maps all types of data", according to Esri, the manufacturer of Arc GIS Pro. This thesis used ArcGIS Pro

version 2.8.29751. All GIS images are credited to Esri's GIS software. For the purposes of this thesis, "GIS" refers to ArcGIS Pro, the current Esri software generation that replaces ArcMAP.

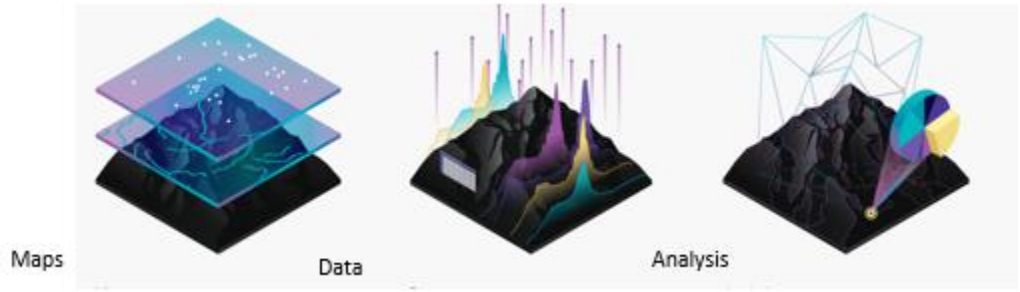

Figure 2.1. ArcGIS Pro capabilities (Esri, 2021).

2.1.2 What is PCSWMM?

The U.S. Environmental Protection Agency (EPA) developed the Stormwater Management Model (SWMM) software. SWMM is a physically-based, discrete-time simulation model used globally for planning, analysis, and design of drainage systems including stormwater runoff systems. The EPA developed SWMM to support local, state, and national stormwater management objectives to reduce runoff through infiltration and retention (EPA, 2021).

This thesis utilizes PCSWMM version 7.4.3200, an advanced proprietary modeling software built on the EPA's SWMM5 engine. PCSWMM is manufactured by Computational Hydraulics International (CHI). Thanks to an educational grant by CHI, this software was available at no cost. For the purposes of this thesis, all graphics and references to "SWMM" refer to CHI's PCSWMM software.

2.2 SWMM COMPUTATIONAL METHODS

SWMM is a physically based, discrete-time simulation model, utilizing the principles of conservation of mass, energy, and momentum where appropriate (Rossman and Huber, 2016).

2.2.1 Visual Objects

SWMM defines subcatchments as "hydrologic units of land whose topography and drainage system elements direct runoff to a single discharge point" (James et al., 2003 p55). Discharge points can be other subcatchments or nodes. SWMM conceptualizes each subcatchment as percentages of pervious area, impervious area and zero-impervious area, as shown in the figure below. Zero impervious areas are impervious areas with no depression storage, such as a sloped metal roof.

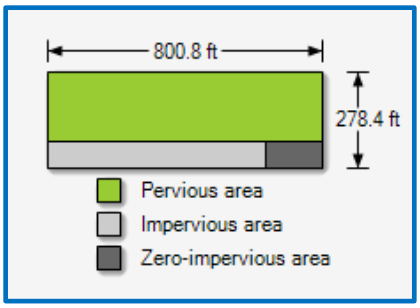

Figure 2.2. SWMM subcatchment conceptualization in SWMM (plan view) (CHI *Software*, 2021e).

Nodes are the points in a drainage system that connect conveyance links and allow external inflows to enter a drainage system. Node types include junctions, outfalls, storage units, and dividers. Nodes require depth and elevation data in SWMM. Links lie between a pair of nodes. Links are the conveyance components of a drainage system. Link types include open and closed conduits, pumps, and flow regulators (James et al., 2003).

2.2.2 Surface Runoff

SWMM treats each subcatchment as a non-linear reservoir. Inflows include precipitation and upstream subcatchments. Outflows include infiltration, evaporation, and surface runoff. The capacity of this subcatchment "reservoir" is the maximum depression storage. An illustration of the subcatchment non-linear reservoir is below:

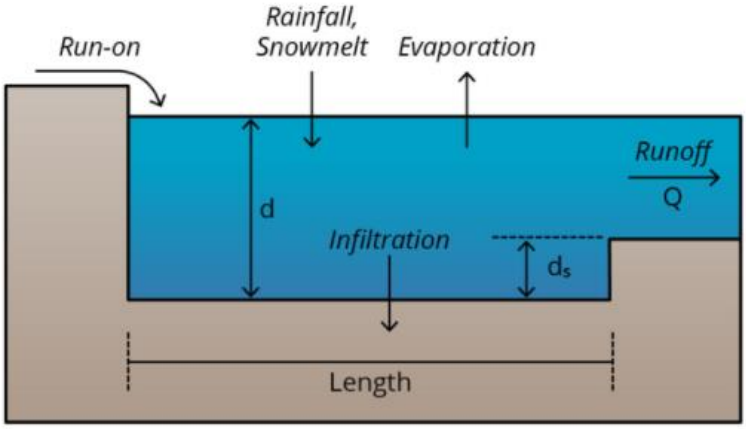

Figure 2.3. Subcatchments as non-linear reservoirs including inflows and outflows (CHI *Surface Runoff*, 2021g).

In SWMM, surface runoff, Q, occurs only when the depth of water, d, in the reservoir, exceeds the maximum depression storage, ds. When this depth is exceeded, the outflow is modeled with Manning's equation in US units:

$$Q = \frac{1.49}{n} W(d - ds)^{5/3} S^{1/2}$$

where Q is the surface runoff volumetric flow rate, n is Manning's surface roughness coefficient for overland flow, W is subcatchment width, d is the depth of water over the subcatchment, ds is the depression storage depth, and S is the average slope of the subcatchment. Depth of water, d, is continuously updated with time.

The runoff flow rate per unit of surface area, q, is calculated by dividing Manning's equation by the surface area of the subcatchment, A (CHI *Surface Runoff*, 2021g):

$$q = \frac{1.49WS^{1/2}}{An}(d - ds)^{5/3}.$$

2.2.3 Infiltration – SCS Curve Number Method for Runoff Estimate

Infiltration is the movement of water from the surface into the soil (Bedient and Huber, 2002). SWMM offers five options for modeling infiltration. The SCS Curve Number Method is utilized in this study.

The Soil Conservation Service (SCS) Curve Number method is a simple, efficient, and widely used method to estimate precipitation excess (runoff) as a function of cumulative precipitation, soil cover, land use, and antecedent moisture condition. The accumulated precipitation excess equation at time t, Pe, in inches, is (NRCS, 1986):

$$Pe = \frac{(P - Ia)^2}{(P - Ia) + S}$$

where P is accumulated rainfall depth at time t in inches, Ia is the initial abstraction (initial loss), and S is the potential maximum retention, which is a measure of a watershed's ability to abstract and retain storm precipitation. Until the accumulated rainfall exceeds the initial abstraction, the precipitation excess (runoff) equals zero. The SCS developed the following relationship between Ia and S from empirical studies:

$$Ia = 0.2S$$

The maximum retention, S, and watershed characteristics are related through the curve number, CN (NRCS, 1986):

$$S = \frac{1000}{CN} - 10.$$

2.2.4 LID Simulation

SWMM simulates low impact development features (LIDs) as nonlinear reservoirs. Inflows are from precipitation falling directly on the LID and from run-on from adjacent impervious and pervious surfaces. SWMM stores water within the LID up to a maximum capacity, after which runoff is released from the LID. SWMM models generate outputs including inflows, outflows, surface and storage depths, evaporation, and infiltration (Rossman, 2015).

In SWMM, LID systems are conceptually incorporated into a subcatchment by specifying the area of the LID feature in each subcatchment. Some or all of the runoff generated in the subcatchment can be routed through the LID (Cothren & Spelman, 2021). After adding LID to a subcatchment, the subcatchment width and percent imperviousness must be modified in the subcatchment attributes.

SWMM conceptually separates each subcatchment into four areas, which are handled differently: LID area, pervious area, impervious area, and directly connected impervious areas (DCIA) (CHI, 2021), as shown in the figure on the left below. DCIA is a type of impervious area with a direct connection to a drainage system or water body via a continuous impervious surface (Hwang, 2017).

LID systems in SWMM provide storage and infiltration. SWMM divides storage into three different model process layers: surface, soil, and storage, as shown in the figure on the right below.

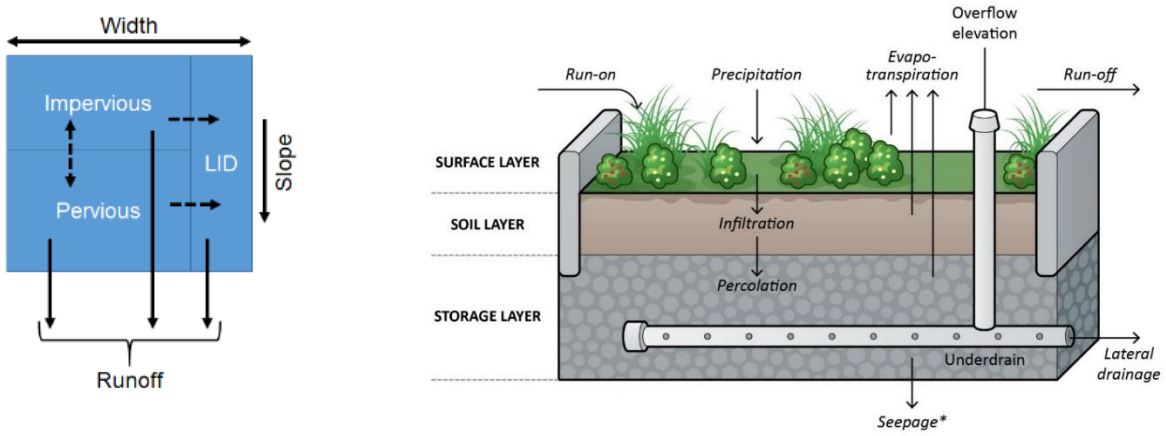

Figure 2.4. Left: LID implementation in SWMM with separate subcatchment conceptual areas (plan view). Right: SWMM model process layers for a bioretention cell LID (CHI *LID Control Editor*, 2021b).

Vegetated swales are channels with sloping sides, covered by grass or other vegetation. Vegetated swales slow the flow rate of runoff and allow more time for the runoff to infiltrate into the soil. Continuous permeable pavement systems are street or parking areas paved with pervious concrete or asphalt mix that sits above an aggregate storage layer. Rainfall passes through the pavement into the storage layer where it can infiltrate into the native soil below. Bioretention cells are depressions that contain vegetation in an engineered soil mixture above an aggregate storage layer. Bioretention cells provide storage, infiltration, evaporation of direct rainfall and runoff from adjacent surfaces (Rossman & Huber, 2016). The figure below illustrates SWMM's interpretation of these LID systems.

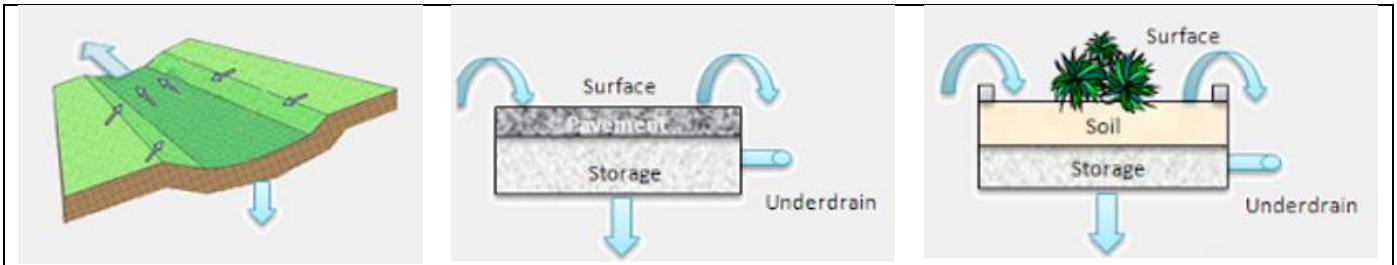

Vegetated Swale **Permeable Pavement** **Bioretention Cell**

Figure 2.5. SWMM's interpretation of three LID systems (Rossman, *SWMM User's Manual Version 5.1*, 2015).

2.3 LID Controls

Several variables impact the hydrologic performance of LID controls including the properties of the soil and aggregate media contained within the unit, the vertical depth of its media layers, and the surface area of the LID unit. Vertical layer attributes are entered in the LID Control Editor. Tabs in the editor correspond to each vertical layer including the surface, pavement, soil, storage, and underdrain, in addition to pollutant removal options. The figure below shows the LID controls designed in this study.

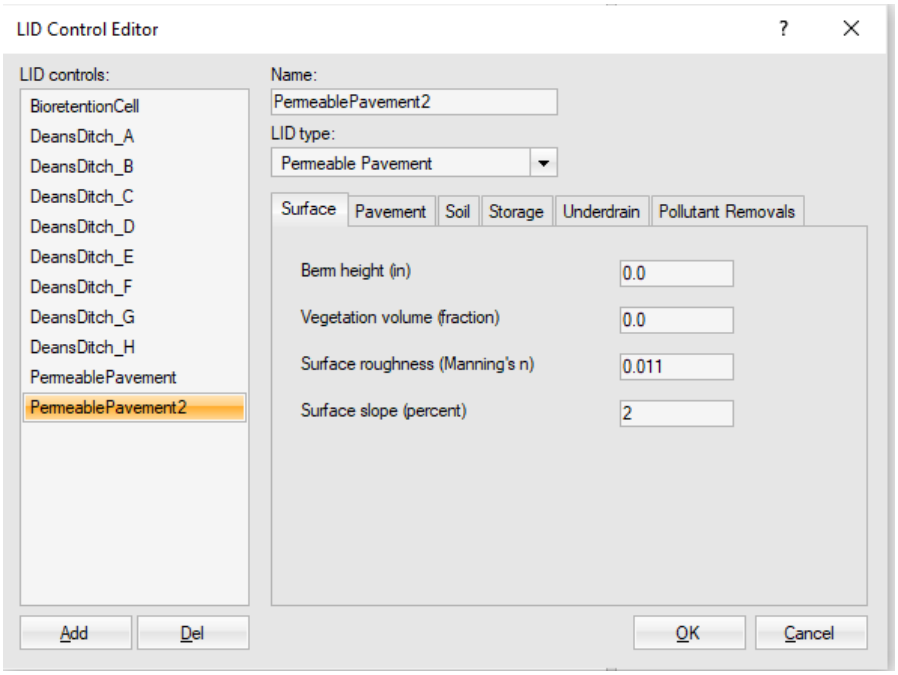

Figure 2.6. LID Control Editor (CHI *Software*, 2021e).

The table below summarizes the layer tabs that are activated in SWMM for each LID control, where R represents required data input, and O represents optional data input.

Table 2.1. LID control required and optional layers for attribute entry; "R" indicates required, "O" indicates optional.

LID Control	Surface	Pavement	Soil	Storage	Underdrain	Pollutant Removal
Vegetated Swale	R					
Permeable Pavement	R	R	O	R	O	O
Bioretention Cell	R		R	R	O	O
*R= Required; O=Optional						

The following description of each LID Control attribute is paraphrased from the EPA's Stormwater Management Model User's Manual Version 5.1 (Rossman, 2015) and Computational Hydraulics International's LID Control Editor publication (CHI, 2021b).

2.3.1 Surface Layer

The LID Control Editor Surface Layer tab describes surface parameters of vegetated swales, permeable pavement, bioretention cells, and infiltration trenches **(**Rossman*, SWMM User's Manual Version 5.1*, 2015). The LID attributes that can be entered in the Surface layer include:

- Storage Depth/Berm Height (inches) – this is the maximum depth to which water can pond above the surface of the unit before overflow occurs, usually present with confining walls, curbs, or berms. For LIDS with overland flow, this is the height of surface depression storage. For vegetated swales, this is the height of the trapezoidal cross section.
- Vegetation volume (fraction) – this is fraction of the volume within the storage depth filled by vegetation stems and leaves—not the surface area of the vegetative coverage. 0.1 and 0.2 can be used for very dense vegetation.
- Surface Roughness – this is Manning's n for overland flow using the aforementioned table of values.
- Surface Slope (%) –this is the slope of the permeable pavement surface or vegetative swale directional flow.
- Swale Side Slope (run/rise) –this is the vegetated swale sidewall cross-sectional slope in run/rise format (Rossman, 2015; CHI, 2021).

2.3.2 Pavement Layer

The Pavement Layer tab in the LID Control Editor includes:

- Thickness (inches)—this is the thickness of the pavement layer.
- Void Ratio (voids/solids)—this is the volume of void space relative to the volume of solids in the pavement for continuous systems or for the fill material used in modular systems.
- Impervious Surface (fraction)—this is the ratio of impervious paved material to the total area.
- Permeability (inches/hour)—in continuous systems, this is the permeability of the concrete. While the permeability of new pervious concrete is high, fines clog the void space over time. Typical flow rates through new pervious concrete are 288 inches/hour (National Ready Mixed Concrete Association, 2011).
- Clogging Factor—this is the number of pavement layer void volumes of treated runoff that it takes to completely clog the pavement. For simplicity, this experiment assumed no clogging and a clogging factor of zero (0) was set in the controls.
- Regeneration Interval (days)—this is the number of days that the pavement layer is allowed to clog before its permeability restored through maintenance. This experiment retained the default value of zero (0) in the controls.
- Regeneration Fraction—this is the fraction of the pavement's original permeability that can be restored after the Regeneration Interval is reached. After the pavement is regenerated, the pavement begins to clog at the Clogging Factor rate. This experiment retained the default value of zero (0) in the controls (Rossman, 2015; CHI, 2021).

2.3.3 Soil Layer

The NRCS Web Soil Survey maps were utilized to determine UNO's soil hydrologic properties (NRCS, 2021). The soil layer is optional in SWMM for permeable pavements, so the Soil Layer was only added to the bioretention cell. The Soil Layer attributes supported in the LID Control Editor include:

- Thickness (inches)—this is the thickness of the soil layer.
- Porosity (volume fraction)—this is the volume of pore space relative to the total volume of soil.

- Field Capacity (volume fraction)—this is the volume of pore water relative to the total volume after the soil drains fully (as a fraction). Vertical drainage of water through the soil layer does not occur below this level.
- Wilting Point (volume fraction)—this is the volume of pore water relative to the total volume for a well-dried soil where only bound water remains (as a fraction). This is the lower limit of the soil moisture content.
- Conductivity (inches/hour)—this is the saturated hydraulic conductivity value for the type of soil used in this layer.
- Conductivity Slope—this is the slope of the curve of log(conductivity) versus soil moisture content (dimensionless). Typical values range from 5 for sands to 15 for silty clay.
- Suction Head (inches)—this is the average value of soil capillary suction along the wetting front (Rossman, 2015; CHI, 2021).

Assuming a "Silty Clay Loam" engineered soil for the bioretention cell, several parameters from CHI's soil characteristics table, shown below were selected. These values were cross-checked with the hydrologic soils group Type D soils parameter ranges listed in the NRCS Hydrology National Engineering Handbook (2009).

Table 2.2. CHI's table of soil characteristics (CHI, 2021f).

US units

Soil Texture Class	Hydraulic Conductivity (in/hr)	Suction Head (in.)	Porosity (fraction)	Field Capacity (fraction)	Wilting Point (fraction)	Initial Deficit (fraction)
Sand	4.74	1.93	0.437	0.062	0.024	0.413
Loamy Sand	1.18	2.40	0.437	0.105	0.047	0.390
Sandy Loam	0.43	4.33	0.453	0.190	0.085	0.368
Loam	0.13	3.50	0.463	0.232	0.116	0.347
Silt Loam	0.26	6.69	0.501	0.284	0.135	0.366
Sandy Clay Loam	0.06	8.66	0.398	0.244	0.136	0.262
Clay Loam	0.04	8.27	0.464	0.310	0.187	0.277
Silty Clay Loam	0.04	10.63	0.471	0.342	0.210	0.261
Sandy Clay	0.02	9.45	0.430	0.321	0.221	0.209
Silty Clay	0.02	11.42	0.479	0.371	0.251	0.228
Clay	0.01	12.60	0.475	0.378	0.265	0.210

2.3.4 Storage Layer

The Storage Layer tab describes the attributes of the designed subsurface layers including aggregates and retention chambers, subbase layer in this study's permeable pavement and bioretention cell systems.

- Height (inches)—this is the thickness of the aggregate layer.

- Void Ratio—this is volume of void space relative to the volume of solids.
- Seepage Rate (inches/hour)—this is the maximum rate at which water infiltrates into the native soil below the LID system Storage Layer. This is also the Saturated Hydraulic Conductivity. If there is an impermeable liner below the layer, then a value of zero (0) is used.
- Clogging Factor—this is the total volume of treated runoff that it takes to completely clog the bottom layer divided by the void volume of the layer. This experiment assumed no clogging and utilized a value of zero (0) (Rossman, 2015; CHI, 2021).

2.3.5 Underdrain

The optional underdrain used in the permeable pavement and bioretention cell LID systems collects stored water from the bottom of the layer and conveys it to a conventional storm drain. The following attributes are entered in the LID Control Editor for underdrains:

- Drain Coefficient—the drain coefficient, C, and drain exponent, n, determine the rate of flow through the underdrain as a function of height of stored water above the drain height, as shown in the following equation:

$$q = C(h - Hd)^n$$

  where q is the outflow in inches/hour, h is the height of the stored water in inches, and Hd is the drain height in inches. For no underdrain, the value is zero (0). This experiment treated the drain like an orifice.
- Drain Exponent—this the n value in the equation above. A value of 0.5 causes the drain to function like an orifice.
- Drain Offset Height (inches)—this is the height of any underdrain piping above the bottom of a storage layer. If the drain is in flush with the bottom of the unit, then the height is zero (0).
- Open Level—this is the water depth in the Storage Layer that causes the drain to open automatically. This experiment assumed that this feature is disabled and retained the default value of zero (0).
- Closed Level—this is the water depth in the storage layer that causes the drain to close automatically. This experiment assumed that this feature is disabled and retained the default value of zero (0).
- Control Curve—this is an optional curve that adjusts the computed drain flow as a function of the head of water above the drain. This experiment left this control blank, as it is not applicable to the LID systems utilized in this study (Rossman, 2015; CHI, 2021).

3. METHODS

3.1 Node Determination Methods

3.1.1 Siting LID Features

To identify LID placement UNO's campus was toured during a rain event to inventory problem flooding areas and to site potential LID features. These areas were identified for problem flooding:

- Founders Road in front of the Cove
- Milneburg Road in front of the Administration Building Parking Lot
- Lafitte Village Parking Lot.

The following five LID features were designed in response to this flooding, shown in the GIS layout below, to evaluate their effectiveness at reducing several stormwater parameters in this preliminary study. These LIDs are illustrated on the following map.

- Dean's Ditch Vegetated Swale
- Administration Building Parking Lot and Permeable Pavement
- The Cove Parking Lot Permeable Pavement
- Lafitte Village Parking Lot Permeable Pavement
- Lafitte Village Parking Lot Bioretention Area

Figure 3.1. Proposed UNO campus LID features in this preliminary SWMM study.

3.1.2 Nodes of Interest

To locate nodes of interest and identify the subcatchments impacted by the experimental LIDS, the GIS LID shapefiles were imported into SWMM. The figure below shows the nodes of interest, which

are the nearest nodes downstream of the proposed LID features. This study will evaluate the hydrographs and hydraulic results at these four nodes of interest, shown on the following map.

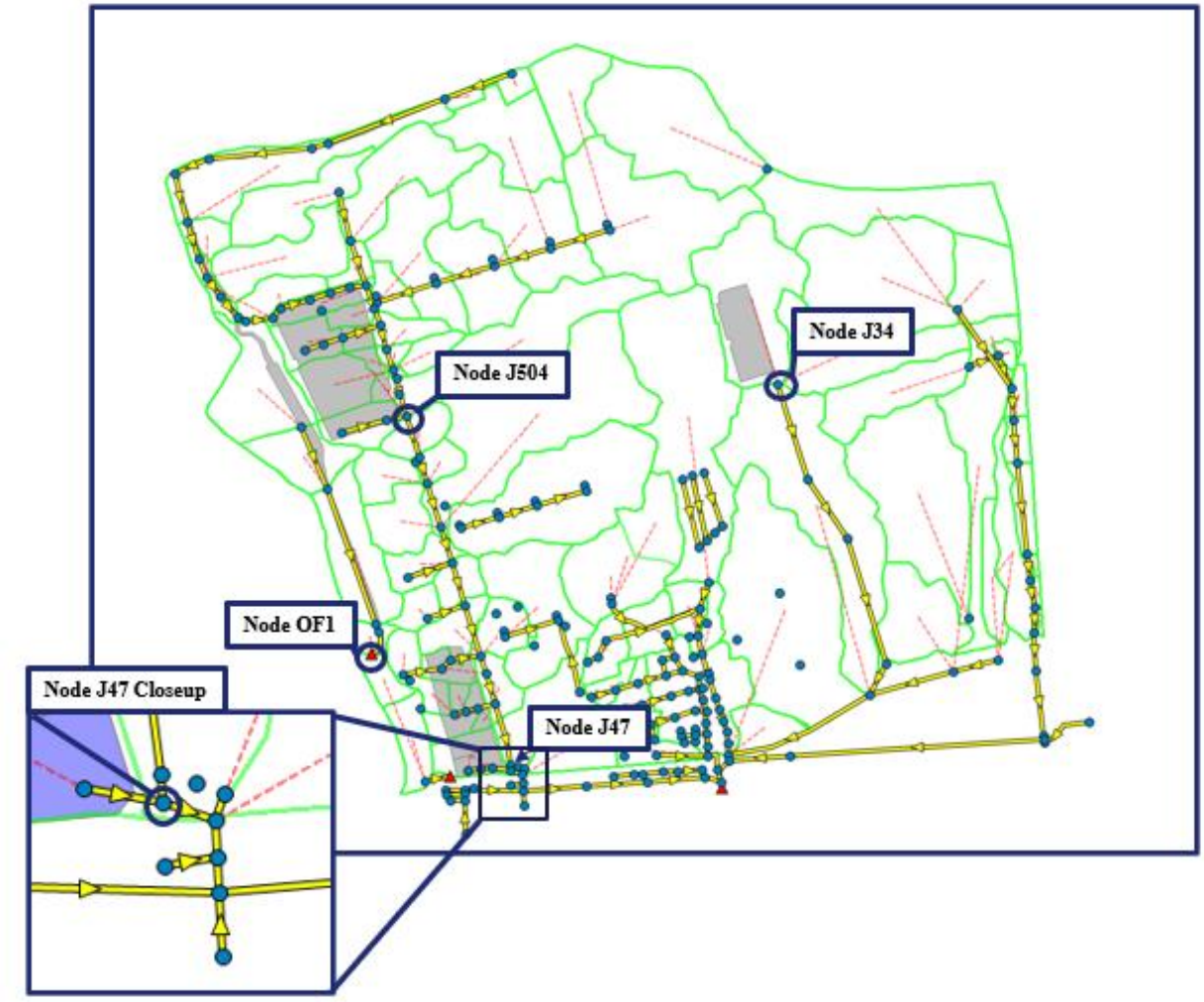

Figure 3.2. Nodes of interest selected in SWMM for each LID feature.

The table below summarizes the nodes of interest for each LID feature. Node J47 serves as the node of interest for both the Lafitte Village Parking Lot bioretention cell and permeable pavement features.

Table 3.1. Nodes of interest.

LID Name	LID Control	Node
Dean's Ditch	Vegetated Swale	OF1
Cove Parking Lot	Permeable Pavement	J504
Admin Building Parking Lot	Permeable Pavement	J34
Lafitte Village Parking Lot	Permeable Pavement	J47
Lafitte Village Parking Lot	Bioretention Cell	J47

3.2 Hydrologic Attribute Determination Methods

The following describes how attributes were selected and assigned in GIS.

3.2.1 GIS Attributes Imported from SWMM

A SWMM subcatchments layer was first imported into GIS. Accompanying each subcatchment were attributes including subcatchment name, subcatchment area, subcatchment width, and percent slope. It is possible to instead devise the subcatchment boundaries in GIS, but the UNO SWMM model including subcatchments had already been under construction and the time of this study.

3.2.2 Attributes Assigned to GIS Layers

To assign hydrologic and land use characteristics to each campus surface, the following attribute fields and selection options were created and applied to each surface layer in GIS, as shown in the table below.

Table 3.2. Assigned attribute fields and selection options.

Attribute Field in GIS	Selection Options
Pervious or Impervious	Pervious / Impervious
Surface Type	Roofs / Parking Lots / Sidewalks / Roads / Open Space
Material	Asphalt / Concrete / Gravel / Roof / Trees / Turf
Land Use	Industrial / Transitional / Open Land
Curve Number	[select value from table]
Manning's n for Overland Flow - Impervious	[select value from table]
Manning's n for Overland Flow - Pervious	[select value from table]
Depression Storage - Impervious	[select value from table]
Depression Storage - Pervious	[select value from table]

3.2.3 Curve Number

Curve Number (CN) values can range from 0 to 100. Lower CN values have higher infiltration rates (NRCS, 1986). For example, 100 is used for water bodies and 30 is used for highly permeable soils. This study assigned a value of 98 for asphalt and concrete surfaces, 91 for gravel surfaces, 98 for smooth roof materials, 83 for trees, and 84 for turf. The following SCS table was used to select CN values representative of each GIS surface material.

Table 3.3. SCS Curve Number Table (NRCS, 1986).

A.4 SCS Curve Numbers[1]

Land Use Description	Hydrologic Soil Group			
	A	B	C	D
Cultivated land				
Without conservation treatment	72	81	88	91
With conservation treatment	62	71	78	81
Pasture or range land				
Poor condition	68	79	86	89
Good condition	39	61	74	80
Meadow				
Good condition	30	58	71	78
Wood or forest land				
Thin stand, poor cover, no mulch	45	66	77	83
Good cover[2]	25	55	70	77
Open spaces, lawns, parks, golf courses, cemeteries, etc.				
Good condition: grass cover on 75% or more of the area	39	61	74	80
Fair condition: grass cover on 50-75% of the area	49	69	79	84
Commercial and business areas (85% impervious)	89	92	94	95
Industrial districts (72% impervious)	81	88	91	93
Residential[3]				
Average lot size (% Impervious[4])				
1/8 ac or less (65)	77	85	90	92
1/4 ac (38)	61	75	83	87
1/3 ac (30)	57	72	81	86
1/2 ac (25)	54	70	80	85
1 ac (20)	51	68	79	84
Paved parking lots, roofs, driveways, etc.[5]	98	98	98	98
Streets and roads				
Paved with curbs and storm sewers[5]	98	98	98	98
Gravel	76	85	89	91
Dirt	72	82	87	89

Source: *SCS Urban Hydrology for Small Watersheds*, 2nd Ed., (TR-55), June 1986.

3.2.4 Hydrologic Soil Group

Hydrologic soil groups are based on estimates of runoff potential (NRCS, 2009). Based on United States Department of Agriculture (USDA) Natural Resources Conservation Service (NCRS) Web Soil Survey maps of UNO's campus area (NRCS, 2021), UNO's campus soils were determined to be predominantly in hydrologic soil group D, which includes clay loam, silty clay loams, sandy clay, and silty clay or clay. Hydrologic soil group D was therefore assumed to apply to all subcatchments.

Group D soils typically has high runoff potential when thoroughly wet and has a large shrink/swell potential. Group D soils are typically comprised of greater than 40% clay, less than 50%

sand, and have clayey textures. Water movement through the soil is typically restricted or very restricted. Soil group D typically has a saturated hydraulic conductivity of 0.05-0.00 inches per hour (NRCS, 2009).

3.2.5 Manning's Roughness

Surface roughness for overland flow is represented by Manning's n. SWMM differentiates between the Manning's n over pervious versus impervious surfaces. For impervious surfaces, this study assigned Manning's n values of 0.011 for asphalt surfaces, 0.012 for concrete surfaces, and 0.010 for roof materials. For pervious surfaces, this study assigned Manning's n values of 0.024 for gravel surfaces, 0.40 for trees, and 0.24 for turf. Manning's n values were selected from the following table.

Table 3.4. Manning's n for overland flow, excerpted from USEPA's SWMM 5 Manual. Original source credited to McCuen, R, et al (1996).

A.6 Manning's n – Overland Flow

Surface	n
Smooth asphalt	0.011
Smooth concrete	0.012
Ordinary concrete lining	0.013
Good wood	0.014
Brick with cement mortar	0.014
Vitrified clay	0.015
Cast iron	0.015
Corrugated metal pipes	0.024
Cement rubble surface	0.024
Fallow soils (no residue)	0.05
Cultivated soils	
Residue cover < 20%	0.06
Residue cover > 20%	0.17
Range (natural)	0.13
Grass	
Short, prairie	0.15
Dense	0.24
Bermuda grass	0.41
Woods	
Light underbrush	0.40
Dense underbrush	0.80

Source: McCuen, R. et al. (1996), *Hydrology*, FHWA-SA-96-067, Federal Highway Administration, Washington, DC

3.2.6 Depression Storage

Depression storage is the ability of land surface to retain water in its pits and depressions, thus preventing the water from flowing off the surface as runoff. SWMM differentiates between depression storage on impervious versus pervious surfaces (Rossman, 2015). For impervious surfaces, this study assigned a depression storage value of 0.05 inches to asphalt and concrete surfaces and a value of 0 inches to roof surfaces, assuming all roofs were sloped and smooth. For pervious surfaces, this study assigned

depression storage values of 0.20 inches for turf and trees, and 0.09 inches for gravel surfaces. Subcatchment depression storage on impervious and pervious surfaces was estimated using the following table.

Table 3.5. Depression storage values, excerpted from USEPA's SWMM 5 Manual (Rossman, 2015). Original source credited to ASCE (1992), Design and Construction of Urban Stormwater Management Systems, New York, New York.

A.5 Depression Storage

Impervious surfaces	0.05 - 0.10 inches
Lawns	0.10 - 0.20 inches
Pasture	0.20 inches
Forest litter	0.30 inches

Source: ASCE, (1992). *Design & Construction of Urban Stormwater Management Systems*, New York, NY.

3.2.7 GIS Area-Weighted Attribute Calculations for the Whole Subcatchment

After determining the attribute values for each campus surface, the area-weighted values representative of a whole subcatchment could then be calculated. This is where GIS becomes a valuable pre-processing tool for SWMM. As an example equation, the equation for the area-weighted curve number (CN) value for a whole subcatchment is:

$$CN_{aw} = \frac{\sum_{i=1}^{n}(CNi * Ai)}{\sum_{i=1}^{n} Ai}$$

where CN_{aw} is the area-weighted curve number for the subcatchment, CN_i is the curve number for each surface type, and Ai is the corresponding area of that surface.

Using geoprocessing tools including "merge", "intersect" and "summarize within", the following area-weighted attributes were calculated in GIS:

- Area-weighted Curve Number (WA_CN)
- Area-weighted Manning's n for overland flow over impervious surfaces (WA_Nimp_Manning)
- Area-weighted Manning's n for overland flow over pervious surfaces (WA_Nperv_Manning)
- Area-weighted Depression Storage on Impervious Surfaces (WA_DstoreImperv)
- Area-weighted Depression Storage on Pervious Surfaces (WA_DstorePerv)

To calculate Percent Imperviousness, %Imperv, the impervious surfaces in the subcatchment were summed then divided by the total subcatchment area, A_{tot}:

$$\%Imperv = \frac{\sum(Impervious\ Surfaces)}{A_{tot}}$$

Percent zero imperviousness refers to the percent of impervious area with no depression storage. For simplicity, this experiment assumed that the only impervious surfaces without depression storage would be smooth, sloped roofs. This experiment assumed that all roofs were both smooth and sloped,

although, in reality, this is not the case. With these assumptions, the calculation for percent zero imperviousness is:

$$\%_{ZEROImperv} = \frac{\sum A_{Roofs}}{A_{tot}}$$

where, %ZEROImperv is percent zero imperviousness, A_{Roofs} is the total area of roof surfaces in the subcatchment, and A_{tot} is the total area of the subcatchment.

3.3 GIS Implementation Methods

3.3.1 GIS Mapping Methods

In GIS, the coordinate system is the "NAD_1983_StatePlane_Louisiana_South_FIPS_ 1702_Feet". The GIS mapping methods began with a GIS base map of UNO's campus, created by three UNO researchers. Quality control was performed on this base map including adjusting roof and parking lot footprints. Other surfaces were redrawn, and new attribute tables were developed for each layer.

The UNO campus was digitized into discrete surface layers including Roads, Sidewalks, Open Spaces, Roofs, and Parking Lots, as shown in the figure below. Sidewalks and roads were created by drawing polylines and "buffering" them to create polygons. The "erase" tool was utilized to create the "Open Spaces" polygon layer in the remaining void spaces.

Figure 3.3. Campus discretized into different surface types in GIS, each with assigned attributes.

Attributes were assigned to each surface layer, as illustrated in the Parking Lot layer figure and corresponding attribute table, as shown in the figure below.

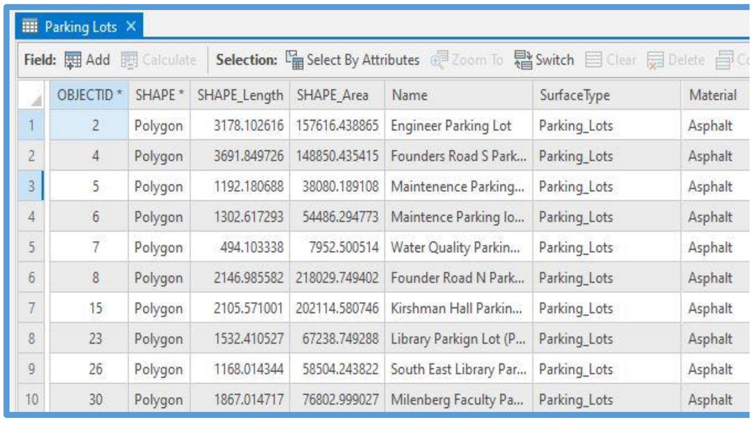

Parking Lots

Field: Add Calculate Selection: Select By Attributes Zoom To Switch Clear Delete

	OBJECTID *	SHAPE *	SHAPE_Length	SHAPE_Area	Name	SurfaceType	Material
1	2	Polygon	3178.102616	157616.438865	Engineer Parking Lot	Parking_Lots	Asphalt
2	4	Polygon	3691.849726	148850.435415	Founders Road S Park...	Parking_Lots	Asphalt
3	5	Polygon	1192.180688	38080.189108	Maintenence Parking...	Parking_Lots	Asphalt
4	6	Polygon	1302.617293	54486.294773	Maintence Parking lo...	Parking_Lots	Asphalt
5	7	Polygon	494.103338	7952.500514	Water Quality Parkin...	Parking_Lots	Asphalt
6	8	Polygon	2146.985582	218029.749402	Founder Road N Park...	Parking_Lots	Asphalt
7	15	Polygon	2105.571001	202114.580746	Kirshman Hall Parkin...	Parking_Lots	Asphalt
8	23	Polygon	1532.410527	67238.749288	Library Parkign Lot (P...	Parking_Lots	Asphalt
9	26	Polygon	1168.014344	58504.243822	South East Library Par...	Parking_Lots	Asphalt
10	30	Polygon	1867.014717	76802.999027	Milenberg Faculty Pa...	Parking_Lots	Asphalt

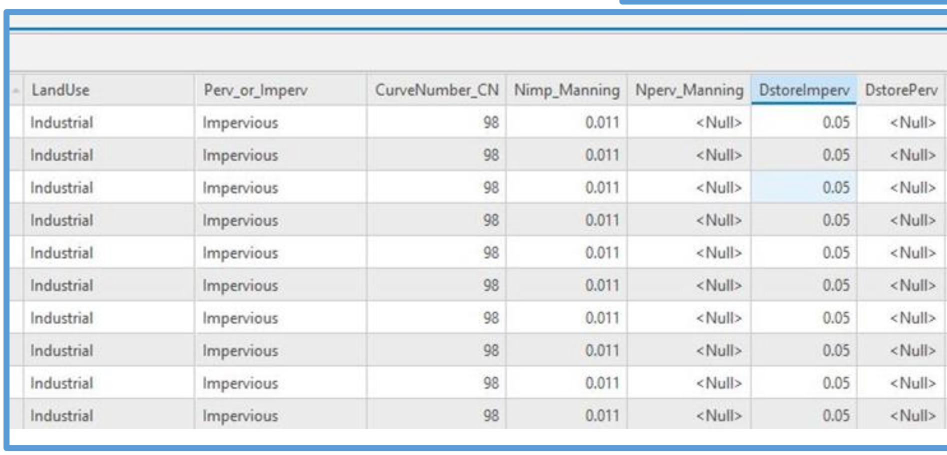

LandUse	Perv_or_Imperv	CurveNumber_CN	Nimp_Manning	Nperv_Manning	DstoreImperv	DstorePerv
Industrial	Impervious	98	0.011	<Null>	0.05	<Null>
Industrial	Impervious	98	0.011	<Null>	0.05	<Null>
Industrial	Impervious	98	0.011	<Null>	0.05	<Null>
Industrial	Impervious	98	0.011	<Null>	0.05	<Null>
Industrial	Impervious	98	0.011	<Null>	0.05	<Null>
Industrial	Impervious	98	0.011	<Null>	0.05	<Null>
Industrial	Impervious	98	0.011	<Null>	0.05	<Null>
Industrial	Impervious	98	0.011	<Null>	0.05	<Null>
Industrial	Impervious	98	0.011	<Null>	0.05	<Null>
Industrial	Impervious	98	0.011	<Null>	0.05	<Null>

Figure 3.4. GIS Parking Lots attribute table and Parking Lots map layer.

The original SWMM model's subcatchment layer was imported into GIS as a shape file then converted it to a "SWMMSubcatchments" feature class in GIS.

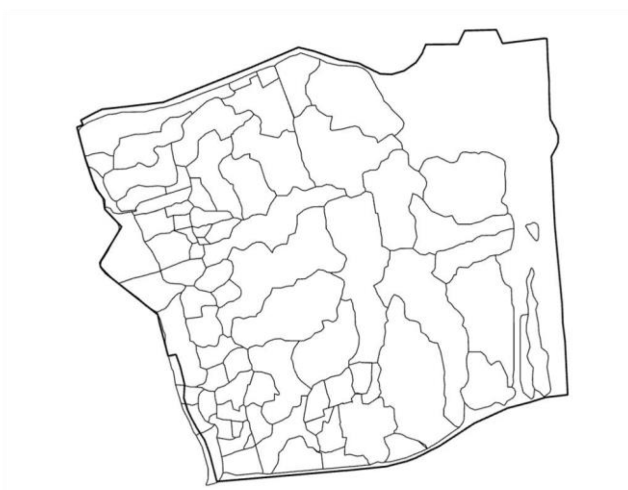

Figure 3.5. Subcatchments layer in GIS imported from SWMM.

3.3.2 GIS Geospatial Analysis

Throughout the geospatial analysis methods, attribute tables across all feature classes were designed with consistent nomenclature, data types, and decimal places to ensure data compatibility through calculations.

All surfaces were first "merged" into a single "SurfacesMergedFinal2" feature class. An additional benefit to using GIS is the ability to visualize different properties of surfaces by "symbolizing" various attributes of interest. For example, the same subcatchment, can be symbolized by Surface Type, Curve Number, or surface Material, as shown in the following figure. This GIS model of campus offers many potential future uses for campus planning.

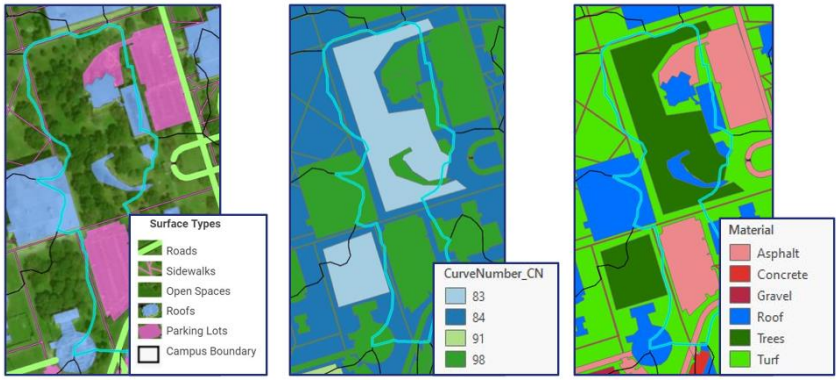

Figure 3.6. A subcatchment symbolized by different attributes in GIS.

To use an analogy, each subcatchment was used like a cookie cutter to cut the other surfaces into parcels within the subcatchment boundary by "intersecting" the "SWMMSubcatchments" and "SurfacesMergedFinal2" layers. This action created a new layer called "IntersectFinal".

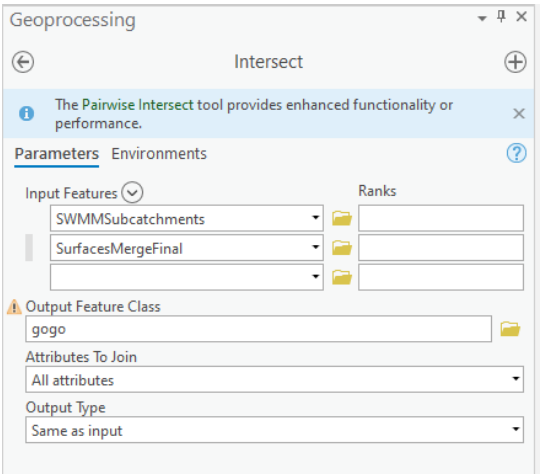

Figure 3.7. Intersect geoprocessing tool window in ArcGIS Pro.

Within the "IntersectFinal" layer, "calculate fields" was utilized to calculate the individual parameters (CNi, for example) times their individual areas (Ai for the CN, for example) within each

subcatchment boundary. These new fields were calculated for all rows (called "ranges" in GIS), using the following Python3 expressions:

CNi_x_Ai = !CurveNumber_CN!*!Shape_Area!
Nimpi_xAi = !Nimp_Manning!*!Shape_Area!
Npervi_xAi= !Nperv_Manning!*!Shape_Area!
DstoreImpervi_xAi = !DstoreImperv!*!Shape_Area!
DstorePervi_xAi = !DstorePerv!*!Shape_Area!
RoofArea = !RoofCode!*!Shape_Area!
ImperviousArea = !ImpervCode!*!Shape_Area!

To continue the area-weighted attribute calculations, the "summarize within" tool was used between "SWMMSubcatchments" and "IntersectFinal2" layers to generate a new feature class called "SummarizeWithinFinal3" that summed the results of the preceding calculations within the whole subcatchment. These calculations generated the following outputs:

SumCN_xAi
SumNimpi_xAi
SumNpervi_xAi
SumDstoreImpervi_xAi
SumDstorePervi_xAi
SumRoofArea
SumImperviousArea

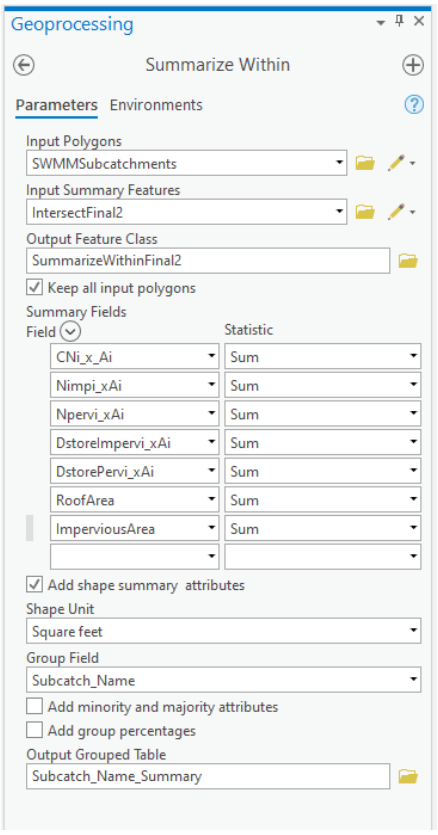

Figure 3.8. Summarize Within geoprocessing tool window.

The following fields were then added to this same "SummarizeWithinFinal3" attribute table and calculated the remainder of the area-weighted value equation by dividing the results from the preceding calculations by the total subcatchment area. To perform these calculations for each attribute, the following Python 3 expressions were created:

WA_CN = !sum_cni_x_ai!/!sum_Area_SQUAREFEET!
WA_Nimp_Manning = !sum_nimpi_xai!/!sum_Area_SQUAREFEET!
WA_Nperv_Manning = !sum_npervi_ai!/!sum_Area_SQUAREFEET!
WA_DstoreImperv = !sum_dstoreimpervi_xai!/!sum_Area_SQUAREFEET!
WA_DstorePerv = !sum_dstorepervi_xai!/!sum_Area_SQUAREFEET!
PercentImperv = !sum_imperviousarea!/!sum_Area_SQUAREFEET!*100
PercentPerv = 100-!PercentImperv!
Percent_ZEROImperv = !sum_roofarea!/!sum_Area_SQUAREFEET!*100

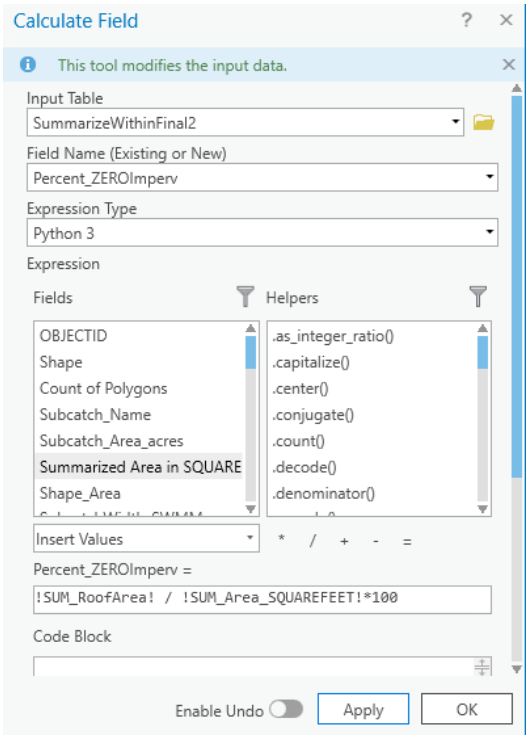

Figure 3.9. The Calculate Field geoprocessing tool window for percent zero impervious surfaces, which sums roof areas in a subcatchment and divides by the total subcatchment area.

3.3.3 GIS Model Area-Weighted Results

The results of this GIS pre-processing model are area-weighted attribute values for each subcatchment that can be imported into SWMM. The area-weighted attributes calculated in GIS include percent imperviousness, Manning's n for overland flow over impervious surfaces, Manning's n for overland flow for pervious surfaces, the depression storage on impervious surfaces, the depression storage on pervious surfaces, the percent zero imperviousness, and the Curve Number. The table excerpt below shows the GIS area-weighted results for 18 of the 82 subcatchments. The full table of results can be found in Appendix A.

Table 3.6. GIS-calculated area-weighted attributes results excerpt (see Appendix A for all results).

Subcatchment Name	Imperv. (%)	N Imperv	N Perv	Dstore Imperv (in)	Dstore Perv (in)	Zero Imperv (%)	Curve Number
S101	60	0.006	0.096	0.022	0.08	16	92
S102	37	0.004	0.152	0.018	0.127	0	89
S105	66	0.007	0.081	0.03	0.068	5	93
S108	80	0.009	0.023	0.032	0.028	16	96
S112	28	0.003	0.173	0.004	0.144	21	88
S114	30	0.003	0.168	0.012	0.14	6	88
S115	40	0.004	0.145	0.011	0.12	18	90
S116	90	0.01	0.024	0.029	0.02	32	97
S117	61	0.007	0.064	0.03	0.063	1	94
S118	9	0.001	0.039	0	0.091	9	91
S119	0	0	0.024	0	0.09	0	91
S120	28	0.003	0.088	0	0.101	28	91
S121	2	0	0.065	0	0.11	2	90
S122	4	0	0.089	0.002	0.12	0	89
S124	77	0.008	0.056	0.037	0.046	3	95
S125	60	0.007	0.095	0.024	0.079	12	92
S127	37	0.004	0.211	0.012	0.126	14	89
S128	75	0.008	0.059	0.033	0.049	9	95

3.3.4 LID Feature Layer Mapping in GIS

To map the proposed LID features in GIS, each LID feature was first mapped as a separate layer. To determine the LID area in each subcatchment, the "split" tool was used to divide each LID feature into smaller polygons within each subcatchment, as illustrated below. These LID GIS shapefiles were imported into SWMM to locate nodes of interest in SWMM and subcatchments impacted by the LID.

Figure 3.10. Proposed pervious pavement area, split by subcatchment in GIS.

The table below summarizes LID areas per subcatchment.

Table 3.7. LID areas per subcatchment.

Node	LID Control	Subcatchment Name	LID Area (sq. ft.)	Total Areas (sq. ft.)
OF1 Dean's Ditch	Vegetative Swale	S247_2	1,393.4	
		S4	11,334.4	
		S43	1,673.5	
		S13_1	4,357.4	
		S13_2	18,856.6	
		S122	10,139.6	
		S27	8,673.5	
		S197_1	1,877.0	58,305.4
J504 Cove Parking Lot	Permeable Pavement	S50_2	34,939.7	
		S66	14,921.8	
		S76_1	13,703.7	
		S76	8,891.1	
		S13_3	8,671.6	
		S108	30,060.5	
		S28	63,658.3	
		S75	39,891.2	214,737.9
J34 Admin Building Parking Lot	Permeable Pavement	S77	58,396.7	58,396.7
J47 Lafitte Village Parking Lot	Permeable Pavement	S117	4,410.2	
		S118	22,016.8	
		S64	20,688.8	
		S63	4,824.3	
		S65	17,841.9	
		S120	8,390.5	
		S119	8,984.7	87,157.2
J47 Lafitte Village	Bioretention Cell	S65	19,108.3	19,108.3

3.4 SWMM Model Implementation Methods

3.4.1 SWMM Model as Received

The UNO research team's SWMM model under development is currently being updated and refined. The SWMM model dated 13 September 2021, called "UNOManualDelineate.pcz" is used as the basis of the SWMM model built in this study (Cothren & Christo, 2021). At the time of this report, the SWMM base model was still being updated with culvert invert elevations, direction of flow through conduits, conduit size, catchment location, etc. Several appropriate modifications to this base model were made based on reasonable assumptions to create a working "Modified Base Model" for this study, as discussed in the following methods.

3.4.2 Modified Base Model Creation

3.4.2.1 GIS Hydrologic Attribute Import to SWMM

The area-weighted ArcGIS Pro attributes were imported into SWMM by matching attribute field names, as shown in SWMM's GIS import wizard below.

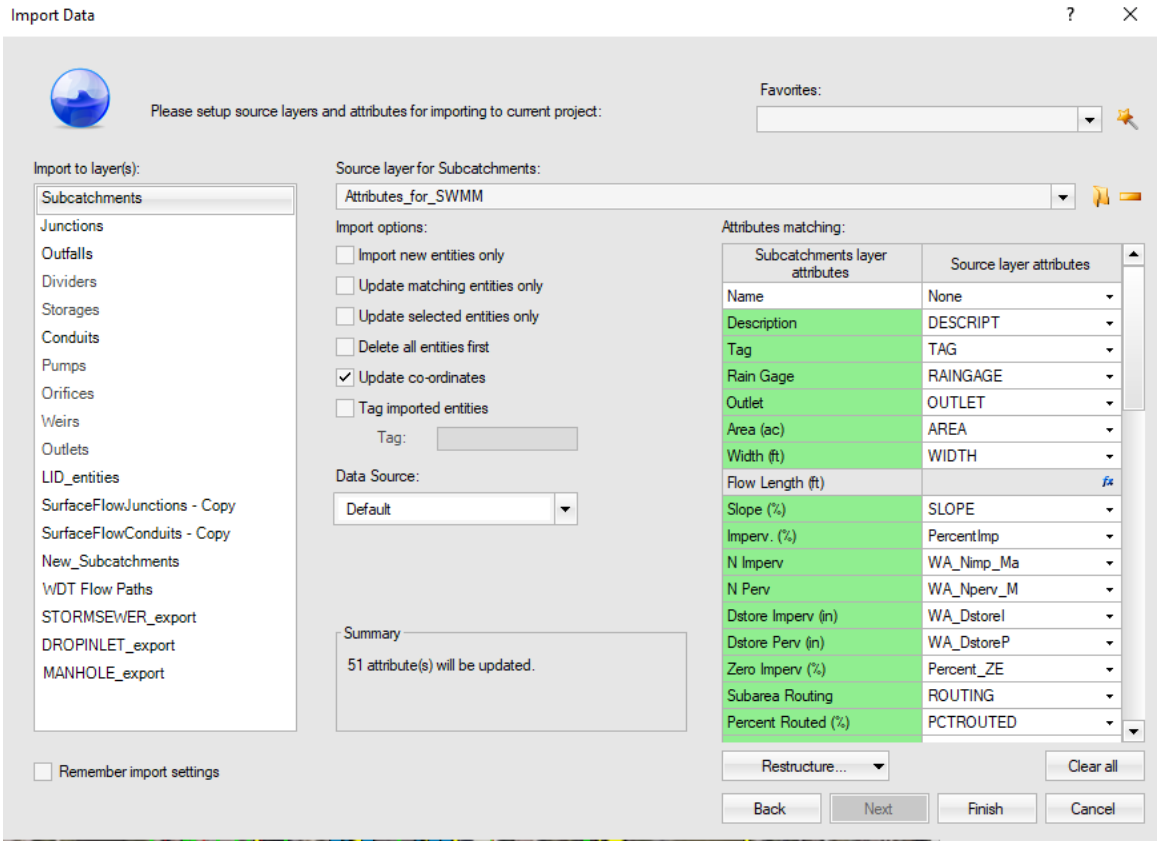

Figure 3.11. GIS area-weighted attributes mapped to the SWMM subcatchment layer (CHI *Software*, 2021e).

3.4.2.2 Duplicate Subcatchment and Name Elimination in SWMM

Only after importing the GIS attributes to SWMM did it become apparent that SWMM had created duplicate subcatchments and additional subcatchment names. This occurred when the subcatchments were first exported from SWMM to GIS because the SWMM command is "Export/Duplicate". The imported area-weighted GIS values populated the new duplicate subcatchments. The subcatchments populated with the area-weighted GIS attributes were retained; the others were deleted. As a result, most SWMM subcatchment names no longer match the subcatchment names in GIS. Future modelers should delete duplicate subcatchments prior to importing GIS attributes.

To note, the UNO research team's SWMM base model contained 82 subcatchments at the time that the GIS model was built (Cothren, 2021). The research team updated the number of subcatchments to 95 at the time of GIS attribute import to SWMM (Cothren, 2021). As a result, there are several subcatchments on the east side of campus that contain default attribute values instead (Appendix E). These subcatchments are not upstream of any nodes of interest.

3.4.2.3 Methods to Ensure GIS-Imported Data is Correct

To ensure the imported GIS values exactly matched those populating subcatchments in SWMM, the GIS and SWMM attribute tables were exported to Excel, subcatchment names were matched, and Excel "if, then" statements were used to identify any data discrepancies. After several corrections, all discrepancies were resolved. Discrepancies originated only from the duplicate subcatchment issue, not from the general GIS import methods.

3.4.2.4 Conduit Geometry Modification

In the 13 September 2021 version of the UNO research team's SWMM base model, the Upper Reach of Dean's Ditch is represented by circular pipes with a 1.25-foot diameter. In the Modified Base Model, these conduits are modified to a trapezoidal channel with a 1.25-foot depth, bottom width of 2-feet, and side slopes of 2 feet/feet (horizontal/vertical), as illustrated in the figure below.

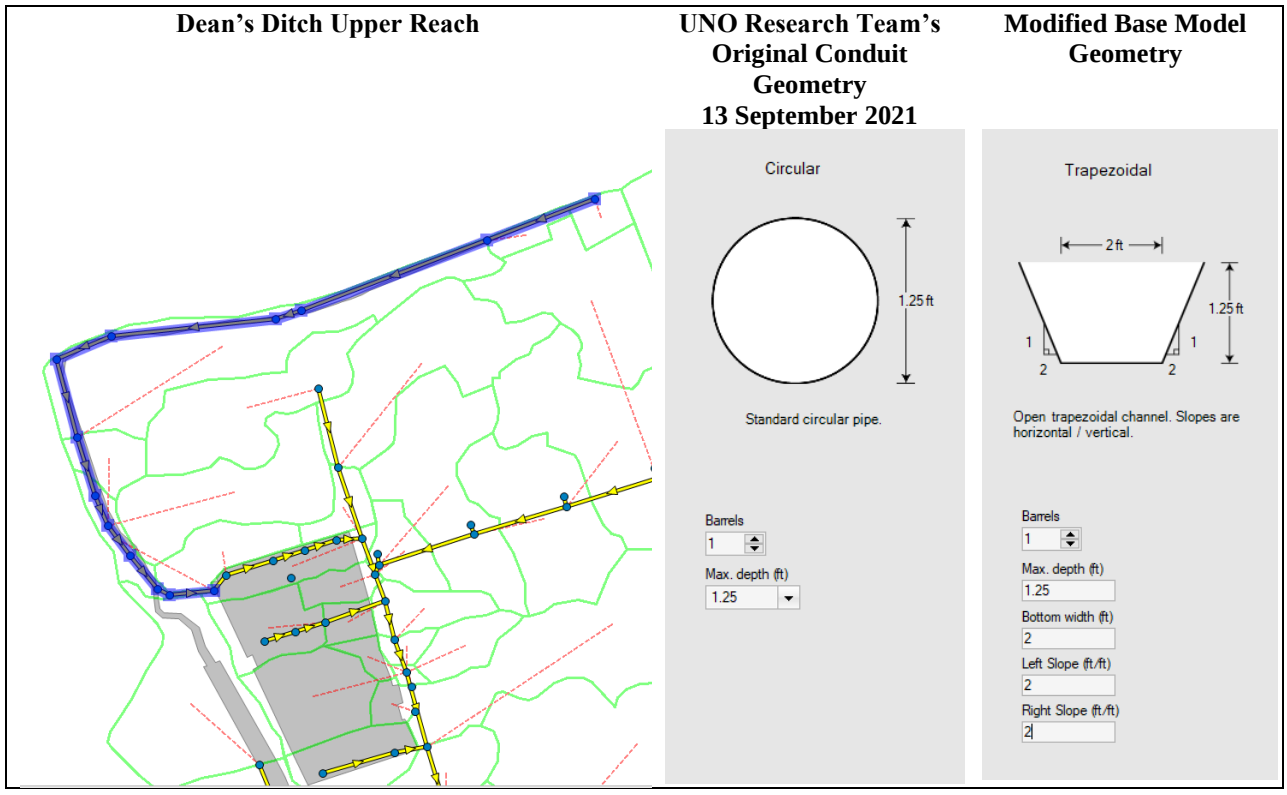

Figure 3.12. Dean's Ditch Upper Reach conduit geometry modification in the Modified Base Model (CHI *Software*, 2021e).

All conduits upstream of Outfall OF1 were already configured as trapezoids with varying geometry in the UNO research team's original SWMM model, as shown in the figure below.

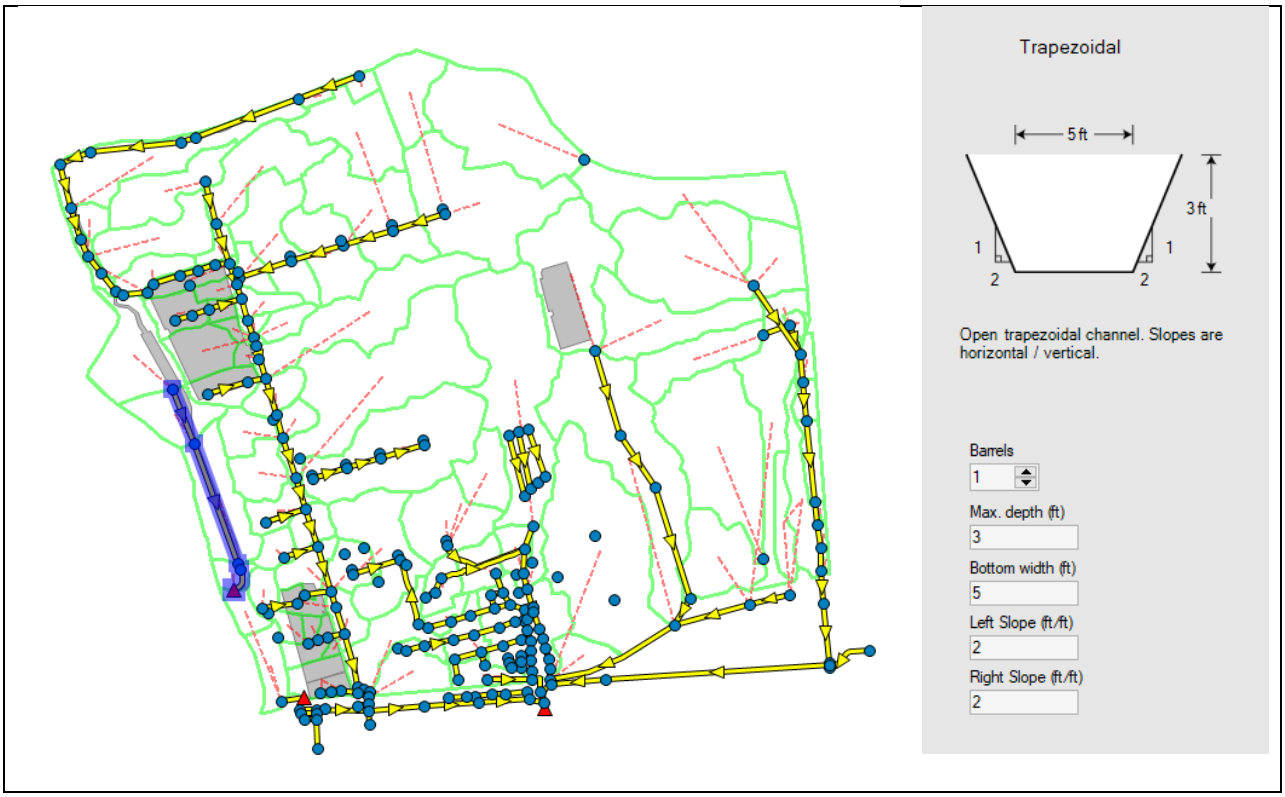

Figure 3.13. Dean's Ditch Lower Reach conduit geometry in the Modified Base Model (CHI *Software*, 2021e).

The table below summarizes the variations in Dean's Ditch trapezoidal geometry in the Modified Base Model. These geometries later populate the SWMM Baseline and LID scenarios.

Table 3.8. Dean's Ditch modified single-barrel trapezoidal geometry.

Segment	Conduit Name	Max Depth	Bottom Width (ft)	Left Slope (ft/ft)	Right Slope (ft/ft)
Upper Reach	Conduits C192 to C123	1.25	2	2	2
Lower Reach	C200	2	2	2	2
	C201	3	3	2	2
	C203_1	3	4	2	2
	C203_2	3	5	2	2

3.4.3 Design Storms

3.4.3.1 Design Storm Selection

Per line 273 of the 2018 *The City of New Orleans Stormwater Code*, "the post-development peak stormwater runoff rate from a development site shall not exceed the pre-development peak stormwater runoff rate from that development site for a 10-year, 24-hour design storm (The City of New Orleans,

2018)." This experiment's design storms therefore all have a 24-hour rainfall duration and 10-year average recurrence interval (return period), meaning that the design storm has a 1/10=0.1=10% chance of being exceeded in any one year. UNO experiences flooding during 2-year to 5-year storm events but this study focused on the Stormwater Code.

3.4.3.2 Multiple Stations to Generate Uncertainty

Precipitation is a primary driver of the SWMM model results. To generate uncertainty in SWMM model results, four 10-year, 24-hour design storms were created using rainfall from four different NOAA Atlas 14 stations near UNO, shown in the figure below. Each station has a different Point Precipitation Frequency Estimate, resulting in four design storms, each with their own total rainfall.

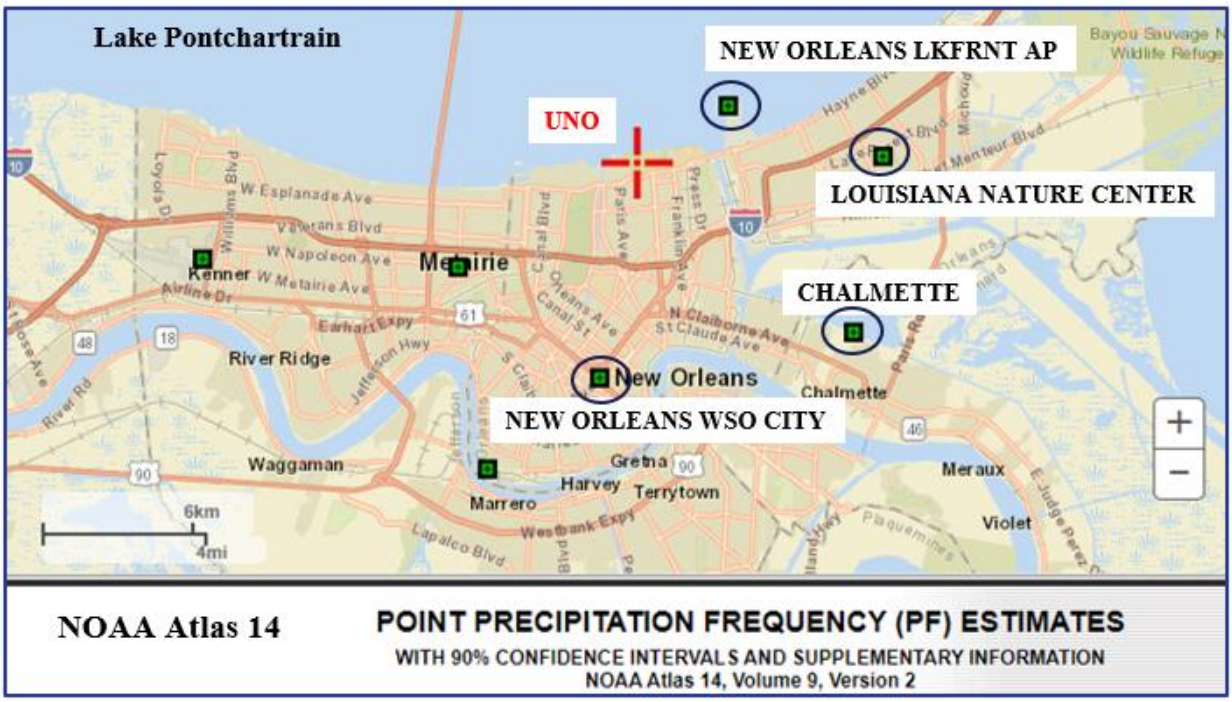

Figure 3.14. NOAA Atlas 14 weather stations map modified with labels (NOAA, 2017).

3.4.3.3 Total Rainfall

SWMM requires a "total rainfall" input to create SCS-method design storms. The NOAA Atlas 14 Partial Duration Series (PDS) Point Precipitation Frequency (PF) Estimate tables with a 90% confidence interval were utilized to identify total rainfall for the four stations. The PF Estimate table for Design Storm 1 can be found in Appendix F. as an example of total rainfall selection. The PDS times series includes all precipitation amounts recorded at a station, for a period of record, if they exceed a pre-defined threshold value. The PDS can include more than one event in any particular year likely resulting in a conservative PF estimate for return periods of 10 years or less for this study site. Total rainfall values (PF) for each station and the corresponding design storms are shown in the table below.

Table 3.9. Total rainfall (PPF) and stations selected for each design storm.

Design Storm Name	Station	Station Number	Point Precipitation Frequency Estimates (inches)
DS1	LOUISIANA NATURE CTR	16-5610	8.26
DS2	NEW ORLEANS LKFRNT AP	16-6667	8.24
DS3	CHALMETTE	16-1639	8.32
DS4	NEW ORLEANS WSO CITY	16-6659	8.35

3.4.3.4 SWMM Design Storm Creator

The SCS rainfall method was selected in SWMM's Design Storm Creator. The "Type III" rainfall distribution storm is required for UNO's location, as shown on the SCS storm distribution boundaries map below.

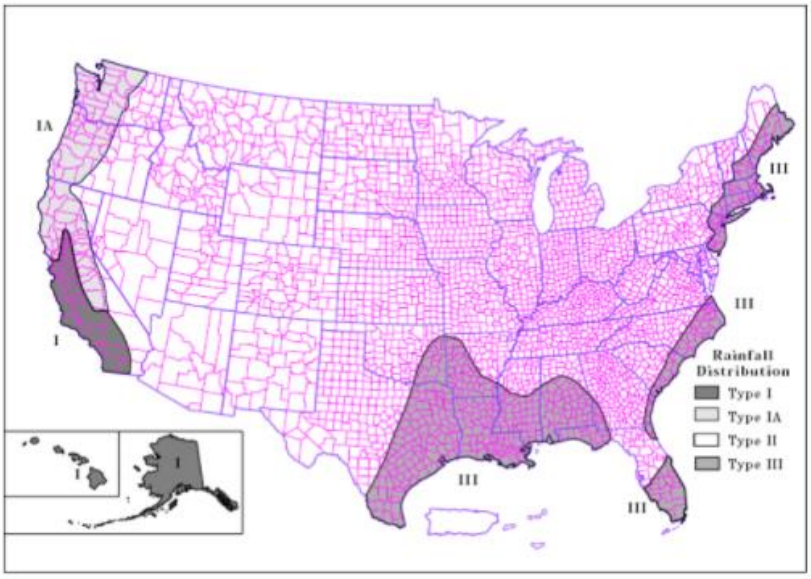

Figure 3.15. SCS storm distribution boundaries. Excerpted from the USACE HEC-HMS Technical Reference Manual (USACE, 2021).

The storm duration was set to "24-hour", the rainfall interval to "6-minute" and the rain format to "intensity" for the 10-year return period. The Design Storm 1 hyetograph is shown in the figure below.

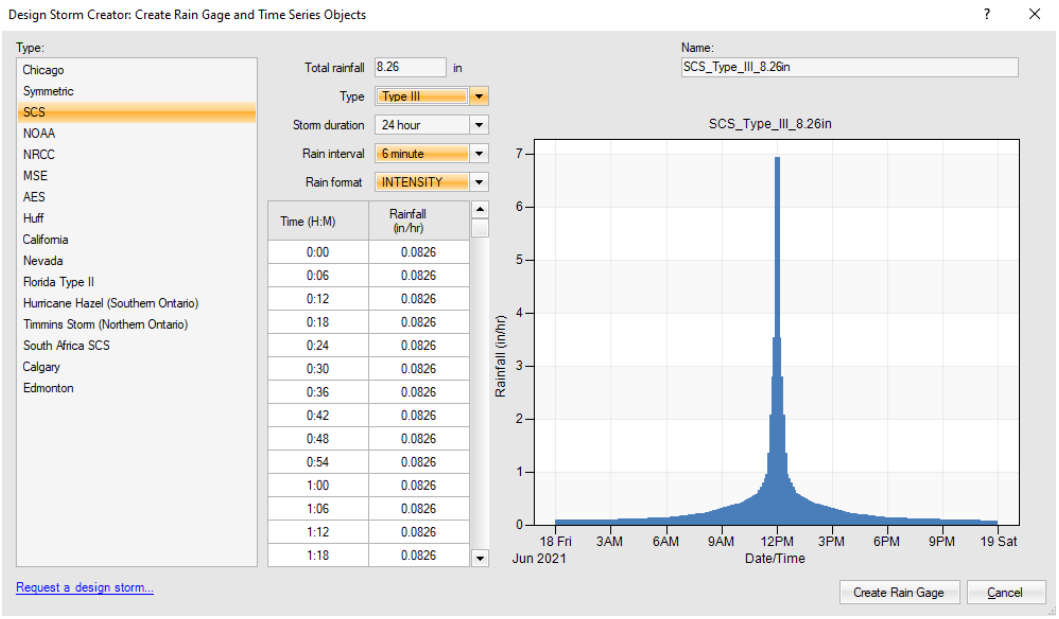

Figure 3.16. SWMM Design Storm Creator with hyetograph (CHI *Software*, 2021e).

3.4.4 Baseline and LID Scenarios

To evaluate the impact of LID features on campus runoff, two scenarios were created from the Modified Base Model within SWMM. The first scenario, called "Baseline", runs the model without any LID. The second scenario, called "LID", includes the five LID features with modified surface drainage outlets, and modified or deleted junctions and conduits. A summary of added and deleted junctions and conduits can be found in Appendix D of this report. A comparison of the Baseline and LID scenario junctions, conduits, and subcatchment outlet configurations are on the following page.

After adding LID features to SWMM, the percent imperviousness for each subcatchment was calculated and manually adjusted.

Baseline Scenario

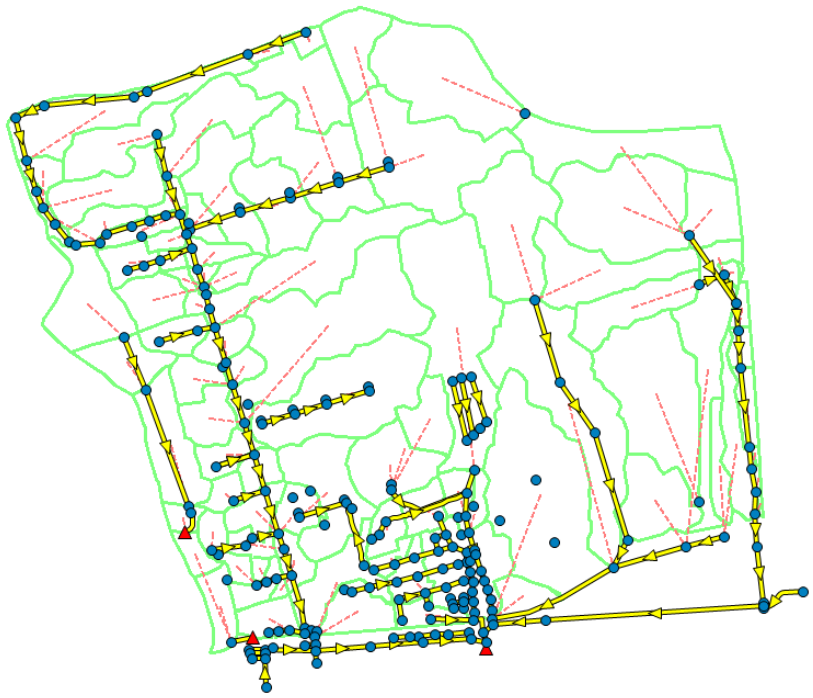

LID Scenario

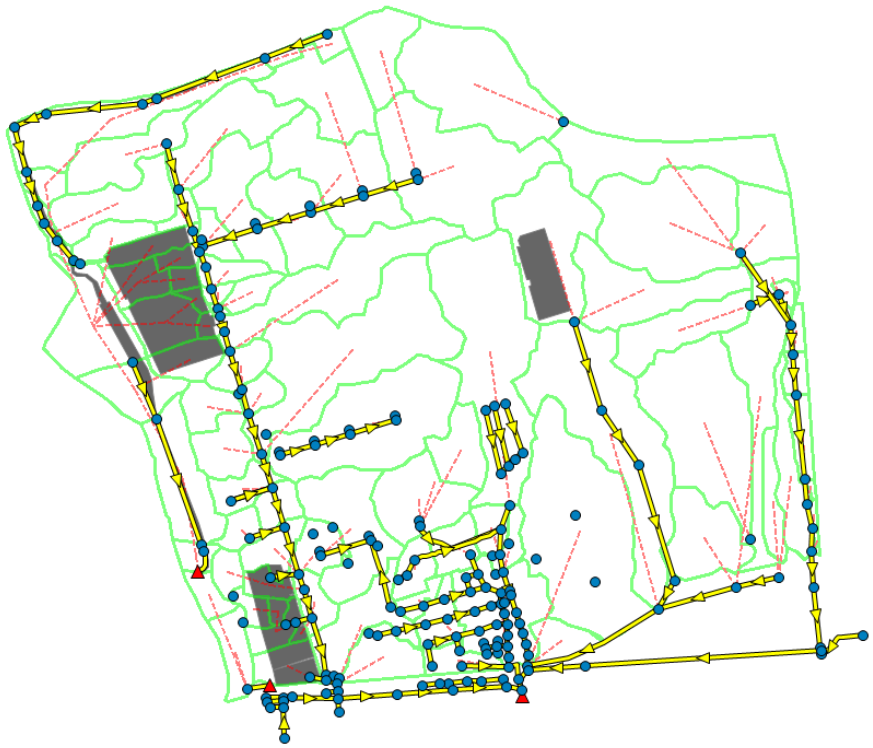

Figure 3.17. Baseline and LID scenarios comparison of junction, conduit and subcatchment outlet configurations (CHI *Software*, 2021e).

The figure below illustrates the original watershed for each node of interest for the Baseline scenario (left) and modified watersheds in the LID scenario (right).

Table 3.10. Watershed for each node of interest in the Baseline versus LID scenarios (CHI *Software*, 2021e).

Node	Baseline Scenario	LID Scenario
OF1 Dean's Ditch		
J504 The Cove Parking Lot	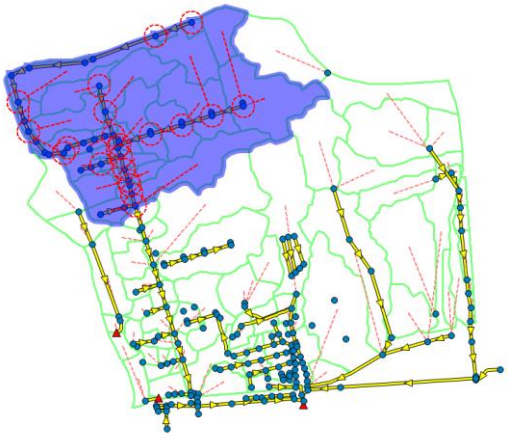	

(Table continued).

(Table continued from previous page).

Node	Baseline Scenario	LID Scenario
J34 Admin Building Parking Lot		
J47 Lafitte Village Parking Lot And Lafitte Village Bioretention Area	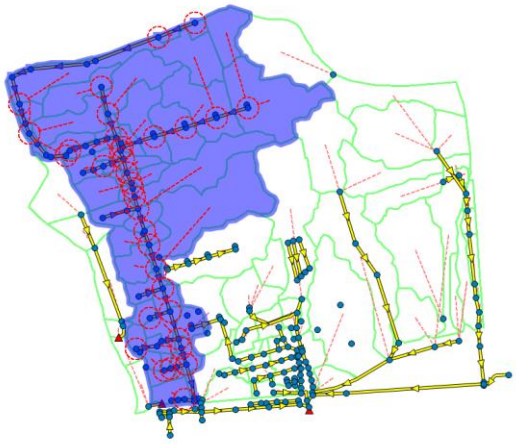	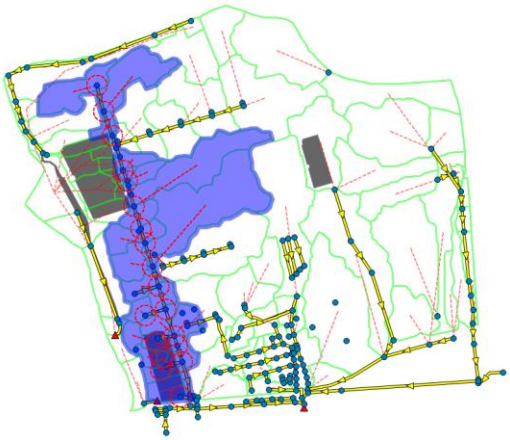

3.4.5 Node Invert Elevation Modification and Conduit Addition

When running preliminary models in both the Baseline and LID scenarios, SWMM reported flooding at many nodes due to conduits with an insufficient slope, a slope of zero (0), or a high invert elevation between two low invert elevations creating a hump. The original model did not show a continuous drop toward each outfall.

To correct this issue the invert elevations for all nodes that impacted the experiment's nodes of interest were recalculated and manually reentered, from each outfall to the upstream reaches of the watershed. A slope of 1-foot drop per 1000-foot run was assumed. Starting with an assumed invert elevation of (-)8-feet at outfall OF11, the length of each conduit in-sequence was used to back-calculate and revise each junction's invert elevation. Thus, a nearly continuous 0.1% upward slope from outfall OF1 was created.

The spreadsheet with these node invert elevation calculations is a tool for future modelers to recalculate campus drainage system node invert elevations simply by entering actual node elevations in the blue cells, and the desired conduit slope upstream. An excerpt of the table of recalculated node invert elevations is below. The full table can be found in Appendix C1-C4 of this report.

Table 3.11. Excerpt of recalculated SWMM node invert elevations. Blue boxes indicate starting elevations. (See Appendix C1-C4 for the full table).

Location	Node d/s	Conduit	Conduit Length	Slope	Original Invert Elevation (ft)	Calculated Invert Elevation(ft)	Notes
Founders Road							
	J499	C130					Added new conduit C130 between J61 and J499 bc J499 had no outlet wasn't connected
	Outfall OF11				0	-8.00	Assigned invert elevation
	J122	C128	27.981	0.001	0	-7.97	
	J73	C112	74.109	0.001	0	-7.90	
	J72	C65	246.311	0.001	0	-7.65	
	J69	C63	262.65	0.001	0	-7.39	
	J62	C62	272.136	0.001	0	-7.12	
	J61	C58	34.264	0.001	0	-7.08	
	J499	C130	36.351	0.001	-4.028	-7.05	
	J47	C68	53.835	0.001	-2.963	-6.99	
	J35	C47	28.158	0.001	0	-6.96	
	J44	C199	269.357	0.001	-1.264	-6.69	
	J78	C198	135.717	0.001	0	-6.56	
	J43	C197	79.414	0.001	-0.656	-6.48	

This process revealed several key junctions (nodes) that were "orphaned" or floating, not actually connected to conduits (links), as shown in the figure on the following page. To correct this, the existing conduits nearby were deleted; new conduits were added in between these junctions, thereby unifying nodes and links. This is an important step because it corrected the SWMM model's understanding of the watershed upstream of each node of interest.

This process also revealed that an important conduit was missing in the Modified Base Model, Baseline scenario, and LID scenarios. As shown on the left in the figure below, the Lafitte Village parking lot and the Founders Road conduits were not routed to any outfalls. In reality this is because field investigations have not made it clear how the upstream node at this gap connects to drainage infrastructure. This experiment assumes that the Founders Road conduits are routed towards outfall OF11, so conduit C130 was to all scenarios in SWMM, as shown below.

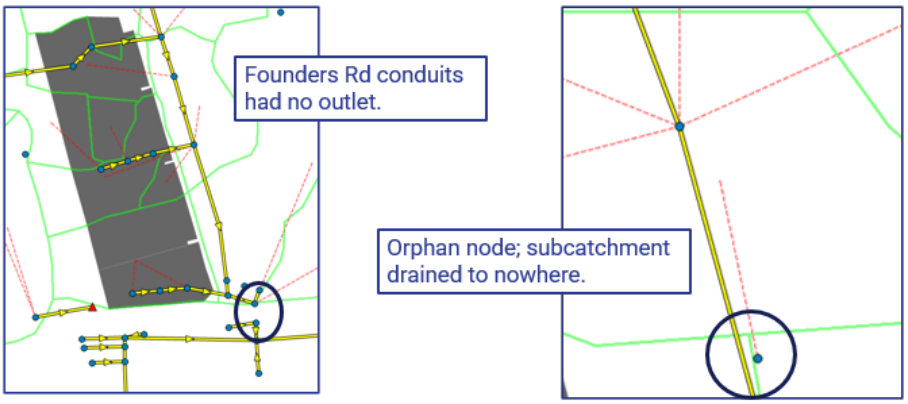

Figure 3.18. Left: Conduit C130 added to route the Founders Road conduits to outfall OF11. Right: orphan nodes connected to conduits (CHI *Software*, 2021e).

3.4.6 Simulation Options

In the Simulation Options editor, the "Rainfall/Runoff" and "Flow Routing" process models were selected. The "Curve Number" method was selected as the infiltration model. Ponding was not selected, so excess flow is lost to the system.

SWMM offers three methods of routing, listed in increasing order of complexity: steady flow routing, kinematic wave routing, and dynamic wave routing. Each routing method uses Manning's equation to relate flow rate to flow depth and bed slope (friction slope). The "Dynamic Wave" routing method was selected. Conduits use continuity and momentum equations. Nodes use a volume continuity equation. Dynamic wave routing accounts for channel storage, entrance and exit losses, flow reversal, backwater, and pressurized flow when a conduit becomes full. Flooding occurs when the water depth at a node exceeds the maximum allowable depth. Excess flow can pond on top of the node and re-enter the drainage system or can be lost to the system. In theory, the dynamic wave routing method produces the most accurate results (CHI, 2021).

Each SWMM scenario was run using the SWMM5.1.013 engine. The coordinate system was set to "NAD83 Louisiana South ft US".

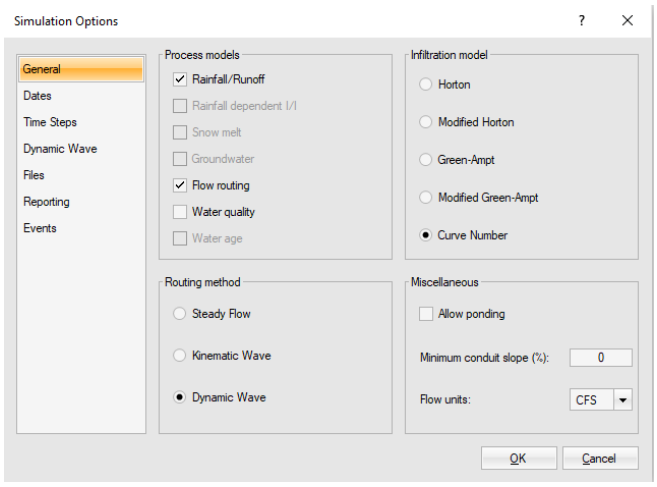

Figure 3.19. SWMM Simulation Option Editor (CHI *Software*, 2021e).

3.5 LID Design and Control Implementation Methods

This preliminary study used three types of SWMM-supported LID systems: a vegetated swale, three permeable pavement systems, and one large bioretention cell system. SWMM also supports rain garden, green roof, infiltration trench, rain barrel, and rooftop disconnection LID systems, but these were not used in this study.

3.5.1 Vegetative Swale for Dean's Ditch

3.5.1.1 Baseline vs LID Scenario – Dean's Ditch

The Baseline "before" scenario represents Dean's Ditch in its current state on campus. Dean's Ditch currently exists as a small ditch divided into two discrete reaches—the Upper Reach and the Lower Reach. The Upper Reach extends from the northeast corner of Privateer Place apartments, flows towards the London Avenue Canal, and turns east at the northwestern corner of the Cove parking lot, where it feeds into junctions that flow into the Founder's Road conduits. The lower reach begins behind the Facility Services building and continues south towards the OF1 outlet. The Baseline scenario models Dean's Ditch as an open channel conduit with trapezoidal geometry. The trapezoidal dimensions in the model were described previously this report.

The LID design for Dean's Ditch expands this small ditch into a long, continuous vegetated swale with varying widths that unites the Upper and Lower Reaches, as shown in the following figure.

Figure 3.20. Dean's Ditch footprint in the LID scenario with runoff routing (CHI *Software*, 2021e).

In the Dean's Ditch LID scenario, several junctions and conduits connecting the Upper Reach to the Lower Reach were deleted. Subcatchment outlets were changed from nodes to adjacent subcatchments. The Cove parking lot runoff was rerouted to flow into Dean's Ditch. Modifications to node OF1's watershed are summarized in the following figure.

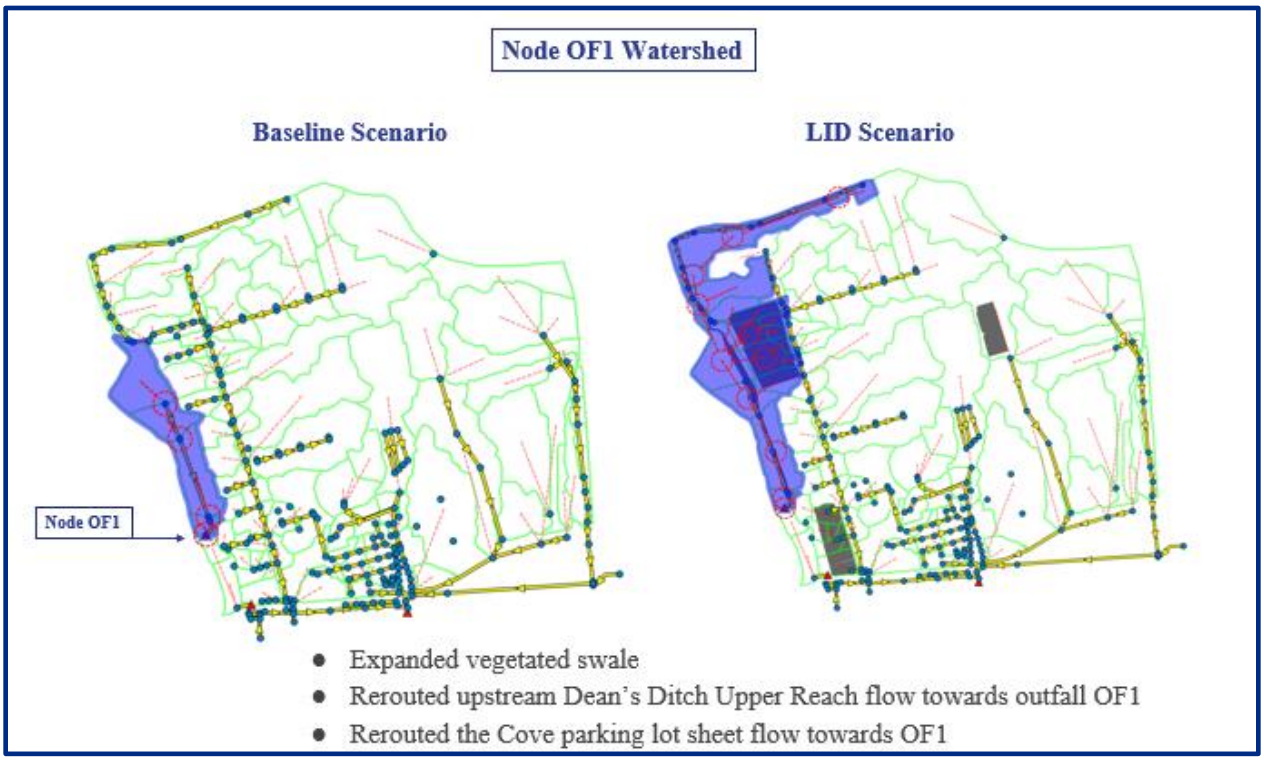

Figure 3.21. Node OF1 Baseline versus LID modified watersheds (CHI *Software*, 2021e).

3.5.1.2 Design –Vegetated Swale

The Dean's Ditch LID feature is a vegetated swale with varying widths, depths, and vegetation. The general LID design for the Upper Reach of Dean's Ditch is a grassed swale with native Bald Cypress trees installed on the side slope and bottom of the swale, as shown in the figure on the following page.

The general LID design for the Lower Reach of Dean's Ditch is native Willow and Bald Cypress trees and diverse shrubs planted on swale berms, side slopes, and bottom. This vegetated and continuous design of Dean's Ditch creates a habitat corridor for wildlife including birds. This swale could become a scenic and educational nature greenway destination on campus.

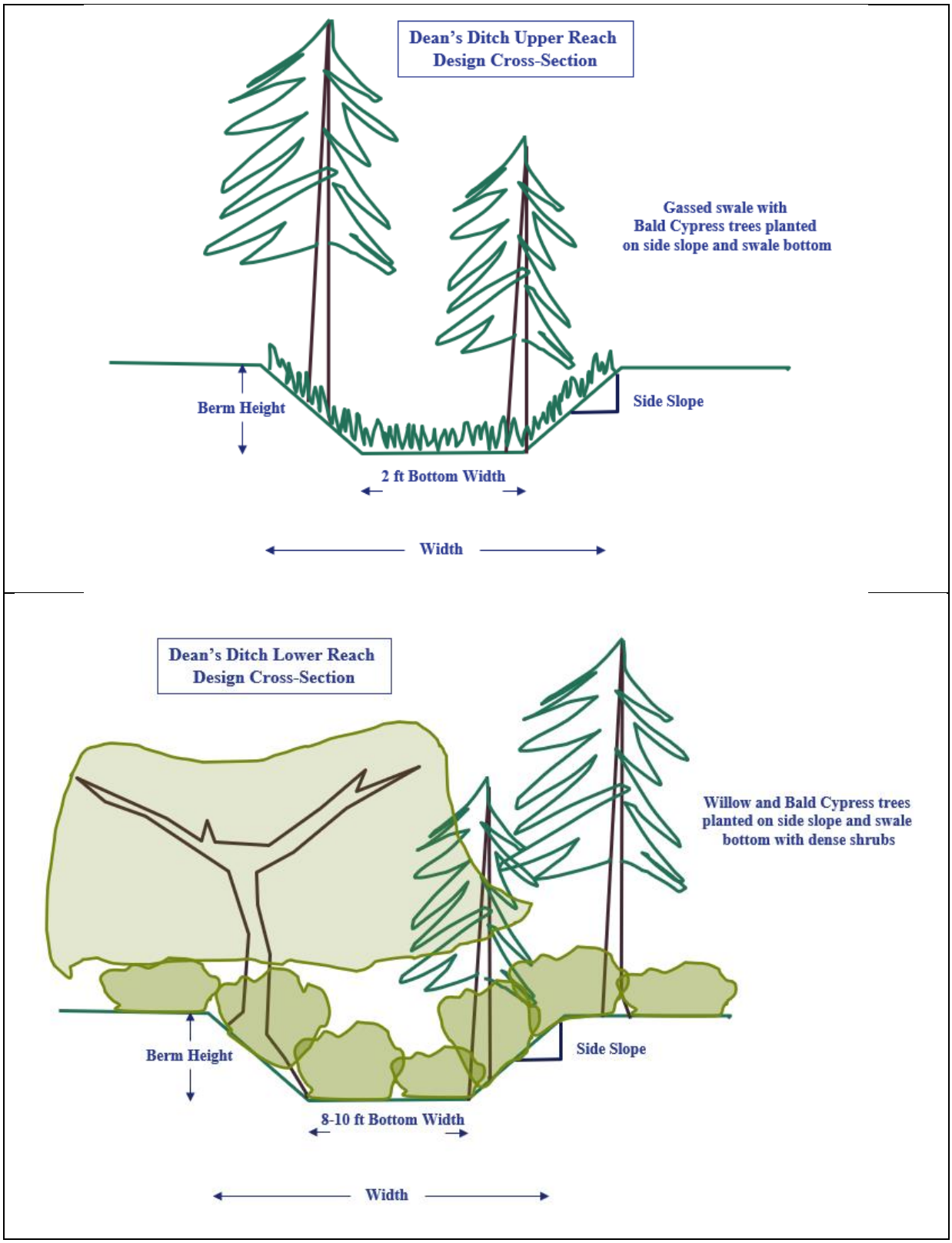

Figure 3.22. Dean's Ditch Upper Reach (top) and Lower Reach (bottom) vegetated swale general design cross sections.

3.5.1.3 LID Controls – Vegetated Swale

The table below summarizes the average vegetated swale characteristics in each subcatchment starting from the Upper Reach of Dean's Ditch to the Lower Reach of Dean's Ditch. For simplified subcatchment LID attribute entry, subcatchments are labeled as segments A-H.

Table 3.12. Dean's Ditch SWMM design parameters.

Segment	Subcatch-ment Name	Swale Width (ft)	LID Area (ft2)	Mean Berm Height (in)	Vegetation Volume (fraction)	Surface Roughness (Manning's n)*	Slope (%)	Swale side slope (run/rise)	Design Notes
A	S247_2	6.4	1393.4	15	0.1	0.41	2	2.6	Bald Cypress trees installed on grassed side slope
B	S4	6.4	11334.4	15	0.1	0.41	2	2.6	Bald Cypress trees installed on grassed side slope
C	S43	6.4	1673.5	15	0.1	0.41	2	2.6	Bald Cypress trees installed on grassed side slope
D	S13_1	6.4	4357.4	18	0.1	0.41	2	2.1	Bald Cypress trees installed on grassed side slope
E	S13_2	35	18856.6	20	0.2	0.6	2	10.5	Willow trees, shrubs
F	S122	40	10139.6	24	0.2	0.6	2	10.0	Willow trees, shrubs
G	S27	13	8673.5	36	0.2	0.8	2	2.2	Mix of Willow and Bald Cypress trees, shrubs
H	S197_1	15	1877.0	36	0.2	0.8	2	2.5	Outlet, mix of Willow and Bald Cypress trees, shrubs
*Manning's n for overland flow from McCuen, R. et al. (1996), Hydrology, FHWA-SA-96-067, Federal Highway Administration, Washington, DC.									

The Manning's n roughness values and vegetated volume fraction values are selected from literature table values, corresponding to the plantings in each Dean's Ditch segment. As shown in the table above, a 2% slope was assumed for the swale, which is a typical slope for overland sheet flow drainage.

3.5.2 Permeable Pavement for the Administration Building, the Cove, and Lafitte Village Parking Lots

The parking lot permeable pavement design is pervious concrete with subsurface arched retention chambers. This design applies to the Cove, Lafitte Village and Administration Building parking lots. These different locations on campus share the same unit-width LID design. The pervious concrete with subsurface arched chambers creates surface permeability, extensive subsurface water storage, and infiltration opportunities at the base.

3.5.2.1 Baseline vs LID Scenario at Each Location—Permeable Pavement

In the Baseline scenario, the Cove parking lot is impervious and is graded to junctions that feed into the Founders Road conduits and pass through node J504. In the LID scenario, the Cove parking lot is pervious concrete and is regraded towards Dean's Ditch, re-routing the runoff from node J504 to node OF1. Modifications to node J504's watershed are illustrated in the figure below. An actual vegetated swale would need to be engineered to accommodate outfall OF1 outlet capacity and optimal slope. Dean's Ditch can likely handle the additional flow, but there may be restrictions where outfall OF1 flow is routed through subsurface conduits and travels south over a short distance to the Southwest corner of Lafitte Village near Leon C. Simon Drive. Reviewing New Orleans Sewerage and Water Board (S&WB)

maps that were scanned and georectified, at this point there an existing 42-inch culvert transports the flow across Leon C. Simon Dr. and then east into a large 36-inch x 54-inch box culvert.

Figure 3.23. Node J504 Baseline versus LID modified watersheds (CHI *Software*, 2021e).

In the Baseline scenario, the Administration Building parking lot is impervious. Runoff is routed through node J34. The only change in the LID scenario is the parking lot surface and subsurface to pervious concrete with subsurface arched retention chambers. Modifications to node J34's watershed are summarized in the figure below.

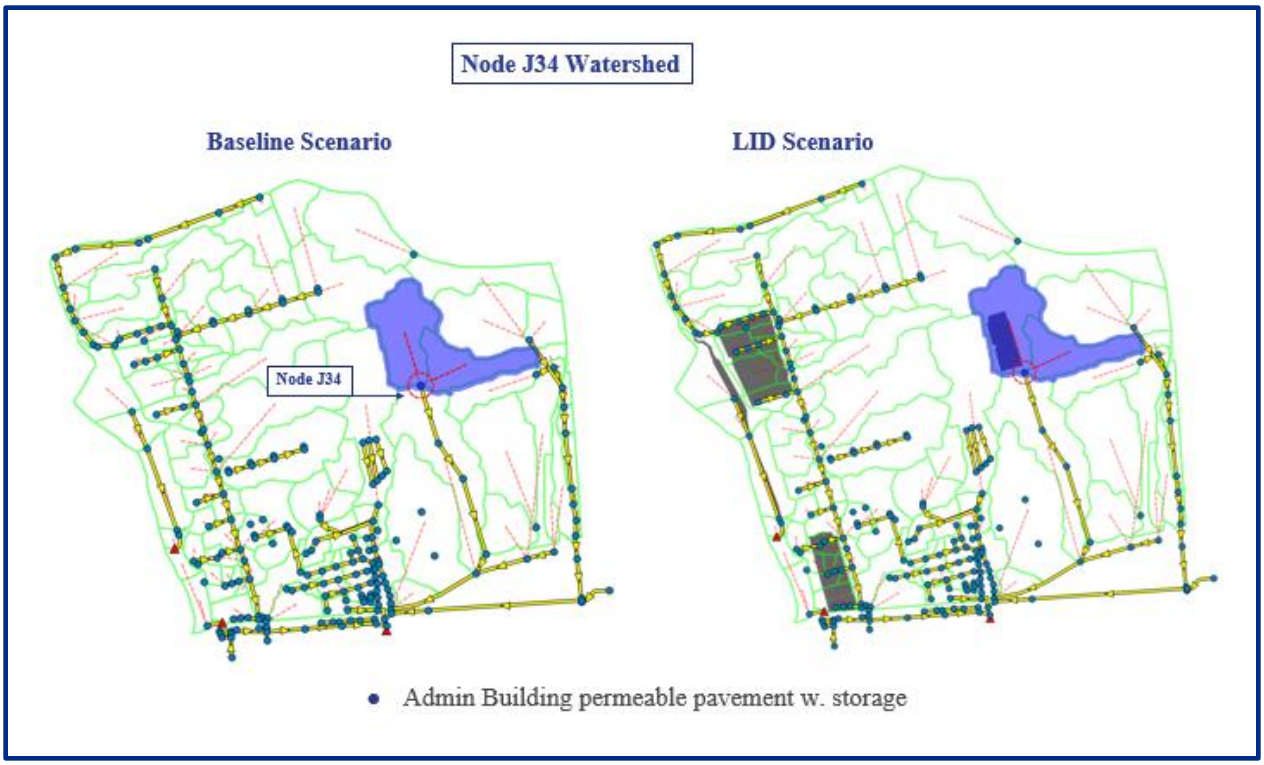

Figure 3.24. Node J34 Baseline versus LID modified watersheds (CHI *Software*, 2021e).

In the Baseline scenario, the Lafitte Village parking lot is impervious, subcatchment outlets are drainage system junctions, and runoff is routed through node J47. In the LID scenario, the Lafite Village parking lot is changed to pervious concrete with arched retention chambers, subcatchment outlets are changed to adjacent subcatchments to create overland flow, and several junctions and conduits are deleted. Modifications to node J47's watershed are summarized in the figure below.

Figure 3.25. Node J47 Baseline versus LID modified watersheds (CHI *Software*, 2021e).

3.5.2.2 Design—Permeable Pavement

The Stormwater Code of the City of New Orleans approves pervious concrete for parking stalls but not the driving lane (City of NO, 2018b, Section 121.7a). For the simplicity of this model exercise, it was assumed that pervious concrete covers the whole parking lot surface with the exception of a 10% impervious surface fraction. The same Stormwater code calls for a maximum contributing drainage area to the permeable pavement surface area ratio to be 4:1 and at least 90% of the area draining to permeable pavement must be impervious to reduce clogging the pores from particulates in runoff from pervious surfaces (City of NO, 2018b, Section 121.7b). The City of New Orleans specifies that all types of permeable pavement maintain a minimum infiltration rate of 200-inches per hour (City of NO, 2018b, Section 121.7c).

The Minnesota Stormwater Manual provided recommendations for the pervious concrete thickness. A 5-inch thickness for the parking lot's surface layer was specified in the SWMM LID controls. This thickness would need to be reevaluated for heavier vehicle size classes.

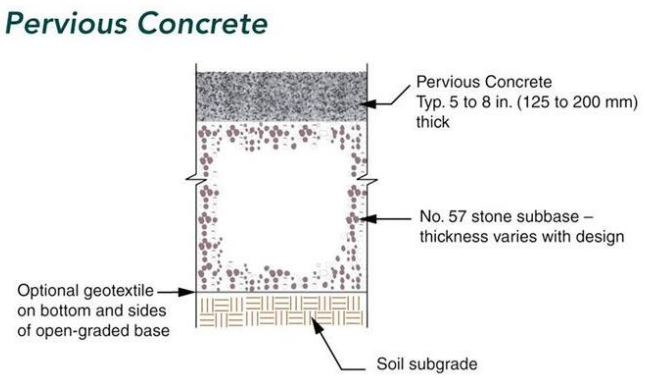

Figure 3.26. Pervious concrete cross section typical design specifications from the Minnesota Stormwater Manual (Minnesota Pollution Control Agency, 2012).

The StormTech SC-160P Chamber subsurface arch chamber was selected to add a substantial amount of storage and infiltration below each parking lot. This chamber was developed for shallow cover applications. The arch itself is only 12-inches tall and 25-inches wide. Each chamber is 85.4-inches long. Each chamber has the storage capacity of 6.85 ft3, creating 15-ft3 of storage after installation when accounting for the storage capacity of the surrounding aggregate in the same footprint (ADS, 2021). In this design, the chambers are installed toe-to-toe to optimize storage capacity, as shown in the ADS design manual specifications below.

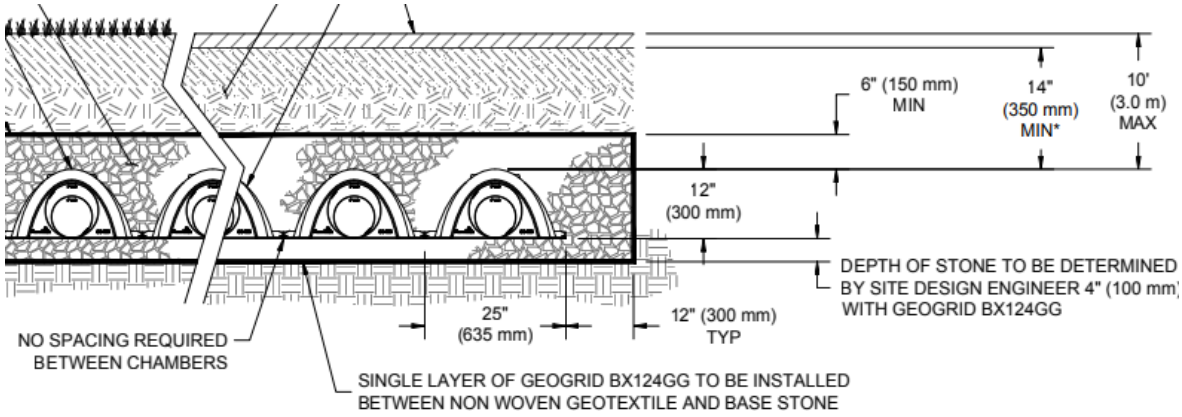

Figure 3.27. StormTech SC-160P detention chamber design specifications (ADS, 2021).

Per the ADS StormTech SC-160LP detention chamber design specifications (ADS, 2021), #57 crushed limestone was specified as the aggregate, which typically has 40% void space. The space inside the arch and in the underdrain are 100% void space. The underdrain is placed 28-inches from the bottom of the aggregate (on-center) and the ADS-specified 14-inch aggregate between the top of the arch and the bottom of the pervious pavement.

The following figure illustrates the proposed pervious concrete design cross section and a photograph of the StormTech SC-160LP retention chamber.

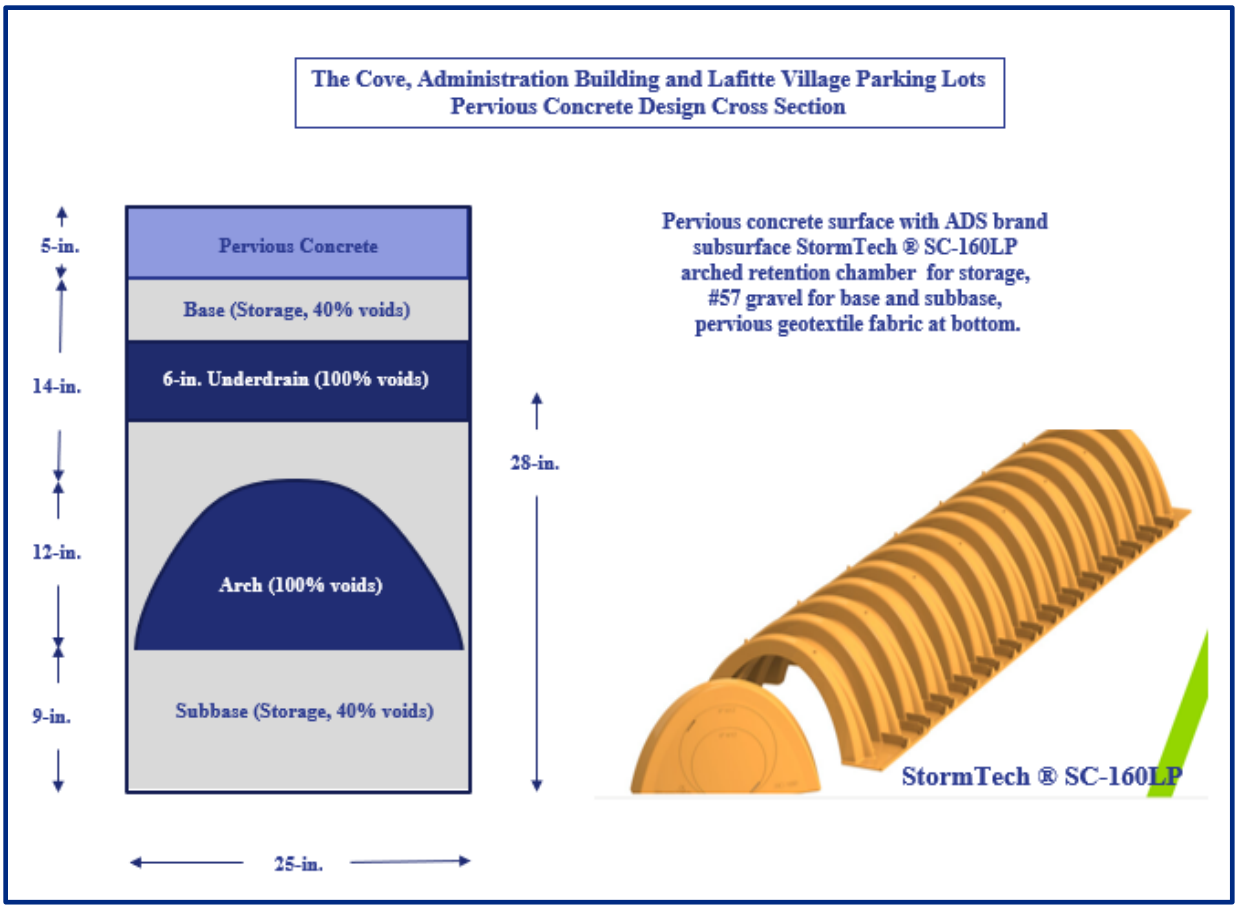

Figure 3.28. Pervious pavement design and StormTech SC-160LP detention arches.

3.5.2.3 LID Controls—Permeable Pavement

The following table summarizes the permeable pavement attributes entered in the SWMM.

Table 3.13. Permeable pavement attributes entered in the SWMM LID Control Editor.

Permeable Pavement			
Layer	**Parameter**	**Value**	**Notes**
Surface	Berm Height (in)	0	
	Vegetation Volume (fraction)	0	
	Surface Roughness (Manning's n)*	0.011	
	Surface Slope (%)	2	
Pavement	Thickness (in)	5	5" per Minnesota Stormwater Manual's Pervious Concrete Specifications
	Void Ratio (voids/solids)	0.33	e=Vv/Vs; 15-25% voids typical for pervious concrete
	Impervious Surface (fraction)	0.1	Assume 10% impervious surface for pavement borders
	Permeability (in/hr)	288	Pervious Pavement Engineering Properties
	Clogging Factor	0	Assume no clogging
	Regeneration Interval (days)	0	Assume 0, feature disabled
	Regeneration Fraction	0	Assume 0, feature disabled
Soil	Thickness (in)	0	
	Porosity (volume fraction)	na	Retained default values; n=Vv/Vtot
	Field Capacity (volume fraction)	na	Retained default values
	Wilting Point (volume fraction)	na	Retained default values
	Conductivity (in/hr)	na	Retained default values
	Conductivity slope	na	Retained default values
	Suction head (in)	na	Retained default values
Storage	Thickness (in)	35	
	Void ratio (voids/solids)	0.9	Subsurface retention chambers add substantial void space. Calculated in a unit width cross section.
	Seepage Rate (in/hr)	0.14	Assuming soil type D; typically be the Saturated Hydraulic Conductivity of the surrounding subcatchment; per USDA Hydrologic Soil Groups
	Clogging Factor	0	Assume no clogging
Underdrain	Drain Coefficient (in/hr)	35	Based on CHI's example scenario and equation
	Drain Exponent	0.6	Typical value used (SWMM)
	Drain Offset Height (in)	28	Assume underdrain is 12 in from the bottom of the storage unit
	Open Level (in)	0	Assume this feature is disabled
	Closed Level (in)	0	Assume this feature is disabled
	Control Curve		Left blank, not applicable

3.5.3 Bioretention Cell for Lafitte Village Parking Lot

3.5.3.1 Baseline vs LID Scenario—Bioretention Cell

In the Baseline scenario, the Lafitte Village parking lot is an impervious asphalt surface with no subsurface storage. The LID scenario contains a large bioretention cell designed to capture sheet flow from the parking lot and provide storage and infiltration. The subcatchment outlets were changed from drainage system junctions to adjacent subcatchments. Several junctions and conduits in the LID scenario were deleted.

The following figure shows the bioretention cell area (in yellow) located on the south side of the Lafitte Village parking lot.

Figure 3.29. Bioretention cell footprint on the Lafitte Village parking lot.

3.5.3.2 Design—Bioretention Cell

The bioretention cell covers the full parking lot length, east-to-west. The bioretention cell has a width ranging from approximately 80-feet to 108-feet, north-to-south.

A shallow 12-inch depression was specified at the surface layer to capture runoff and allow it time to soak through the soil layer. The berm height closest to Leon C Simon Drive is 4-inches lower than the Lafitte Village parking lot side, creating an overflow outlet for runoff. In the design cross section below, a 4-inch underdrain is positioned 7-inches (on center) from the bottom of the unit, centered in a #57 size crushed aggregate storage layer.

The bioretention cell design features dense native Bald Cypress tree plantings with a diverse native shrub understory. The engineered soil is 48-inch thick to allow a moderate amount of space for the cypress tree roots. The total depth of this bioretention cell unit is 74-inches, as shown in the bioretention cell cross section below.

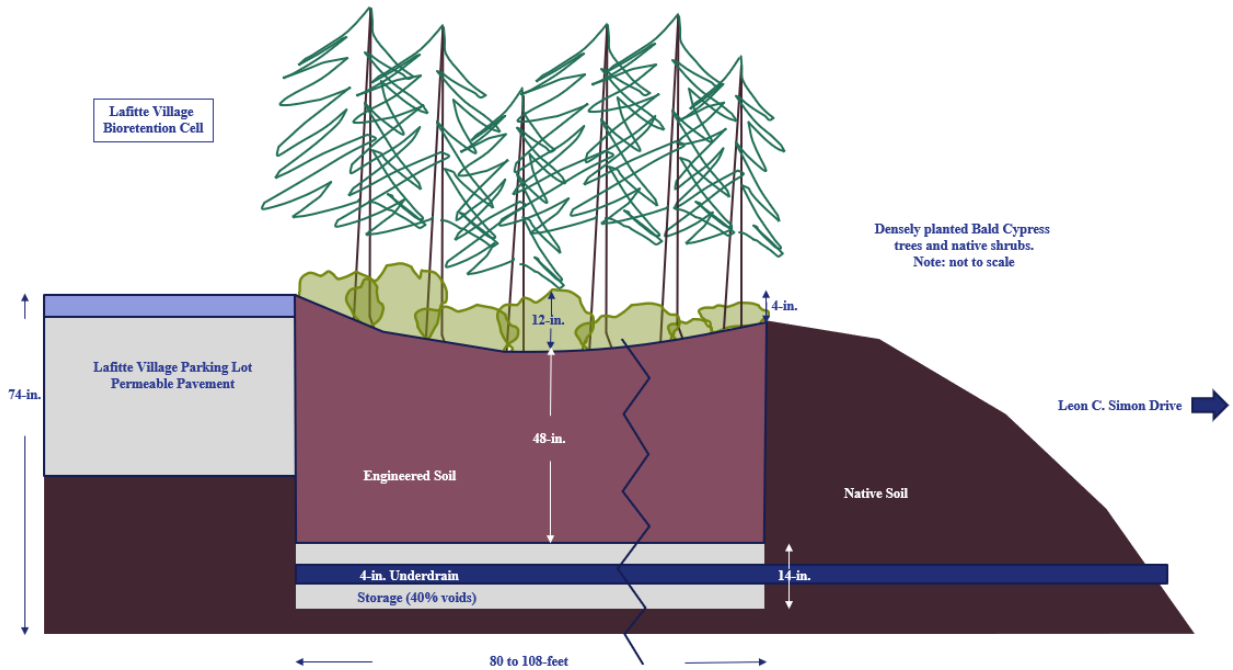

Figure 3.30. Bioretention cell design for the Lafitte Village parking lot.

3.5.3.3 LID Controls—Bioretention Cell

The following table summarizes the attributes entered in the SWMM LID Control Editor for the Lafitte Village parking lot bioretention cell.

Table 3.14. Bioretention Cell attributes entered in the SWMM LID Control Editor.

Bioretention Cell			
Layer	**Parameter**	**Value**	**Notes**
Surface	Berm Height (in)	12	
	Vegetation Volume (fraction)	0.2	
	Surface Roughness (Manning's n)*	0.8	
	Surface Slope (%)	2	
Soil	Thickness (in)	48	
	Porosity (volume fraction)	0.471	n=Vv/Vtot; NRCS
	Field Capacity (volume fraction)	0.342	From NRCS Literature
	Wilting Point (volume fraction)	0.210	From NRCS Literature
	Conductivity (in/hr)	0.04	From NRCS Literature
	Conductivity slope	15	Per CHI's slope of the curve of log(conductivity) versus soil moisture content (dimensionless). Typical values range from 5 for sands to 15 for silty clay.
	Suction head (in)	10.63	
Storage	Thickness (in)	14	
	Void ratio (voids/solids)	0.4	Typical #57 size aggregate void ratio
	Seepage Rate (in/hr)	0.14	Assuming soil type D; typically be the Saturated Hydraulic Conductivity of the surrounding subcatchment; per USDA Hydrologic Soil Groups
	Clogging Factor	0	Assume no clogging
Underdrain	Drain Coefficient (in/hr)	35	Based on CHI's example scenario and equation
	Drain Exponent	0.6	Typical value used (SWMM)
	Drain Offset Height (in)	7	Assume underdrain is 7 in from the bottom of the cell
	Open Level (in)	0	Assume this feature is disabled
	Closed Level (in)	0	Assume this feature is disabled
	Control Curve		Left blank because not applicable

3.6 Statistical Analysis Methods

3.6.1 Hypotheses

To evaluate the effectiveness of LID features on campus, seven null hypotheses paired with seven alternative hypotheses were created, summarized on the following pages. These hypotheses were evaluated with the paired t-test statistic.

Intuitively, for nodes J504 for the Cove Permeable Pavement, J34 for the Admin Building Permeable Pavement, and J47 for the Lafitte Village Permeable Pavement and Bioretention Cell, it was hypothesized that there will be a significant reduced Peak Flow, significant reduced Mean Total Inflow, and significant reduced Total Inflow Volume in through the nodes of interest after adding LID due to the increased infiltration and storage. These alternative hypotheses correlate to the hypotheses on the table Ha4, Ha5, and Ha6, respectively.

Conversely, at these same nodes (J504, J34, and J47), the paired null hypotheses would be that there is no significant reduction in Peak Flow, no significant reduction in Mean Total Inflow, and no significant reduction in Total Inflow Volume after adding LID. These null hypotheses correlate to the hypotheses on the table H04, H05, and H06, respectively.

It was hypothesized that node OF1 for Dean's Ditch will experience an opposite result because more water is diverted into Dean's Ditch after adding the Cove LID and after re-grading the Cove parking lot towards Dean's Ditch. It was hypothesized that there will be a significant increase in Peak Flow, increase in Total Mean Inflow, and increase in Total Volume Inflow at node OF1 after adding LID and redirecting runoff into Dean's Ditch. These alternative hypotheses correlate to the hypotheses on the table Ha1, Ha2, and Ha3, respectively.

Conversely, at node OF1, the paired null hypotheses would be that there is no significant increase in Peak Flow, no significant increase in Mean Total Inflow, and no significant increase in Total Inflow Volume. These null hypotheses correlate to the hypotheses on the table H01, H02, and H03, respectively.

For Time to Peak, it was hypothesized that at all four nodes (OF1, J504, J34 and J47), there will be a significant delay in time to peak, because a large volume of storage is added through the LID features; this is alternative hypothesis Ha7. Conversely, the null hypothesis at all nodes of interest is that there is no significant delay in Time to Peak; this is null hypothesis H07.

On the tables, $\mu 1$ is the Baseline mean and $\mu 2$ is the LID mean of the four design storm results. The mean paired difference is the Baseline mean minus the paired LID mean to compare "before" vs "after" adding LID: $\mu d = \mu 1 - \mu 2$.

The exception for this nomenclature is for the Time to Peak hypotheses where the assigned $\mu 1$ and $\mu 2$ are reversed. For the Time to Peak hypotheses, $\mu 1$ is the LID mean and $\mu 2$ represents the Baseline mean.

Table 3.15a. Hypotheses applied at node OF1 Dean's Ditch for each experimental parameter.

Nodes	LID Feature	Parameters	Hypotheses	Baseline (μ1) vs LID (μ2) Means	Mean Paired Difference		Hypo-thesis ID
OF1	Dean's Ditch	Peak Flow, Qp (cfs)	Null Hypothesis, H0		μd ≥ 0	"There is no significant increase in Peak Flow after redirecting runoff into Dean's Ditch and adding LID"	H01
			Alternative Hypothesis, Ha	μ1 < μ2	μd < 0	"There is a signficant increase in Peak Flow after redirecting runoff into Dean's Ditch and adding LID"	Ha1
		Mean Total Inflow, Qmean (cfs)	Null Hypothesis, H0		μd ≥ 0	"There is no significant increase in Mean Total Inflow after redirecting runoff into Dean's Ditch and adding LID"	H02
			Alternative Hypothesis, Ha	μ1 < μ2	μd < 0	"There is a significant increase in Mean Total Inflow after redirecting runoff into Dean's Ditch and adding LID"	Ha2
		Total Inflow Volume, V (ft3)	Null Hypothesis, H0		μd ≥ 0	"There is no significant increase in Total Inflow Volume after redirecting runoff into Dean's Ditch and adding LID"	H03
			Alternative Hypothesis, Ha	μ1 < μ2	μd < 0	"There is a significant increase in Total Inflow Volume after redirecting runoff into Dean's Ditch and adding LID"	Ha3

Table 3.15b. Hypotheses applied at each node of interest for each experimental parameter.

Nodes	LID Feature	Parameters	Hypotheses	Baseline (μ1) vs LID (μ2) Means	Mean Paired Difference		Hypo-thesis ID
J504	Cove Permeable Pavement	Peak Flow, Qp (cfs)	Null Hypothesis, H0		μd ≤ 0	"There is no significant reduction in Peak Flow after adding LID"	H04
			Alternative Hypothesis, Ha	μ1 > μ2	μd > 0	"There is signficant reduction in Peak Flow after adding LID"	Ha4
J34	Admin Building Permeable Pavement	Mean Total Inflow, Qmean (cfs)	Null Hypothesis, H0		μd ≤ 0	"There is no significant reduction in Total Inflow after adding LID"	H05
			Alternative Hypothesis, Ha	μ1 > μ2	μd > 0	"There is signficant reduction in Total Inflow after adding LID"	Ha5
J47	Lafitte Vlillage Permeable Pavement and Bioretention Cell	Total Inflow Volume, V (ft3)	Null Hypothesis, H0		μd ≤ 0	"There is no significant reduction in Total Inflow Volume after adding LID"	H06
			Alternative Hypothesis, Ha	μ1 > μ2	μd > 0	"There is signficant reduction in Total Inflow Volume after adding LID"	Ha6
OF1	All Nodes	Time to Peak, Tp (Hrs:mins)	Null Hypothesis, H0		μd ≤ 0	"There is no significant delay in Time to Peak"	H07
J504			Alternative Hypothesis, Ha	μ1 < μ2*	μd > 0	"There is a significant delay in Time to Peak"	Ha7
J34							
J47			*Here μ1 represents the LID, μ2 represents Baseline				

3.6.2 Percent Runoff Reduction

To evaluate the percent runoff reduction for each paired Baseline and LID scenario parameter, the following equation was used:

$$R(\%) = \frac{QLID - QBaseline}{QBaseline} \times 100\%,$$

where R is the reduction rate, $Q_{Baseline}$ is the modeled parameter before adding LID, such as Peak Flow in cfs, Mean Total Inflow in cfs, or Total Inflow Volume in ft3. Q_{LID} is the paired modeled parameter after adding LID.

3.6.3 Precision and Uncertainty

Several analyses were used to describe uncertainty among 1) the Baseline results for the four design storms, 2) the LID results for the four design storms, and 3) the paired differences between the Baseline and LID results for the four design storms.

The sample mean, $\bar{y}$ is calculated by adding the numerical values (y1,y2,y3..yi) of each analysis and dividing by the sum of measurements used, n. The experimental mean, $\bar{y}$ is the best estimate of the true mean, μ.

$$\bar{y} = \frac{\Sigma yi}{n}$$

The standard deviation evaluates the distribution of values about its mean. A higher standard deviation indicates a greater level of data dispersion about the mean. The numerator represents the deviation from the mean; the denominator represents the degrees of freedom, df=n-1. The sample standard deviation, Sy, is an estimate of the true standard deviation, σ:

$$Sy = \sqrt{\frac{\sum_{i=1}^{n}(yi - \bar{y})^2}{(n-1)}}$$

The coefficient of variation, CV, evaluates the relative standard deviation by dividing the standard deviation by the mean. A higher the coefficient of variation, indicates a greater level of data dispersion about the mean. The coefficient of variation in analyses here is expressed as a percent. Assuming $\bar{y}$ =μ and Sy=σ:

$$CV = \frac{\sigma}{\mu} \times 100\%$$

Confidence limits for the mean are the interval estimate around an experimental mean, $\bar{y}$, within which the true result is likely to lie within a stated probability (Rincon, 2018). A confidence interval generates a lower and upper limit for the mean, indicating the level of uncertainty for the estimate of the true mean. The narrower the interval, the more precise the estimate. The confidence limit, CL, is expressed as the experimental mean, $\bar{y}$, plus or minus the critical t value, ta, times the sample standard deviation, Sy, divided by the square root of the sum of measurements used, n. The critical t value, ta, is the value on a one-tailed normal distribution which determines if the null hypotheses is accepted or rejected. Ta was selected from statistical tables. Analyses performed here use a 95% confidence interval: thus, a=0.05 and ta=2.353.

$$CL = \bar{y} \pm ta \times \frac{Sy}{\sqrt{n}}$$

The margin of error describes the amount of random variation underlying the experimental results. For a 95% confidence level, the "true" results would fall within the margin of error 95% of the time. The higher the margin of error, the more likely the experimental results differ from the "true" values. The margin of sampling error is the latter portion of the confidence limit expression:

$$Margin\ of\ Error = ta \times \frac{Sy}{\sqrt{n}}$$

3.6.4 Paired T-Test

Paired t-tests compare the means of two populations by using a paired sample. In this experiment, at each of the four nodes, the Baseline Scenario mean results generated from the four design storms are compared to the LID Scenario mean results generated from the four design storms. Thus, the paired t-test analysis evaluates the "before" versus "after" adding LID at each node and can determine if the LID significantly impacted the experimental parameters.

The mean of the paired differences equals the difference between the two population means, represented as:

$$\mu d = \mu 1 - \mu 2$$

where μd is the mean of the paired differences, d is the paired difference variable, μ1 is the mean of the Baseline Scenario (before) sample results averaged over the four design storms at the node of interest, and μ2 is the mean of the LID Scenario (after) sample results, also averaged over the four design storms at the node of interest.

Assuming the paired difference variable, d, is normally distributed, then for paired samples of size n, the degree of freedom, df=n-1, the calculated test statistic value, tc, is:

$$tc = \frac{\overline{d} - \mu d}{Sd/\sqrt{n}}$$

where tc is the calculated test statistic value, $\overline{d}$ is the mean of the paired differences, Sd is the standard deviation of the paired difference variable from the four design storms at the node of interest, and n is the sample size.

Because the null hypotheses, H0, includes the hypothesis that the mean results will not change after adding LID, it is hypothesized that μ1 = μ2, thereby making μd=0. Therefore, the calculated test statistic equation can be rewritten as:

$$tc = \frac{\overline{d}}{Sd/\sqrt{n}}$$

The mean of the paired differences at the node of interest for the four design storms is the calculated as:

$$\bar{d} = \frac{\Sigma di}{n}$$

The standard deviation of the paired differences at the node of interest for the four design storms is:

$$Sd = \sqrt{\frac{\Sigma di^2 - (\Sigma di)^2/n}{n-1}}$$

Paired t-tests assume a normal distribution. The critical t-value, ta, separates the "accept" versus "reject" regions of the null hypothesis, H0, under the curve. In the analysis, the calculated test statistic value, tc, is compared to the critical t-value, ta, as shown in the following figure.

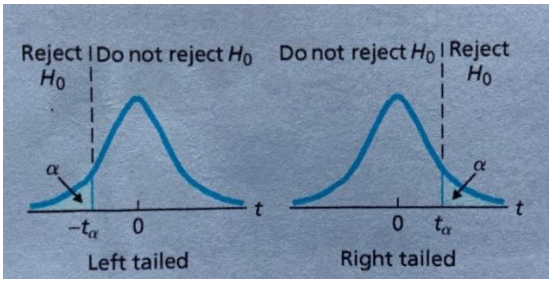

Figure 3.31. Paired t-test one-tailed normal distributions.

If the value of the test statistic, tc, falls within the rejection region of the normal distribution curve, the null hypothesis, H0, is rejected. Otherwise, the null hypothesis is not rejected (Weiss, 2016).

3.6.5 Nash-Sutcliffe Efficiency Coefficient

The Nash-Sutcliffe efficiency (NSE) is a normalized statistic that compares the relative magnitude of the residual variance, or "noise", to the measured data variance, or "signal".

While the NSE analyses is not a statistically rigorous assessment, it is useful to compare the shapes of two Total Inflow time series curves. This makes NSE a good complementary analysis to the Paired t-Test. Challenges with the NSE analysis include that the NSE thresholds are subjective and the NSE analysis is sensitive to extreme values and, as a result, weighs towards peak flows.

NSE is typically used to describe how well the plot of observed data matches modeled data and is widely used to calibrate hydrological models. The NSE is commonly represented by the equation:

$$NSE = 1 - \frac{\sum_{i=1}^{n}(Qi\ obs - Qi\ mod)^2}{\sum_{i=1}^{n}(Qi\ obs - \overline{Qi}\ obs)^2}$$

where Qi_{obs} represents the observed data, $\overline{Qi}_{obs}$ represents the mean of the observed data, and Qi mod represents the modeled data, and n is the total number of observations (Nash, 1970).

Nash-Sutcliffe efficiency values range from negative infinity to one (1). NSE=1 represents a perfect match of modeled data to observed data. NSE=0 indicates that the model predictions are as accurate as the mean of the observed data because the model estimation of error variance (numerator) matches the variance of the observed time series (denominator). NSE<0 indicates that the observed mean is a better predictor than the model because the estimation error variance (numerator) is much larger than the variance of observations.

For the purposes of this thesis, the NSE equation was adapted to evaluate the similarity of the shapes of the Baseline and the LID Total Inflow (cfs) time series curves at each node for a single design storm. Observed data for this model is not available; rather, the modeled results from two different scenarios will be compared: "before" versus "after" adding LID. Therefore, the NSE equation's observed

data is substituted with the Baseline data, and the NSE equation's modeled data is substituted with theLID data. The adapted NSE equation for this experiment is:

$$NSE = 1 - \frac{\Sigma(Qi\ Baseline - Qi\ LID)^2}{(Qi\ Baseline - \overline{Qi}\ Baseline)^2}$$

where $Qi_{Baseline}$ represents the Baseline Total Inflow data (cfs), $\overline{Qi}_{\ Baseline}$ represents the mean Baseline Total Inflow data (cfs), and Qi_{LID} represents the LID Total Inflow data (cfs).

In this case, NSE=1 represents a perfect match of the Baseline data to the LID data time series curves, indicating that there is no significant difference to the shape Total Inflow curves before versus after adding the LID. NSE=0 and NSE <1 indicate that there is a statistically insignificant correlation between the Baseline and LID curve shapes.

4. RESULTS AND DISCUSSION

4.1 Continuity Errors

The Baseline Scenario and LID Scenario models were each run for the four 10-year, 24-hour design storms over a simulation period of 24-hours, dated June 18, 4:54 am 2021to June 19th, 5:00 am 2021 in the model. SWMM reported runoff quantity continuity percent errors and flow routing continuity percent errors as less than one (<1) in all cases, indicating successful model runs.

Table 4.1. SWMM model runoff quantity and flow routing continuity of errors for each model run.

	Percent Error (%)							
	DS1_8.26 in		DS2_8.24in		DS3_8.32in		DS4_8.35in	
Scenario:	**Baseline**	**LID**	**Baseline**	**LID**	**Baseline**	**LID**	**Baseline**	**LID**
Runoff Quantity Continuity:	-0.055	-0.071	-0.055	-0.07	-0.058	-0.076	-0.055	-0.074
Flow Routing Continuity:	-0.003	-0.003	-0.003	-0.003	-0.003	-0.003	-0.003	-0.003

Results for the four nodes of interest are organized in order of increasing complexity below.

4.2 Results

4.2.1 Node J34 Results – Administration Building Parking Lot Permeable Pavement

Node J34, the Administration Building parking lot permeable pavement is designed with pervious concrete with subsurface arches to create substantial storage volume for runoff. Node J34 offers the simplest LID effectiveness evaluation because the LID is wholly contained in one subcatchment (S77) and because there are only two subcatchments (S77 and S88) upstream of node J34, allowing for simpler "before" and "after" adding LID interpretations.

4.2.1.1 Hydrographs at Node J34

Baseline and LID scenario hydrographs below show the rate of flow over the 24-hour simulation period at node J34. Paired hyetographs show the distribution of the design storm rainfall intensity over time. The hydrographs and hyetographs below share a common Date/Time x-axis displayed as 3:00am on

day 1 to 3:00 am on day 2. The hydrograph y-axis is Total Inflow (cfs); the design storm hyetographs above show rainfall (in/hr).

Peak flow for all four design storms, for both the Baseline and LID scenarios, occurred at 12:05pm at node J34, as shown in the hydrographs below.

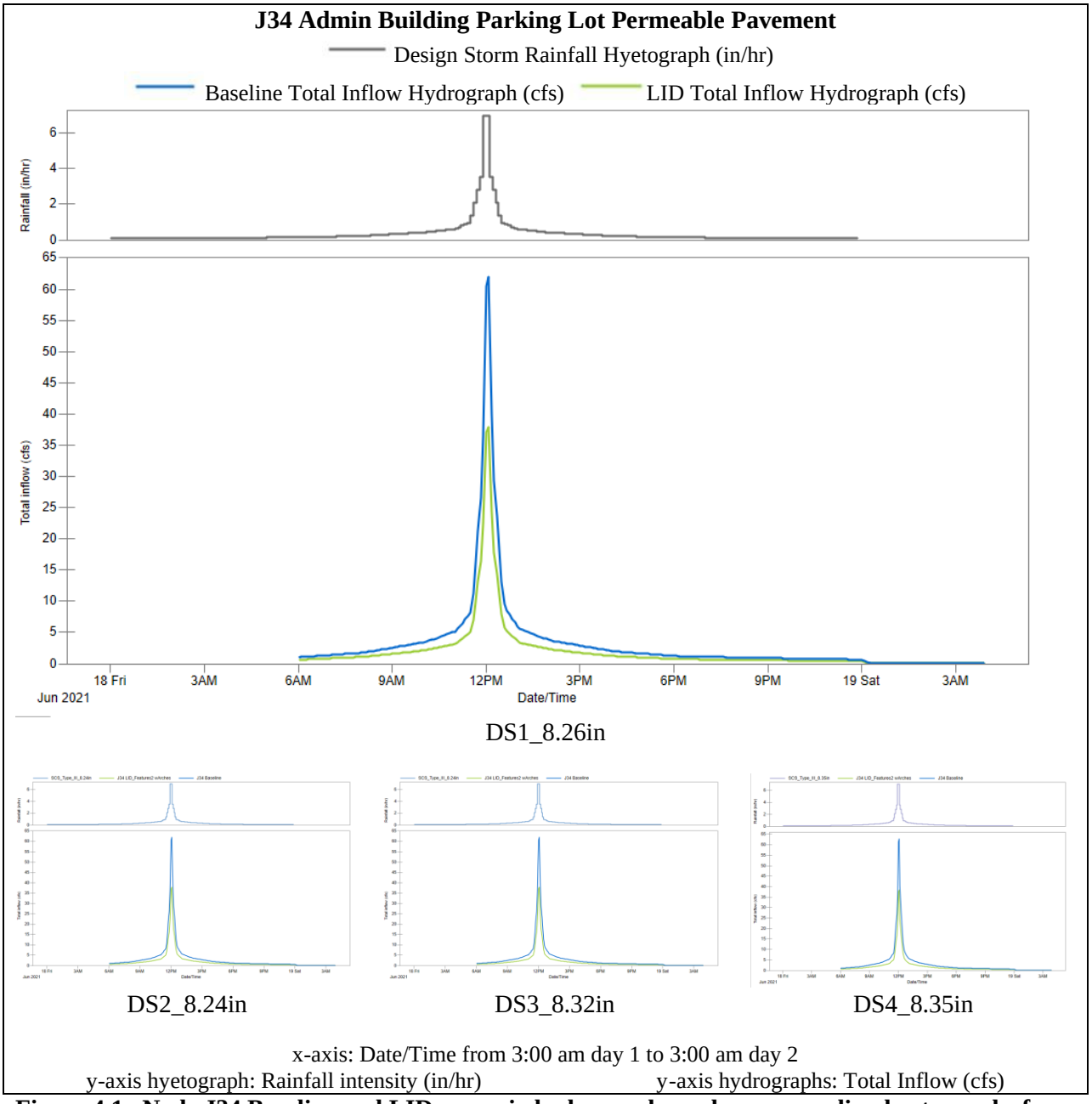

Figure 4.1. Node J34 Baseline and LID scenario hydrographs and corresponding hyetographs for four 10-year, 24-hour design storms based on four different design depths.

4.2.1.2 Peak Flow, Mean Total Inflow, and Total Inflow Volume Results at Node J34

Baseline and LID scenario SWMM results for Peak Flow, Qp, in cubic feet per second, Mean Total Inflow, Qmean, in cubic feet per second, Total Inflow Volume, V, in feet cubed, and the Time of Peak are shown in the table below. Flow parameter results produced the following ranges:

- The Peak Flows ranged between 62.05 cfs and 62.89 cfs for the Baseline and ranged between 37.97 cfs and 38.49 cfs for the LID.
- The Mean Total Inflows ranged between 3.134 cfs and 3.169 cfs for the Baseline and ranged between 1.916 cfs and 1.942 for the LID.
- The Total Inflow Volumes ranged between 246600 ft3 and 250000 ft3 for the Baseline and ranged between 151000 ft3 and 153200 ft3 for the LID.

Table 4.2. SWMM model results for node J34, for the four 10-year, 24-hour design storms.

Node	LID Feature	Design Storm	Parameter	Baseline	LID
J34	Admin Building Parking Lot Permeable Pavement	DS1_8.26in	Maximum Total Inflow (Peak Flow), Qp (cfs)	62.20	38.06
			Mean Total Inflow, Qmean (cfs)	3.134	1.920
			Total Inflow Volume, V (ft3)	247300	151500
			Time of Peak (Hrs:mins)	12:05 PM	12:05 PM
		DS2_8.24in	Maximum Total Inflow (Peak Flow), Qp (cfs)	62.05	37.97
			Mean Total Inflow, Qmean (cfs)	3.126	1.916
			Total Inflow Volume, V (ft3)	246600	151100
			Time of Peak (Hrs:mins)	12:05 PM	12:05 PM
		DS3_8.32in	Maximum Total Inflow (Peak Flow), Qp (cfs)	62.66	38.35
			Mean Total Inflow, Qmean (cfs)	3.157	1.935
			Total Inflow Volume, V (ft3)	249100	152600
			Time of Peak (Hrs:mins)	12:05 PM	12:05 PM
		DS4_8.35in	Maximum Total Inflow (Peak Flow), Qp (cfs)	62.89	38.49
			Mean Total Inflow, Qmean (cfs)	3.169	1.942
			Total Inflow Volume, V (ft3)	250000	153200
			Time of Peak (Hrs:mins)	12:05 PM	12:05 PM

4.2.2 Node J504 Results – Cove Parking Lot Permeable Pavement

In the Baseline "before" scenario, the Cove parking lot is impervious and drains towards Founder's Road and then through node J504.

In the LID "after" scenario, the Cove parking lot is reconstructed using pervious concrete and subsurface arches to create a pervious surface with substantial storage volume for runoff. The Cove parking lot is also re-graded to drain towards Dean's Ditch. These modifications redirect runoff away from the Founder's Road and towards Dean's Ditch, thus diverting water away from node J504.

4.2.2.1 Hydrographs at Node J504

Baseline and LID scenario hydrographs below show the rate of flow over the 24-hour simulation period at node J504. Peak flow for all four design storms, for both the Baseline and LID scenarios, occurred at 12:05pm at node J504, as shown in the hydrographs below. This is the same time to peak as node J34 Baseline and LID scenarios.

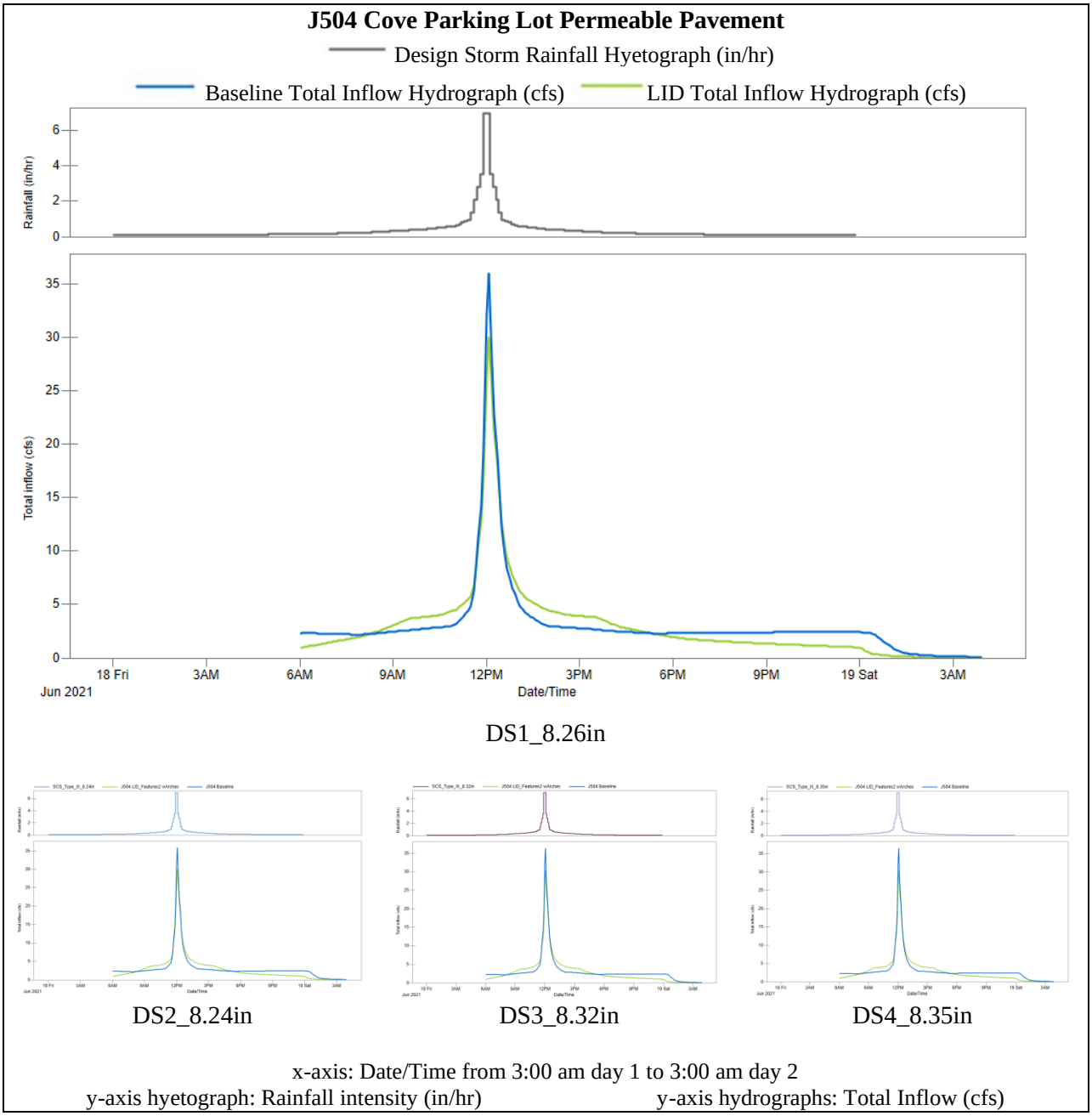

Figure 4.2. Node J504 Baseline and LID scenario hydrographs and corresponding hyetographs for four 10-year, 24-hour design storms based on four different design depths.

4.2.2.2 Peak Flow, Mean Total Inflow, and Total Inflow Volume Results at Node J504

Baseline and LID scenario SWMM results for Peak Flow, Qp, Mean Total Inflow, Qmean, Total Inflow Volume, V, and the Time of Peak are shown in the table below. Flow parameter results produced the following ranges:

- The Peak Flows ranged between 35.91 cfs and 36.48 cfs for the Baseline and ranged between 29.95 cfs and 30.40 cfs for the LID.
- The Mean Total Inflows ranged between 3.087 cfs and 3.109 cfs for the Baseline and ranged between 2.902 cfs and 2.929 for the LID.
- The Total Inflow Volumes ranged between 243600 ft3 and 245300 ft3 for the Baseline and ranged between 228300 ft3 and 231100 ft3 for the LID.

Table 4.3. SWMM model results for node J34, for the four 10-year, 24-hour design storms.

Node	LID Feature	Design Storm	Parameter	Baseline	LID
J504	Cove Parking Lot Permeable Pavement	DS1_8.26in	Maximum Total Inflow (Peak Flow), Qp (cfs)	36.01	30.03
			Mean Total Inflow, Qmean (cfs)	3.091	2.902
			Total Inflow Volume, V (ft3)	243900	228900
			Time of Peak (Hrs:mins)	12:05 PM	12:05 PM
		DS2_8.24in	Maximum Total Inflow (Peak Flow), Qp (cfs)	35.91	29.95
			Mean Total Inflow, Qmean (cfs)	3.087	2.896
			Total Inflow Volume, V (ft3)	243600	228300
			Time of Peak (Hrs:mins)	12:05 PM	12:05 PM
		DS3_8.32in	Maximum Total Inflow (Peak Flow), Qp (cfs)	36.32	30.28
			Mean Total Inflow, Qmean (cfs)	3.103	2.920
			Total Inflow Volume, V (ft3)	244800	230400
			Time of Peak (Hrs:mins)	12:05 PM	12:05 PM
		DS4_8.35in	Maximum Total Inflow (Peak Flow), Qp (cfs)	36.48	30.40
			Mean Total Inflow, Qmean (cfs)	3.109	2.929
			Total Inflow Volume, V (ft3)	245300	231100
			Time of Peak (Hrs:mins)	12:05 PM	12:05 PM

4.2.3 Node OF1 Results– Dean's Ditch Vegetated Swale

In the Baseline "before" scenario, Dean's Ditch was represented by an open channel conduit with trapezoidal geometry split into two separate reaches—the Upper Reach, which fed into the Founder's Road conduit upstream of node J504, and the Lower Reach, which fed into outfall OF1.

In the LID "after" scenario, there were several significant modifications to Dean's Ditch. First, the runoff from the Cove parking lot and several adjacent subcatchments was redirected into Dean's Ditch as overland flow. Second, the Dean's Ditch routing was changed at the northwest corner of the Cove parking lot; rather than flowing into the Founder's Road conduit, the water from the Upper Reach of Dean's Ditch was redirected to flow across subcatchment S13_2 and connect to the Lower Reach then into outfall OF1; this created one long, continuous vegetated swale starting near the northeast corner of Privateer Place and ending at outfall OF1 . Third, rather than representing Dean's Ditch solely by an open conduit with trapezoidal geometry, vegetated swale LID controls were added to every subcatchment that this long vegetated swale passes through.

Overall, this means that more water is routed to node OF1 after adding LID because the Cove parking lot, adjacent subcatchments, and the Upper Reach of Dean's Ditch were re-routed towards node OF1.

4.2.3.1 Hydrographs at Node OF1

Baseline and LID scenario hydrographs below show the rate of flow over the 24-hour simulation period at node OF1. Peak flow for all four design storms, for the Baseline scenario occurred at 12:00 pm. Peak flow for all four LID scenarios was delayed to 12:20pm, as shown in the hydrographs below. These times to peak differ from the J34 and J504 Baseline and LID scenarios.

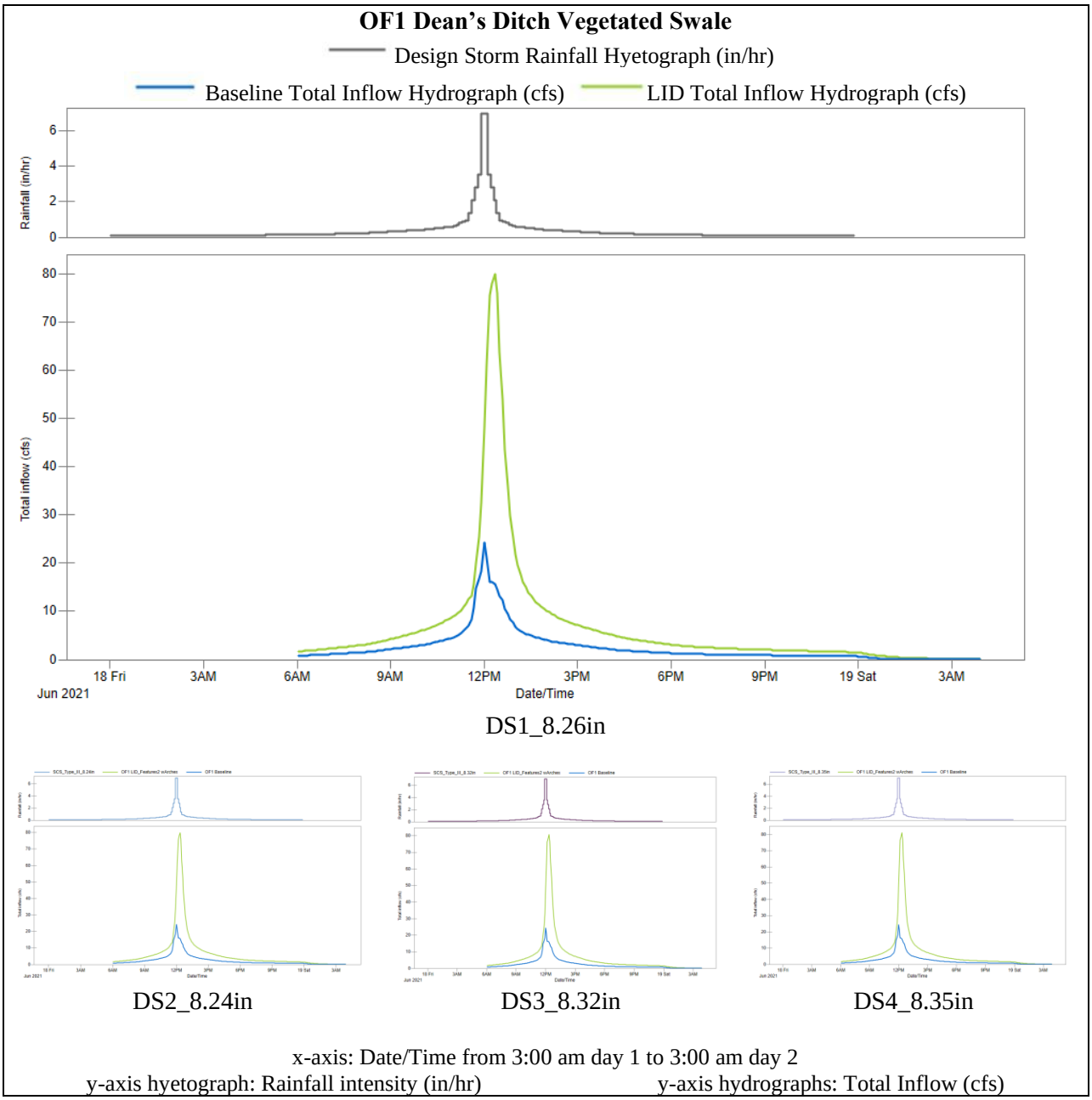

Figure 4.3. Node OF1 Baseline and LID scenario hydrographs and corresponding hyetographs for four 10-year, 24-hour design storms based on four different design depths.

4.2.3.2 Peak Flow, Mean Total Inflow, and Total Inflow Volume Results at Node OF1

Baseline and LID scenario SWMM results for Peak Flow, Qp, Mean Total Inflow, Qmean, Total Inflow Volume, V, and the Time of Peak are shown in the table below. Flow parameter results produced the following ranges:

- The Peak Flows ranged between 24.24 cfs and 24.38 cfs for the Baseline and ranged between 79.94 cfs and 81.16 cfs for the LID.

- The Mean Total Inflows ranged between 2.459 cfs and 2.487 cfs for the Baseline and ranged between 6.510 cfs and 6.600 for the LID.
- The Total Inflow Volumes ranged between 19400 ft3 and 196200 ft3 for the Baseline and ranged between 513600 ft3 and 520700 ft3 for the LID.

Table 4.4. SWMM model results for node OF1, for the four 10-year, 24-hour design storms.

Node	LID Feature	Design Storm	Parameter	Baseline	LID
OF1	Dean's Ditch Vegetated Swale	DS1_8.26in	Maximum Total Inflow (Peak Flow), Qp (cfs)	24.26	80.16
			Mean Total Inflow, Qmean (cfs)	2.464	6.525
			Total Inflow Volume, V (ft3)	194400	514800
			Time of Peak (Hrs:mins)	12:00 PM	12:20 PM
		DS2_8.24in	Maximum Total Inflow (Peak Flow), Qp (cfs)	24.24	79.94
			Mean Total Inflow, Qmean (cfs)	2.459	6.510
			Total Inflow Volume, V (ft3)	194000	513600
			Time of Peak (Hrs:mins)	12:00 PM	12:20 PM
		DS3_8.32in	Maximum Total Inflow (Peak Flow), Qp (cfs)	24.34	80.03
			Mean Total Inflow, Qmean (cfs)	2.479	6.575
			Total Inflow Volume, V (ft3)	195600	518800
			Time of Peak (Hrs:mins)	12:00 PM	12:20 PM
		DS4_8.35in	Maximum Total Inflow (Peak Flow), Qp (cfs)	24.38	81.16
			Mean Total Inflow, Qmean (cfs)	2.487	6.600
			Total Inflow Volume, V (ft3)	196200	520700
			Time of Peak (Hrs:mins)	12:00 PM	12:20 PM

4.2.4 Node J47 Results– Lafitte Village Parking Lot Permeable Pavement and Bioretention Cell

Of the four nodes of interest, node J47 has the most complex upstream modifications and, consequently, most complex results.

In the Baseline "before" scenario, the Lafitte Village parking lot was an impervious surface that drained to the Founder's Road conduit. In the LID "after" scenario, the Lafitte Village Parking Lot became a pervious surface reconstructed as pervious concrete with subsurface arches creating substantial storage volume for runoff and infiltration. A large bioretention cell was also added, creating additional storage volume and infiltration. In theory, much of the runoff that previously routed through node J47 would be stored and infiltrated under this new parking lot and in the bioretention cell, reducing the volume of water from the Lafitte Village parking lot routed through node J47. There are many catchments upstream of node J47, adding further complexity to both the Baseline and LID scenario total inflow results.

4.2.4.1 Hydrographs at Node J47

The Baseline and LID scenario hydrographs below show the rate of flow over the 24-hour simulation period at node OF1. For the Baseline scenarios, Peak Flow occurred at 11:40am for design storms 1 and 3, and at 11:35am for design storms 2 and 4. This is the only node of interest where there are differing times of peak rainfall, in the Baseline scenario run. For the LID scenarios, Peak Flow for all four design storms occurred at 12:45pm.

Node J47 experiences both the earliest and latest peak flow events compared to the other nodes of interest. These times to peak differ from the times to peak at the other nodes of interest, as shown on the hydrograph on the following page.

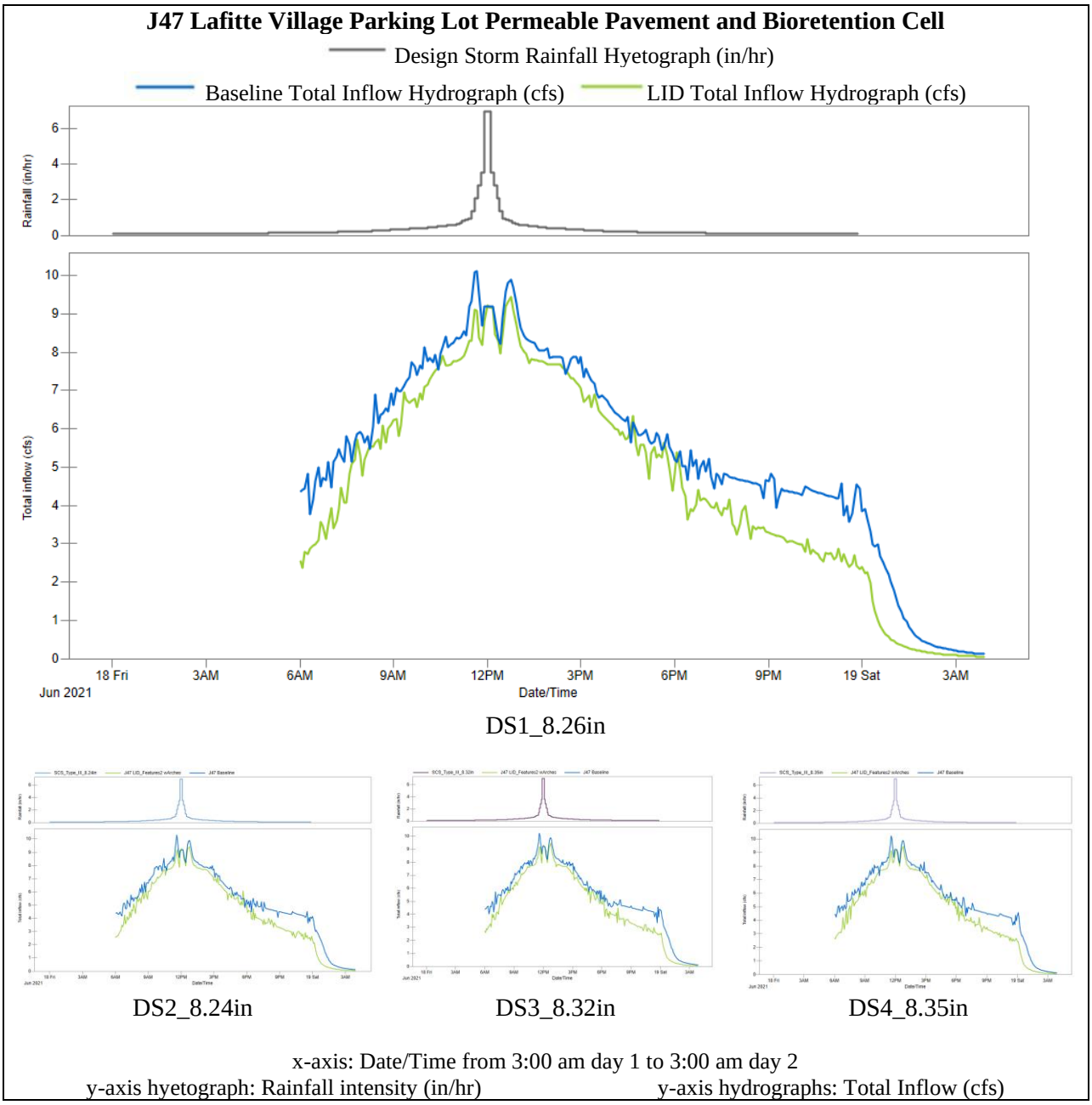

Figure 4.4. Node J47 Baseline and LID scenario hydrographs and corresponding hyetographs for four 10-year, 24-hour design storms based on four different design depths.

4.2.4.2 Peak Flow, Mean Total Inflow, and Total Inflow Volume Results at Node J47

Baseline and LID scenario SWMM results for Peak Flow, Qp, Mean Total Inflow, Qmean, Total Inflow Volume, V, and the Time of Peak are shown in the table below. Flow parameter results produced the following ranges:

- The Peak Flows ranged between 10.11 cfs and 10.28 cfs for the Baseline and ranged between 9.438 cfs and 9.449 cfs for the LID.

- The Mean Total Inflows ranged between 5.299 cfs and 5.354 cfs for the Baseline and ranged between 4.537 cfs and 4.583 for the LID.
- The Total Inflow Volumes ranged between 418100 ft3 and 422400 ft3 for the Baseline and ranged between 357900 ft3 and 361600 ft3 for the LID.

Table 4.5. SWMM model results for node J47, for the four 10-year, 24-hour design storms.

Node	LID Feature	Design Storm	Parameter	Baseline	LID
J47	Lafitte Village Parking Lot Permeable Pavement and Bioretention Cell	DS1_8.26in	Maximum Total Inflow (Peak Flow), Qp (cfs)	10.11	9.449
			Mean Total Inflow, Qmean (cfs)	5.311	4.537
			Total Inflow Volume, V (ft3)	419000	357900
			Time of Peak (Hrs:mins)	11:40 AM	12:45 PM
		DS2_8.24in	Maximum Total Inflow (Peak Flow), Qp (cfs)	10.28	9.438
			Mean Total Inflow, Qmean (cfs)	5.299	4.539
			Total Inflow Volume, V (ft3)	418100	358100
			Time of Peak (Hrs:mins)	11:35 AM	12:45 PM
		DS3_8.32in	Maximum Total Inflow (Peak Flow), Qp (cfs)	10.21	9.449
			Mean Total Inflow, Qmean (cfs)	5.318	4.571
			Total Inflow Volume, V (ft3)	419600	360700
			Time of Peak (Hrs:mins)	11:40 AM	12:45 PM
		DS4_8.35in	Maximum Total Inflow (Peak Flow), Qp (cfs)	10.21	9.447
			Mean Total Inflow, Qmean (cfs)	5.354	4.583
			Total Inflow Volume, V (ft3)	422400	361600
			Time of Peak (Hrs:mins)	11:35 AM	12:45 PM

4.2.5 Time to Peak at All Nodes Results

The Time to Peak, Tp, is the duration of time from the start of the rain event to the Peak Flow. The model began the design storm rain event at 4:54 am on day 1. As shown in the table below, the times to peak at each node of interest ranged between 6 hours 41 minutes and 7 hours 51 minutes.

Table 4.6. Time to Peak calculations at each node for the four design storms with different depths.

			Time to Peak, Tp (hh:mm)	
Node	**LID Feature**	**Design Storm**	**Baseline**	**LID**
OF1	Dean's Ditch Vegetated Swale	DS1_8.26in	7:06	7:26
		DS2_8.24in	7:06	7:26
		DS3_8.32in	7:06	7:26
		DS4_8.35in	7:06	7:26
J504	Cove Parking Lot Permeable Pavement	DS1_8.26in	7:11	7:11
		DS2_8.24in	7:11	7:11
		DS3_8.32in	7:11	7:11
		DS4_8.35in	7:11	7:11
J34	Admin Building Parking Lot Permeable Pavement	DS1_8.26in	7:11	7:11
		DS2_8.24in	7:11	7:11
		DS3_8.32in	7:11	7:11
		DS4_8.35in	7:11	7:11
J47	Lafitte Village Parking Lot Permeable Pavement and Bioretention Cell	DS1_8.26in	6:46	7:51
		DS2_8.24in	6:41	7:51
		DS3_8.32in	6:46	7:51
		DS4_8.35in	6:41	7:51

4.3 Analysis

This experiment evaluated the effectiveness of the LID at reducing Peak Flow, Mean Total Inflow, Total Inflow Volume, and delayed Time to Peak using several statistical analyses for each experimental parameter, at each node. First, statistical analysis evaluated the precision and uncertainty of results generated by the four design storms. Second, the paired t-test statistically determined the effectiveness of the LID and accept or reject the null hypotheses. Third, the Nash-Sutcliffe efficiency coefficient (NSE) analysis evaluated the similarities of the Baseline and LID time series curves to determine if there is a statistically significant difference between them.

4.3.1. Summary of Analysis

All model runs reported low runoff quantity and flow routing continuity errors, indicating successful model runs. Statistical analysis of all trials (all parameters for all design storms) showed low standard deviation, coefficient of variation, and low margin of error values, indicating the results across the four design storms are precise with low uncertainties.

Only two null hypotheses were accepted based on paired t-test analysis: there was not a significantly delayed Time to Peak at either the Cove node J504 or at the Administration Building node J34. All other experimental trials resulted in the acceptance of the alternative hypotheses.

As hypothesized, the Dean's Ditch Vegetated Swale node OF1 experienced an *increase* in Peak Flow, Mean Total Inflow, and Total Inflow Volume after adding LID and rerouting Cove parking lot runoff into Dean's Ditch.

As hypothesized, the Cove node J504, the Administration Building node J34, and the Lafitte Village node J47 experienced a significant *reduction* in Peak Flow, Mean Total Inflow, and Total Inflow Volume after adding the LID features.

As hypothesized, the Dean's Ditch node OF1 and the Lafitte Village node J47 experienced a significant *delay* in Time to Peak. A summary of accepted hypotheses based on paired t-tests is presented in the table on the following page.

Table 4.7. Accepted hypotheses based on paired t-tests.

Node	LID Feature	Parameters	Hypo-thesis ID	Hypotheses Accepted	Baseline (μ1) vs LID (μ2) Means	Mean Paired Difference μd = μ1 - μ2	Statements
OF1	Dean's Ditch	Peak Flow, Qp (cfs)	Ha1	Alternative Hypothesis, Ha	$\mu1 < \mu2$	$\mu d < 0$	"There is a signficant increase in Peak Flow after redirecting runoff into Dean's Ditch and adding LID"
		Mean Total Inflow, Qmean (cfs)	Ha2	Alternative Hypothesis, Ha	$\mu1 < \mu2$	$\mu d < 0$	"There is a significant increase in Mean Total Inflow after redirecting runoff into Dean's Ditch and adding LID"
		Total Inflow Volume, V (ft3)	Ha3	Alternative Hypothesis, Ha	$\mu1 < \mu2$	$\mu d < 0$	"There is a significant increase in Total Inflow Volume after redirecting runoff into Dean's Ditch and adding LID"
		Time to Peak, Tp (Hrs:mins)	Ha7	Alternative Hypothesis, Ha	$\mu1 < \mu2$*	$\mu d > 0$	"There is a significant delay in Time to Peak" *Here μ1 represents the LID, μ2 represents Baseline
J504	Cove Permeable Pavement	Peak Flow, Qp (cfs)	Ha4	Alternative Hypothesis, Ha	$\mu1 > \mu2$	$\mu d > 0$	"There is signficant reduction in Peak Flow after adding LID"
		Mean Total Inflow, Qmean (cfs)	Ha5	Alternative Hypothesis, Ha	$\mu1 > \mu2$	$\mu d > 0$	"There is signficant reduction in Total Inflow after adding LID"
		Total Inflow Volume, V (ft3)	Ha6	Alternative Hypothesis, Ha	$\mu1 > \mu2$	$\mu d > 0$	"There is signficant reduction in Total Inflow Volume after adding LID"
		Time to Peak, Tp (Hrs:mins)	H07	Null Hypothesis, H0		$\mu d \leq 0$	"There is no significant delay in Time to Peak" *Here μ1 represents the LID, μ2 represents Baseline
J34	Admin Building Permeable Pavement	Peak Flow, Qp (cfs)	Ha4	Alternative Hypothesis, Ha	$\mu1 > \mu2$	$\mu d > 0$	"There is signficant reduction in Peak Flow after adding LID"
		Mean Total Inflow, Qmean (cfs)	Ha5	Alternative Hypothesis, Ha	$\mu1 > \mu2$	$\mu d > 0$	"There is signficant reduction in Total Inflow after adding LID"
		Total Inflow Volume, V (ft3)	Ha6	Alternative Hypothesis, Ha	$\mu1 > \mu2$	$\mu d > 0$	"There is signficant reduction in Total Inflow Volume after adding LID"
		Time to Peak, Tp (Hrs:mins)	H07	Null Hypothesis, H0		$\mu d \leq 0$	"There is no significant delay in Time to Peak". *Here μ1 represents the LID, μ2 represents Baseline.
J47	Lafitte Village Permeable Pavement and Bioretention Cell	Peak Flow, Qp (cfs)	Ha4	Alternative Hypothesis, Ha	$\mu1 > \mu2$	$\mu d > 0$	"There is signficant reduction in Peak Flow after adding LID"
		Mean Total Inflow, Qmean (cfs)	Ha5	Alternative Hypothesis, Ha	$\mu1 > \mu2$	$\mu d > 0$	"There is signficant reduction in Total Inflow after adding LID"
		Total Inflow Volume, V (ft3)	Ha6	Alternative Hypothesis, Ha	$\mu1 > \mu2$	$\mu d > 0$	"There is signficant reduction in Total Inflow Volume after adding LID"
		Time to Peak, Tp (Hrs:mins)	Ha7	Alternative Hypothesis, Ha	$\mu1 < \mu2$*	$\mu d > 0$	"There is a significant delay in Time to Peak" *Here μ1 represents the LID, μ2 represents Baseline.

The following bar graphs including margin of error bars illustrate the mean results over the four design storms at each node of interest. The margin of error bars are barely visible because the margin of errors for each design storm model run were so low.

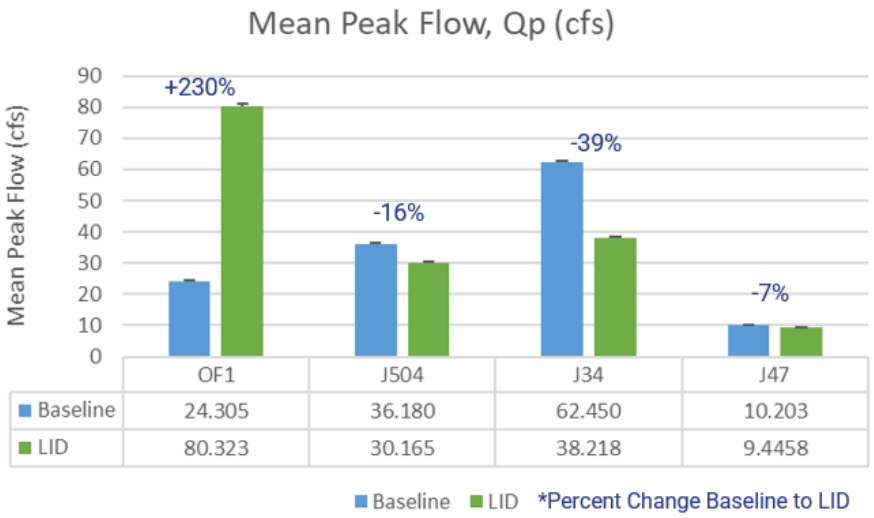

Figure 4.5. Mean Peak Flow results bar graphs for each node with margin of error bars and percent change between the Baseline and LID scenarios.

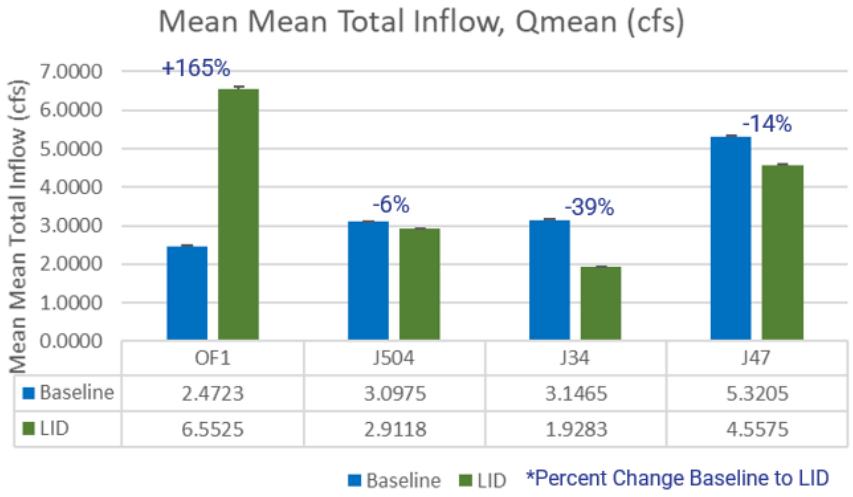

Figure 4.6. Mean Mean Total Inflow results bar graphs for each node with margin of error bars and percent change between the Baseline and LID scenarios.

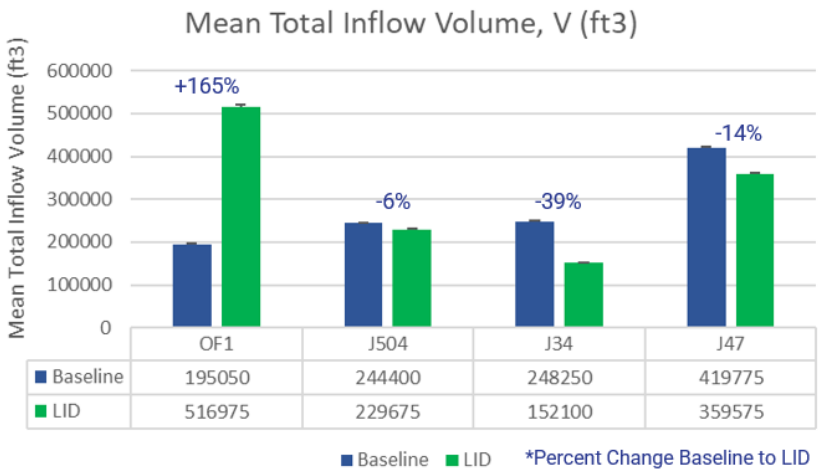

Figure 4.7. Mean Total Inflow Volume results bar graphs for each node with margin of error bars and percent change between the Baseline and LID scenarios.

As the bar graphs illustrate, Dean's Ditch node OF1 shows an *increased* mean Peak Flow (+230%), mean Mean Total Inflow (+165%), and mean Total Inflow Volume (+165%) in the LID scenario because 1) the designed vegetated swale LID system was added, 2) the flow from the Upper Reach of Dean's Ditch was rerouted from the Founder's Road conduits to the Lower Reach of Dean's Ditch, and 3) runoff was rerouted from the Cove parking lot and adjacent subcatchments to Dean's Ditch.

The Cove node J504, the Administration Building node J34, and Lafitte Village node J47 all show *decreased* mean Peak Flow, mean Mean Total Inflow, and mean Total Inflow Volume after adding the LID system, as expected.

The Cove node J504, however, shows only a *slight decrease* in the mean Mean Total Inflow (-6%) and mean Total Inflow Volume (-6%) in the LID scenario compared to the Baseline scenario. A greater decrease in these parameters was anticipated between the two scenarios because 1) the pervious concrete with arched retention chambers added substantial storage and permeability, and 2) the Cove parking runoff was diverted away from node J504. The paired t-test analysis proved even these slight decreases in flow in the LID scenarios to be statistically significant. SWMM results report flooding at node J504 indicating that 62162 ft3 of water may be lost to the system at this node because "no ponding" was specified.

Another odd trend is that while Dean's Ditch node OF1 shows a substantial *increase* in the mean Peak Flow (+230%), mean Mean Total Inflow (+165%), and mean Total Inflow Volume (+165%) in the LID scenario , the Cove node J504 *does not show a proportional decrease* in these parameters. By comparison, the Cove node J504 shows only a 16% reduction in mean Peak Flow, a 6% reduction in mean Mean Total Inflow, and a 6% reduction in mean Mean Total Inflow Volume. Because a large volume of runoff was diverted from node J504 to node OF1, some relationship between the volume of water gains at OF1 and losses at J504 was anticipated. Future modelers should investigate the sources of this trend.

Node J47 at Lafitte Village shows only a very *slight reduction* in mean Peak Flow after adding LID (-7%). A greater reduction in Peak Flow was expected at this node because a significant volume of water was diverted away from node J47 upstream including: 1) the Cove parking lot runoff was rerouted to Dean's Ditch, 2) the Cove and Lafitte Village pervious concrete parking lots with subsurface retention

chambers added substantial subsurface storage and permeability, 3) and the Lafitte Village bioretention cell adds storage capacity and permeability. Paired t-tests prove even this slight mean Peak Flow decrease to be statistically significant.

Across all the model runs for each individual design storm, only one trial for all nodes shows any variation in the Time of Peak flow among the four design storms—the Baseline scenario for Lafitte Village node J47. The other trials for all scenarios and all nodes recorded the same time of peak flow for all four design storms.

All nodes of interest were expected to show a significant delay in Time to Peak due to the significant increase in permeable surfaces and the large storage capacity created in the designed LID systems. Instead, only two nodes show any delay in Time to Peak—Dean's Ditch node OF1 (20-minute delay) and Lafitte Village node J47 (68-minute delay), as illustrated in the bar graph below.

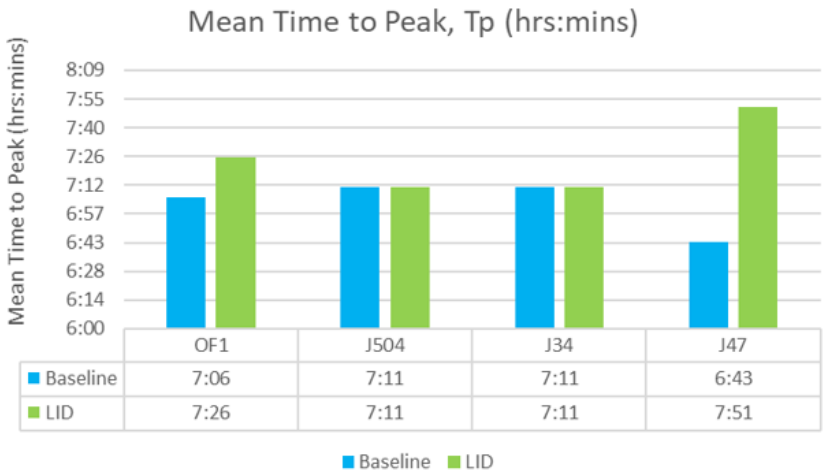

Figure 4.8. Mean Time to Peak results bar graphs at each node.

Surprisingly, the Cove node J504 and the Administration Building node J34 show no delay in Time to Peak despite the substantial storage capacity added via the subsurface arch retention chambers below the pervious concrete surfaces. Storage typically produces a delayed time to peak. This anomaly suggests that the next modelers should examine the potential sources of this error. Nodes J504 and J34 are both LID features with only permeable pavement LID controls. Other non-permeable pavement LID controls, including the Dean's Ditch vegetated swale and the Lafitte Village bioretention cell, do demonstrate a delayed time to peak. This trend may suggest that there is an error with the SWMM model concerning permeable pavement and subsurface storage.

From upstream to downstream, stormwater flows first through node J47 near the Cove then through node J47 near Lafitte Village. Because there is no delayed Time to Peak at node J504 upstream yet there is a substantially delayed Time to Peak downstream at node J47, this suggests that the Lafitte Village Parking Lot Permeable Pavement and Bioretention Cell LID systems are primarily responsible for intercepting runoff and delaying Time to Peak.

The Nash-Sutcliffe Efficiency coefficient (NSE) analysis method evaluated the similarity of the Baseline and LID total inflow timeseries curve shapes. NSE results are presented in the table below. For simplicity, only Design Storm 1 curves were analyzed. Nodes J504 near the Cove, node J34 near the

Administration building, and node J47 near Lafitte Village all produced NSE values that approximate one (1), indicating that the Baseline and LID curves are not statistically different in shape. Only node OF1 for Dean's Ditch has a negative NSE value, suggesting that the Baseline and LID curves are statistically different in shape.

Table 4.8. Nash-Sutcliffe Efficiency Coefficient analysis summary at each node for Design Storm 1.

Node	NSE Coefficient	NSE Interpretation	Statistically Significant Correlation Between Baseline and LID Curves?
OF1	-4.5013	NSE<0	NO
J504	0.9253	NSE≈1	YES
J34	0.8200	NSE≈1	YES
J47	0.8618	NSE≈1	YES

While this NSE analysis is informative of curve shape, it does not provide statical rigor to override the conclusions of the paired t-tests, especially given the subjective thresholds for the paired t-tests. NSE analysis also has disadvantages including that it weighs heavily towards peak flow.

The following node-by-node detailed analysis is arranged in order of increasing complexity.

4.3.2 Node J34 Analysis – Administration Building Parking Lot Permeable Pavement

The following analysis supports the Summary Analysis section with an in-depth review of statistical analysis at node J34.

4.3.2.1 Precision of Results and Uncertainty at Node J34

Results from the four design storms with different depths were averaged and compared to one another via statistical analysis to evaluate precision. At node J34, mean results show a significant reduction in Peak Flow, Mean Total Inflow, and Total Inflow Volume after adding LID features, suggesting that the LID features are effective, as shown in the table below.

Table 4.9. Node J34 statistical analysis of the Baseline and LID model for four 10-year, 24-hour design storms based on four different design depths.

Node: J34, Admin Building Parking Lot Permeable Pavement

Parameter	**Uncertainty**		
PEAK FLOW, Qp (cfs)	**Baseline, µ1**	**LID, µ2**	**Percent Reduction from Baseline to LID**
Mean	62.450	38.218	38.803%
SD	0.39166	0.24350	6.7953E-05
Coefficient of Variation	0.62716%	0.63714%	0.017512%
Margin of Error	0.46079	0.28648	7.9947E-05
MEAN TOTAL INFLOW, Qmean (cfs)	**µ1**	**µ2**	
Mean	3.1465	1.9283	38.715%
SD	0.019942	0.012285	1.4406E-04
Coefficient of Variation	0.63377%	0.63710%	0.03721%
Margin of Error	0.023461	0.014453	1.6949E-04
TOTAL INFLOW VOLUME, V (ft3)	**µ1**	**µ2**	
Mean	248250	152100	38.739%
SD	1571.6	969.54	6.2794E-06
Coefficient of Variation	0.63308%	0.63743%	0.0016209%
Margin of Error	1849.0	1140.7	7.3877E-06
TIME TO PEAK (hh:mm)	**µ2***	**µ1***	
Mean	7:11	7:11	
SD	0:00	0:00	
Coefficient of Variation	0.0%	0.0%	
Margin of Error	0:00	0:00	

*Unlike the other parameters, for Time to Peak, µ1 represents the LID, µ2 represents Baseline.

4.3.2.1.1 Peak Flow at Node J34 –Precision of Results and Uncertainty

The Peak Flow percent reduction and precision analysis is as follows:

- There was a 39% reduction in mean Peak Flow rate from the Baseline to the LID scenario.
- With a 95% confidence limit, at node J34, the mean Baseline Peak Flow is 62.450 ± 0.461 cfs and the mean LID Peak Flow is 38.218 ± 0.286 cfs.
- The percent reduction Peak Flow from the Baseline to the LID scenario is approximately 38.8%, indicating that the LIDs are effective at reducing Peak Flow at node J34.
- The low standard deviation of results for the four design storms for the Baseline and LID scenarios, at 0.39166 and 0.24350, respectively, indicate that the data points are close to the mean, with little variation, and are therefore precise.
- The low coefficient of variation of results for the four design storms for the Baseline and LID scenarios, at 0.62716% and 0.63714%, respectively, indicating that the results are reasonably precise.
- The low margin of error of results for the four design storms for the Baseline and LID scenarios, at 0.46079 and 0.28648, respectively, indicating a larger confidence in the results.

4.3.2.1.2 Mean Total Inflow at Node J34–Precision of Results and Uncertainty

The Mean Total Inflow percent reduction and precision analysis is as follows:

- There was a 39% reduction in mean Mean Total Inflow from the Baseline to the LID scenario.
- With a 95% confidence limit, at node J34, the mean Baseline Mean Total Inflow is 3.1465 ± 0.0235 cfs and the mean LID Mean Total Inflow is 1.9283 ± 0.0145 cfs.
- The percent reduction in Mean Total Inflow from the Baseline to the LID scenario is approximately 38.7%, indicating that the LIDs are effective at reducing Mean Total Inflow at node J34.
- The low standard deviation of results for the four design storms for the Baseline and LID scenarios, at 0.39166 and 0.24350, respectively, indicate that the data points are close to the mean, with little variation, and are therefore precise.
- The low coefficient of variation of results for the four design storms for the Baseline and LID scenarios, at 0.62716% and 0.63714%, respectively, indicating that the results are reasonably precise.
- The low margin of error of results for the four design storms for the Baseline and LID scenarios, at 0.46079 and 0.28648, respectively, indicating a larger confidence in the results.

4.3.2.1.3 Total Inflow Volume at Node J34–Precision of Results and Uncertainty

The Total Inflow Volume percent reduction and precision analysis is as follows:

- There was a 39% reduction in mean Total Inflow Volume from the Baseline to the LID scenario.
- With a 95% confidence limit, the mean Baseline Total Inflow Volume is 248,250 ± 1849 ft3 and the mean LID Total Inflow Volume is 152,100 ± 1141.
- The percent reduction in Total Inflow Volume from the Baseline to the LID scenario is approximately 38.7%, indicating that the LIDs are effective at reducing Total Inflow Volume.
- The low standard deviation of results for the four design storms for the Baseline and LID scenarios, at 0.39166 and 0.24350, respectively, indicate that the data points are close to the mean, with little variation, and are therefore precise.
- The low coefficient of variation of results for the four design storms for the Baseline and LID scenarios, at 0.62716% and 0.63714%, respectively, indicating that the results are reasonably precise.
- The low margin of error of results for the four design storms for the Baseline and LID scenarios, at 0.46079 and 0.28648, respectively, indicating a larger confidence in the results.

4.3.2.1.4 Time to Peak at Node J34–Precision of Results and Uncertainty

With both the Baseline and LID scenarios reporting a mean Time to Peak of 7 hours and 11 minutes, there is no delay in Time to Peak at this node. All four design storms produced the same time to peak. The standard deviation, coefficient of variation and the margin of error for both the Baseline and LID scenarios are all zero (0).

4.3.2.2 Paired T-Test Analysis at Node J34

The paired t-test compares the mean of the Baseline scenario results to the paired mean of the LID scenario results for each design storm. For example, the Baseline results for Design Storm 1 are paired and compared with the LID results for Design Storm 1.

Assuming a normal distribution with a 95% confidence limit, for the four design storms, the critical t-value, ta, selected from a table is 2.353. This critical t-value defines the boundary under the normal distribution where the null hypothesis, H0, is accepted or rejected, as shown in the table below. A calculated test statistic value, tc, for each parameter is compared to the critical t-value. If the value of the test statistic, tc, falls within the rejection region of the normal distribution curve, the null hypothesis, H0, is rejected in favor of the alternative hypothesis, Ha. At this node, all four parameters used a right-tailed t-test distribution curve, as shown in the table below.

Table 4.10. Node J34 paired t-test statistical analysis and the corresponding hypothesis conclusion.

Parameter	Paired T-Test						
PEAK FLOW, Qp (cfs)	**Paired Difference, μd = μ1 - μ2**	**H0**	**Ha**	**Critical t-value from table, ta**	**Calculated Test Statistic, tc**	**Normal Distribution Curve**	**Accept or Reject Null Hypothesis**
Mean	24.233	μd ≤ 0	μd > 0	2.353	327.06	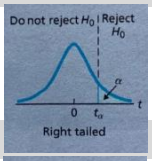	REJECT
SD	0.14818						
Coefficient of Variation	0.61151%		μ1 > μ2				
Margin of Error	0.17434						
MEAN TOTAL INFLOW, Qmean (cfs)							
Mean	1.2183	μd ≤ 0	μd > 0	2.353	317.43	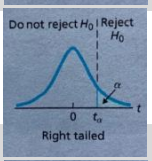	REJECT
SD	0.0076757						
Coefficient of Variation	0.63006%		μ1 > μ2				
Margin of Error	0.0090305						
TOTAL INFLOW VOLUME, V (ft3)							
Mean	96150	μd ≤ 0	μd > 0	2.353	319.03	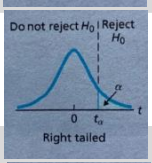	REJECT
SD	602.77						
Coefficient of Variation	0.62691%		μ1 > μ2				
Margin of Error	709.16						
TIME TO PEAK (hh:mm)	**Tp Delay, μd = μ1 - μ2**						
Mean	0:00	μd ≤ 0	μd > 0	2.353	[div/0]	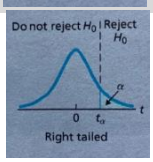	ACCEPT
SD	0:00						
Coefficient of Variation	0.0%		μ1 < μ2*				
Margin of Error	0:00						

*Unlike the other parameters, for Time to Peak, μ1 represents the LID, μ2 represents Baseline.

4.3.2.2.1 Peak flow at Node J34 – Paired T-Test

The Peak Flow paired t-test results are as follows:

- The mean paired Peak Flow difference between the Baseline and LID scenarios at this node is 24.233 ± 0.174 cfs. This indicates that flow was reduced after adding LID at this node.
- The paired Peak Flow differences demonstrate low values for the standard deviation, coefficient of variation, and margin of error at 0.14818, 0.61151%, and 0.17434, respectively. These indicate low variability in the differences among paired Baseline and LID results for each design storm.

- The calculated test statistic, tc lies to the right of the critical t value on the distribution. The null hypothesis, H04, that "there is no significant reduction in Peak Flow after adding LID" is therefore rejected.
- The mean of the paired differences, μd, is greater than zero, further supporting rejection of the null hypothesis.
- The alternative hypothesis, Ha4, that "there is significant reduction in Peak Flow after adding LID" is therefore accepted.

4.3.2.2.2 Mean Total Inflow at Node J34– Paired T-Test

The Mean Total Inflow paired t-test results are as follows:

- The mean paired Mean Total Inflow difference between the Baseline and LID scenarios at this node is 1.2183 ± 0.009 cfs.
- The paired Mean Total Inflow differences demonstrate low values for the standard deviation, coefficient of variation, and margin of error at 0.0076757, 0.63006%, and 0.0090305, respectively. These indicate low variability in the differences among paired Baseline and LID results for each design storm.
- The calculated test statistic, tc lies to the right of the critical t value on the distribution. The null hypothesis, H05, that "there is no significant reduction in Mean Total Inflow after adding LID" is therefore rejected.
- The mean of the paired differences, μd, is greater than zero, further supporting rejection of the null hypothesis.
- The alternative hypothesis, Ha5, that "there is significant reduction in Mean Total Inflow after adding LID" is therefore accepted.

4.3.2.2.3 Total Inflow Volume at Node J34– Paired T-Test

The Total Inflow Volume paired t-test results are as follows:

- The mean paired Total Inflow Volume difference between the Baseline and LID scenarios at this node is 96,150 ±709 ft3.
- The paired Total Inflow Volume differences demonstrate low values for the standard deviation, coefficient of variation, and margin of error at 602.77, 0.62691%, and 709.16, respectively. These indicate low variability in the differences among paired Baseline and LID results for each design storm.
- The calculated test statistic, tc lies to the right of the critical t value on the distribution. The null hypothesis, H06, that "there is no significant reduction in Total Inflow Volume after adding LID" is therefore rejected.
- The mean of the paired differences, μd, is greater than zero, further supporting rejection of the null hypothesis.
- The alternative hypothesis, Ha6, that "there is significant reduction in Total Inflow Volume after adding LID" is therefore accepted.

4.3.2.3 Time to Peak at Node J34– Paired T-Test

The mean paired Time to Peak is zero (0) at this node because both the Baseline and LID scenarios showed no difference in time to peak for all design storms. There is no statistical difference

between the Time to Peak for the Baseline vs LID scenarios. The calculated test statistic, tc, is not able to be calculated because the denominator in the calculation would be zero. Based on the mean of paired differences equaling zero, the null hypothesis, H07, that "there is no significant difference in time to peak" is therefore accepted.

4.3.2.3 Nash-Sutcliffe Efficiency Coefficient (NSE) Analysis at Node J34

The Nash-Sutcliffe Efficiency Coefficient (NSE) is a normalized statistic adapted to this experiment to compare the similarity of the shapes of the Baseline and the LID Total Inflow (cfs) time series curves for Design Storm 1 only. While the NSE analyses is not a statistically rigorous assessment but is useful to compare the shapes of two Total Inflow time series curves, making NSE a good complementary analysis to the Paired t-Test. Challenges with the NSE analysis include that the NSE thresholds are subjective, and the NSE analysis is sensitive to extreme values and, as a result, weighs towards peak flows.

Design Storm 1 was selected for this analysis because the NOAA 14 total rainfall value of 8.26 inches from the Louisiana Nature Center station data matches the total rainfall amount when looking up the Point Precipitation Frequency for UNO's exact address.

Table 4.11. Nash-Sutcliffe Efficiency Coefficient (NSE) to evaluate Baseline and LID scenario Total Inflow time series curve shape similarity at node J34, Admin Building Parking Lot Permeable Pavement.

NSE Coefficient	NSE Interpretation	Statistically Significant Correlation Between Baseline and LID Curves?
0.82	NSE≈1	YES

The calculated NSE value is 0.82. This value was interpreted to approximate one (1), indicating that there is a statistically significant correlation between Baseline and LID curves. This means that the Baseline and LID Total Inflow time series curves are not different enough statistically to suggest that the LID were effective on changing the Total Inflow curve.

For the purposes of this analysis, based on the hydrograph and the paired t-test results discussed earlier in this report, this NSE conclusion is informative of curve shape but does not provide sufficient statistical rigor to override the previous conclusion that the LIDs do have effective impact on Total Inflow at this node.

4.3.3 Node J504 Analysis – Administration Building Parking Lot Permeable Pavement

The following analysis supports the Summary Analysis section with an in-depth review of statistical analysis at node J504.

4.3.3.1.1 Precision of Results and Uncertainty at Node J504

At node J504, there is a significant reduction in Peak Flow, Mean Total Inflow, and Total Inflow Volume after adding LID features, suggesting that the LID features are effective, as shown in the table below.

Table 4.12. Node J504 statistical analysis of the Baseline and LID model results for four 10-year, 24-hour design storms based on four different design depths.

Node: J504, Cove Parking Lot Permeable Pavement

Parameter	**Uncertainty**		
PEAK FLOW, Qp (cfs)	**Baseline, μ1**	**LID, μ2**	**Percent Reduction from Baseline to LID**
Mean	36.180	30.165	16.625%
SD	0.26546	0.21048	3.1007E-04
Coefficient of Variation	0.73371%	0.69775%	0.18651%
Margin of Error	0.31231	0.24762	3.6480E-04
MEAN TOTAL INFLOW, Qmean (cfs)	**μ1**	**μ2**	
Mean	3.0975	2.9118	5.9248%
SD	0.010247	0.015370	1.3632E-03
Coefficient of Variation	0.33081%	0.52788%	2.30089%
Margin of Error	0.012056	0.018083	1.6038E-03
TOTAL INFLOW VOLUME, V (ft3)	**μ1**	**μ2**	
Mean	244400	229675	5.9259%
SD	787.40	1297.1	1.5581E-03
Coefficient of Variation	0.32218%	0.56476%	2.6293%
Margin of Error	926.38	1526.1	1.8331E-03
TIME TO PEAK (hh:mm)	**μ2***	**μ1***	
Mean	7:11	7:11	
SD	0.00	0.00	
Coefficient of Variation	0.0%	0.0%	
Margin of Error	0:00	0:00	

*Unlike the other parameters, for Time to Peak,

μ1 represents the LID, μ2 represents Baseline.

4.3.3.1.1 Peak Flow at Node J504—Precision of Results and Uncertainty

The Peak Flow percent reduction and precision analysis results are as follows:

- There is a 17% reduction in mean Peak Flow between the Baseline and LID scenarios.
- With a 95% confidence limit, at node J504, the mean Baseline Peak Flow is 36.180 ± 0.312 cfs and the mean LID Peak Flow is 30.165 ± 0.248 cfs.
- The percent reduction Peak Flow from the Baseline to the LID scenario is approximately 16.6%, suggesting that the LIDs are effective at reducing Peak Flow at node J504.

- The low standard deviation of results for the four design storms for the Baseline and LID scenarios, at 0.26546 and 0.21048, respectively, indicate that the data points are close to the mean, with little variation, and are therefore precise.
- The low coefficient of variation of results for the four design storms for the Baseline and LID scenarios, at 0.73371% and 0.69775%, respectively, indicate that the results are reasonably precise.
- The low margin of error of results for the four design storms for the Baseline and LID scenarios, at 0.31231 and 0.24762, respectively, indicate confidence in the results.

4.3.3.1.2 Mean Total Inflow at Node J504—Precision of Results and Uncertainty

The Mean Total Inflow percent reduction and precision analysis results are as follows:

- There is a 6% reduction in mean Mean Total Inflow between the Baseline and LID scenarios.
- With a 95% confidence limit, at node J504, the mean Baseline Mean Total Inflow is 3.0975 ± 0.0121 cfs and the mean LID Mean Total Inflow is 2.9118 ± 0.0181 cfs.
- The percent reduction in Mean Total Inflow from the Baseline to the LID scenario is approximately 5.9%, indicating that the LIDs are somewhat effective at reducing Mean Total Inflow at node J504.
- The low standard deviation of results for the four design storms for the Baseline and LID scenarios, at 0.010247 and 0.015370, respectively, indicate that the data points are close to the mean, with little variation, and are therefore precise.
- The low coefficient of variation of results for the four design storms for the Baseline and LID scenarios, at 0.33081% and 0.52788%, respectively, indicate that the results are reasonably precise.
- The low margin of error of results for the four design storms for the Baseline and LID scenarios, at 0.012056 and 0.018083, respectively, indicate confidence in the results.

4.3.3.1.3 Total Inflow Volume at Node J504—Precision of Results and Uncertainty

The Total Inflow Volume percent reduction and precision analysis results are as follows:

- There is a 6% reduction in Total Inflow Volume between the Baseline and LID scenarios.
- With a 95% confidence limit, the mean Baseline Total Inflow Volume is 244,400 ± 926 ft3 and the mean LID Total Inflow Volume is 229,675 ± 1526 ft3.
- The percent reduction in Total Inflow Volume from the Baseline to the LID scenario is approximately 5.9%, suggesting that the LIDs are effective at reducing Total Inflow Volume.
- The low standard deviation of results for the four design storms for the Baseline and LID scenarios, at 787.40 and 1297.1, respectively, indicate that the data points are close to the mean, with little variation, and are therefore precise.
- The low coefficient of variation of results for the four design storms for the Baseline and LID scenarios, at 0.32218% and 0.56476%, respectively, indicate that the results are reasonably precise.
- The low margin of error of results for the four design storms for the Baseline and LID scenarios, at 926.38 and 1526.1, respectively, indicate confidence in the results.

4.3.3.1.4 Time to Peak at Node J504—Precision of Results and Uncertainty

With both the Baseline and LID scenarios reporting a mean Time to Peak of 7 hours and 11 minutes, there is no delay in Time to Peak at this node. All four design storms produced the same time to peak. The standard deviation, coefficient of variation and the margin of error for both the Baseline and LID scenarios are all zero (0).

4.3.3.2 Paired T-Test Analysis

The paired t-test compares the mean of the Baseline scenario results to the paired mean of the LID scenario results for each design storm. For example, the Baseline results for Design Storm 1 are paired and compared with the LID results for Design Storm 1. Assuming a normal distribution with a 95% confidence limit, for the four design storms, the critical t-value, ta, selected from a table is 2.353. This critical t-value defines the boundary under the normal distribution where the null hypothesis, H0, is accepted or rejected, as shown in the table below.

A calculated test statistic value, tc, for each parameter is compared to the critical t-value. If the value of the test statistic, tc, falls within the rejection region of the normal distribution curve, the null hypothesis, H0, is rejected in favor of the alternative hypothesis. At this node, all four parameters used a right-tailed t-test distribution curve, as shown in the table below.

Table 4.13. Node J504 paired t-test statistical analysis and the corresponding hypothesis conclusion.

Node: J504, Cove Parking Lot Permeable Pavement

Parameter	**Paired T-Test**						
PEAK FLOW, Qp (cfs)	**Paired Difference, μd = μ1 - μ2**	**H0**	**Ha**	**Critical t-value from table, ta**	**Calculated Test Statistic, tc**	**Normal Distribution Curve**	**Accept or Reject Null Hypothesis**
Mean	6.0150	μd ≤ 0	μd > 0	2.353	218.43	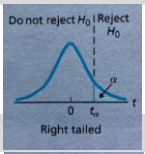	REJECT
SD	0.055076						
Coefficient of Variation	0.91564%		μ1 > μ2				
Margin of Error	0.064797						
MEAN TOTAL INFLOW, Qmean (cfs)							
Mean	0.18575	μd ≤ 0	μd > 0	2.353	72.51	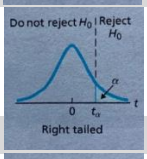	REJECT
SD	0.0051235						
Coefficient of Variation	2.7583%		μ1 > μ2				
Margin of Error	0.0060278						
TOTAL INFLOW VOLUME, V (ft3)							
Mean	14725	μd ≤ 0	μd > 0	2.353	57.48	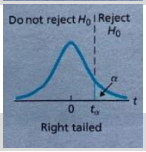	REJECT
SD	512.35						
Coefficient of Variation	3.4794%		μ1 > μ2				
Margin of Error	602.78						
TIME TO PEAK (hh:mm)	**Mean Tp Delay, μd = μ1 - μ2**						
Mean	0:00	μd ≤ 0	μd > 0	2.353	[div/0]	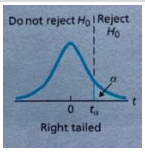	ACCEPT
SD	0:00						
Coefficient of Variation	0.0%		μ1 < μ2*				
Margin of Error	0:00						

*Unlike the other parameters, for Time to Peak, μ1 represents the LID, μ2 represents Baseline.

4.3.3.2.1 Peak flow at Node J504—Paired T-Test

The Peak Flow paired t-test results are as follows:

- The mean paired Peak Flow difference between the Baseline and LID scenarios at this node is 6.0150 ± 0.0648 cfs. This indicates that flow is reduced after adding LID at this node.
- The paired Peak Flow differences show low values for the standard deviation, coefficient of variation, and margin of error at 0.055076, 0.91564%, and 0.064797, respectively. These indicate low variability in the differences among paired Baseline and LID results for each design storm.
- The calculated test statistic, tc lies to the right of the critical t value on the distribution. The null hypothesis, H04 that "there is no significant reduction in Peak Flow" is therefore rejected.
- The mean of the paired differences, μd, is greater than zero, further supporting rejection of the null hypothesis.
- The alternative hypothesis, Ha4, that "there is significant reduction in Peak Flow after adding LID" is therefore accepted.

4.3.3.2.2 Mean Total Inflow at Node J504—Paired T-Test

The Mean Total Inflow paired t-test results are as follows:

- The mean paired Mean Total Inflow difference between the Baseline and LID scenarios at this node is 0.18575 ± 0.00602 cfs.
- The paired Mean Total Inflow differences demonstrate low values for the standard deviation, coefficient of variation, and margin of error at 0.0051235, 2.7583%, and 0.0060278, respectively. These indicate low variability in the differences among paired Baseline and LID results for each design storm.
- The calculated test statistic, tc lies to the right of the critical t value on the distribution. The null hypothesis, H05, that "there is no significant reduction in Mean Total Inflow" is therefore rejected.
- The mean of the paired differences, μd, is greater than zero, further supporting rejection of the null hypothesis.
- The alternative hypothesis, Ha5, that "there is significant reduction in Mean Total Inflow after adding LID" is therefore accepted at node J504.

4.3.3.2.3 Total Inflow Volume at Node J504—Paired T-Test

The Total Inflow Volume paired t-test results are as follows:

- The mean paired Total Inflow Volume difference between the Baseline and LID scenarios at this node is 14725 ± 603 ft3.
- The paired Total Inflow Volume differences demonstrate low values for the standard deviation, coefficient of variation, and margin of error at 512.35, 3.4794%, and 602.78, respectively. These indicate low variability in the differences among paired Baseline and LID results for each design storm.
- The calculated test statistic, tc lies to the right of the critical t value on the distribution. The null hypothesis, H06, that "there is no significant reduction in Total Inflow Volume after adding LID" is therefore rejected.
- The mean of the paired differences, μd, is greater than zero, further supporting rejection of the null hypothesis.

- The alternative hypothesis, Ha6, that "there is significant reduction in Mean Total Inflow after adding LID" is therefore accepted at node J504.

4.3.3.2.4 Time to Peak at Node J504—Paired T-Test

The mean paired Time to Peak is zero (0) at this node because both the Baseline and LID scenarios showed no difference in time to peak for all design storms. There is no statistical difference between the Time to Peak for the Baseline vs LID scenarios.

The calculated test statistic, tc, is unable to be calculated because the denominator value in the calculation is equal to zero. Because the mean of the paired differences, μd, is equal to zero, the null hypothesis, H07, that "there is no significant delay in Time to Peak" is accepted at node J504.

4.3.3.3 Nash-Sutcliffe Efficiency Coefficient (NSE) Analysis at Node J504

The Nash-Sutcliffe Efficiency Coefficient (NSE) is a normalized statistic adapted to this experiment to compare the similarity of the shapes of the Baseline and the LID Total Inflow (cfs) time series curves for Design Storm 1 only.

Table 4.14. Nash-Sutcliffe Efficiency Coefficient (NSE) to evaluate Baseline and LID scenario Total Inflow time series curve shape similarity at node J504, the Cove Parking Lot Permeable Pavement.

NSE Coefficient	NSE Interpretation	Statistically Significant Correlation Between Baseline and LID Curves?
0.93	NSE≈1	YES

The calculated NSE value is 0.93. This value was interpreted to approximate 1, indicating that there is a statistically significant correlation between Baseline and LID curves. This means that the Baseline and LID Total Inflow time series curves are not different enough statistically to suggest that the LID were effective on changing the Total Inflow curve.

This NSE conclusion is informative of curve shape but does not provide sufficient statistical rigor to override the previous conclusion that the LIDs do have effective impact on Total Inflow at this node per the preceding paired t-test analysis, especially given the subjective thresholds for NSE tests.

4.3.4 Node OF1 Analysis – Dean's Ditch Vegetated Swale

Node OF1corresponds to Dean's Ditch, where more water is diverted into this vegetated swale after regrading the Cove parking lot towards Ditch and re-routing water from Dean's Ditch Upper Reach to the Lower Reach. The following analysis supports the Summary Analysis section with an in-depth review of statistical analysis at node OF1.

4.3.4.1 Precision of Results and Uncertainty at Node OF1

The model results show an increase in Peak Flow, Mean Total Inflow and Total Inflow Volume after adding the vegetated swale LID and re-routing runoff, accordingly. This node also shows a delayed Time to Peak in the LID scenario, as shown in the table below.

Table 4.15. Node OF1 statistical analysis of the Baseline and LID model results for four 10-year, 24-hour design storms based on four different design depths.

Node: OF1, Dean's Ditch Vegetated Swale

Parameter	**Uncertainty**		
PEAK FLOW, Qp (cfs)	**Baseline, μ1**	**LID, μ2**	**% Increase from Baseline to LID**
Mean	24.305	80.323	230.48%
SD	0.066081	0.56559	
Coefficient of Variation	0.27188%	0.70415%	
Margin of Error	0.15549	0.66542	
MEAN TOTAL INFLOW, Qmean (cfs)	**μ1**	**μ2**	
Mean	2.4723	6.5525	165.04%
SD	0.012997	0.042131	
Coefficient of Variation	0.52571%	0.64297%	
Margin of Error	0.015291	0.049567	
TOTAL INFLOW VOLUME, V (ft3)	**μ1**	**μ2**	
Mean	195050	516975	165.05%
SD	1024.7	3333.0	
Coefficient of Variation	0.52535%	0.64472%	
Margin of Error	1205.6	3921.3	
TIME TO PEAK (hh:mm)	**μ2***	**μ1***	
Mean	7:06	7:26	
SD	0.00	0.00	
Coefficient of Variation	0.0%	0.0%	
Margin of Error	0:00	0:00	

*Unlike the other parameters, for Time to Peak, μ1 represents the LID, μ2 represents Baseline.

4.3.4.1.1 Peak Flow at Node OF1—Precision of Results and Uncertainty

The Peak Flow percent reduction and precision analysis results are as follows:

- There is a 230% increase in mean Peak Flow between the Baseline and LID scenarios.
- With a 95% confidence limit, at node OF1, the mean Baseline Peak Flow is 24.305 ± 0.155 cfs and the mean LID Peak Flow is greater, at 80.323 ± 0.665 cfs.
- The percent reduction Peak Flow from the Baseline to the LID scenario is approximately (-) 230.5%. The negative percent is expected because the Baseline scenario has a lower Peak Flow

than the LID scenario, suggesting that there is a significant increase in Peak Flow in the LID scenario, as predicted.

- The low standard deviation of results for the four design storms for the Baseline and LID scenarios, at 0.066081 and 0.56559, respectively, indicate that the data points are close to the mean, with little variation, and are therefore precise.
- The low coefficient of variation of results for the four design storms for the Baseline and LID scenarios, at 0.27188% and 0.70415%, respectively, indicate that the results are reasonably precise.
- The low margin of error of results for the four design storms for the Baseline and LID scenarios, at 0.15549 and 0.66542, respectively, indicate a larger confidence in the results.

4.3.4.1.2 Mean Total Inflow at Node OF1—Precision of Results and Uncertainty

The Mean Total Inflow percent reduction and precision analysis results are as follows:

- There is a 165% increase in mean Mean Total Inflow between the Baseline and LID scenarios.
- With a 95% confidence limit, at node OF1, the mean Baseline Mean Inflow is 2.4723 ± 0.0152 cfs and the mean LID Mean Total Inflow is 6.5525 ± 0.049567 cfs.
- The percent reduction in Mean Total Inflow from the Baseline to the LID scenario is approximately (-) 165.0%, indicating that the LID scenario shows a greater Mean Total Inflow than the Baseline at node OF1.
- The low standard deviation of results for the four design storms for the Baseline and LID scenarios, at0.012997 and 0.042131, respectively, indicate that the data points are close to the mean, with little variation, and are therefore precise.
- The low coefficient of variation of results for the four design storms for the Baseline and LID scenarios, at 0.52571% and 0.64297%, respectively, indicating that the results are reasonably precise.
- The low margin of error of results for the four design storms for the Baseline and LID scenarios, at 0.015291 and 0.049567, respectively, indicate confidence in the results.

4.3.4.1.3 Total Inflow Volume at Node OF1—Precision of Results and Uncertainty

The Total Inflow Volume percent reduction and precision analysis results are as follows:

- There is a 165% increase in mean Total Inflow Volume between the Baseline and LID scenarios.
- With a 95% confidence limit, the mean Baseline Total Inflow Volume is 195050± 1205 ft3 and the mean LID Total Inflow Volume is 516975 ± 3921.
- The percent reduction in Total Inflow Volume from the Baseline to the LID scenario is approximately (-) 165.1%, indicating that the LID scenario shows a higher Total Inflow Volume than the Baseline scenario.
- The relatively low standard deviation of results for the four design storms for the Baseline and LID scenarios, at 1024.7 and 3333.0, respectively, indicate that the data points are close to the mean, with little variation, and are therefore precise.
- The low coefficient of variation of results for the four design storms for the Baseline and LID scenarios, at 0.52535% and 0.64472%, respectively, indicate that the results are reasonably precise.
- The relatively low margin of error of results for the four design storms for the Baseline and LID scenarios, at 1205.6 and 3921.3, respectively, indicate a larger confidence in the results.

4.3.4.1.4 Time to Peak at Node OF1—Precision of Results and Uncertainty

For all four design storms, the Time to Peak in the Baseline scenario is 7 hours 6 minutes. For all four design storms, the LID scenario shows a delayed time to peak of 20 minutes, with a Time to Peak at 7 hours 26 minutes.

4.3.4.2 Paired T-Test Analysis

The paired t-test compares the mean of the Baseline scenario results to the paired mean of the LID scenario results for each design storm. For example, the Baseline results for Design Storm 1 are paired and compared with the LID results for Design Storm 1.

Assuming a normal distribution with a 95% confidence limit, for the four design storms, the critical t-value, ta, selected from a table is 2.353. This critical t-value defines the boundary under the normal distribution where the null hypothesis, H0, is accepted or rejected, as shown in the table below. A calculated test statistic value, tc, for each parameter is compared to the critical t-value. If the value of the test statistic, tc, falls within the rejection region of the normal distribution curve, the null hypothesis, H0, is rejected in favor of the alternative hypothesis, Ha.

At this node, because the null hypotheses differ from the other nodes of interest, Peak Flow, Mean Total Inflow, and Total Inflow Volume use a left-tailed distribution curve to perform the t-test. The Time to Peak, which has the same null hypothesis as the other nodes of interest, still uses a right-tailed normal distribution curve.

Table 4.16. Node OF1 paired t-test statistical analysis and the corresponding hypothesis conclusion.

Node: OF1, Dean's Ditch Vegetated Swale

Parameter	Paired T-Test						
PEAK FLOW, Qp (cfs)	**Paired Difference, μd = μ1 - μ2**	**H0**	**Ha**	**Critical t-value from table, ta**	**Calculated Test Statistic, tc**	**Normal Distribution Curve**	**Accept or Reject Null Hypothesis**
Mean	-56.018	μd ≥ 0	μd < 0	2.353	-216.51	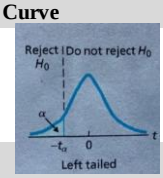	REJECT
SD	0.51745						
Coefficient of Variation	-0.92374%		μ1 < μ2				
Margin of Error	0.60878						
MEAN TOTAL INFLOW, Qmean (cfs)							
Mean	-4.0803	μd ≥ 0	μd < 0	2.353	-280.08	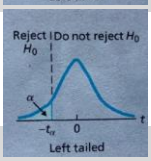	REJECT
SD	0.029136						
Coefficient of Variation	-0.71408%		μ1 < μ2				
Margin of Error	0.034279						
TOTAL INFLOW VOLUME, V (ft3)							
Mean	-321925	μd ≥ 0	μd < 0	2.353	-278.90	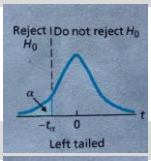	REJECT
SD	2308.5						
Coefficient of Variation	-0.71709%		μ1 < μ2				
Margin of Error	2715.9						
TIME TO PEAK (hh:mm)	**Mean Tp Delay, μd = μ1 - μ2**						
Mean	0:20	μd ≤ 0	μd > 0	2.353	[div/0]	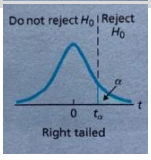	REJECT
SD	0.00						
Coefficient of Variation	0.0%		μ1 < μ2*				
Margin of Error	0.00						

*Unlike the other parameters, for Time to Peak, μ1 represents the LID, μ2 represents Baseline.

4.3.4.2.1 Peak flow at Node OF1—Paired T-Test

The Peak Flow paired t-test results are as follows:

- The mean paired Peak Flow difference between the Baseline and LID scenarios at this node is (-) 56.018 ± 0.608 cfs, indicating that flow is increased after adding LID at this node.
- The paired Peak Flow differences demonstrate low values for the standard deviation, coefficient of variation, and margin of error at 0.51745, -0.92374%, and 0.60878, respectively. These indicate low variability in the differences among paired Baseline and LID results for each design storm.
- The calculated test statistic, tc lies to the left of the critical t value on the distribution. The null hypothesis, H01, that "there is no significant increase in Peak flow after rerouting runoff into Dean's Ditch" is therefore rejected.
- The mean of the paired differences, μd, is less than zero, further supporting rejection of the null hypothesis.
- The alternative hypothesis, Ha1, that there is a significant increase in Peak Flow after rerouting runoff into Dean's Ditch" is therefore accepted.

4.3.4.2.2 Mean Total Inflow at Node OF1—Paired T-Test

The Mean Total Inflow paired t-test results are as follows:

- The mean paired Mean Total Inflow difference between the Baseline and LID scenarios at this node is (-) ± 4.0803 cfs.
- The paired Mean Total Inflow differences demonstrate low values for the standard deviation, coefficient of variation, and margin of error at 0.029136, (-)0.71408%, and 0.034279, respectively. These indicate low variability in the differences among paired Baseline and LID results for each design storm.
- The calculated test statistic, tc lies to the left of the critical t value on the distribution. The null hypothesis, H02, that "there is no significant increase in Mean Total Inflow after rerouting runoff into Dean's Ditch and adding LID" is therefore rejected.
- The mean of the paired differences, μd, is less than zero, further supporting rejection of the null hypothesis.
- The alternative hypothesis, Ha2, that "there is a significant increase in mean Total Inflow after rerouting runoff into Dean's Ditch and adding LID" is therefore accepted.

4.3.4.2.3 Total Inflow Volume at Node OF1—Paired T-Test

The Total Inflow Volume paired t-test results are as follows:

- The mean paired Total Inflow Volume difference between the Baseline and LID scenarios at this node is (-)321925 ±_2716 ft3, indicating a decrease in Total Inflow Volume in the LID scenario compared to the Baseline scenario.
- The paired Total Inflow Volume differences demonstrate relatively low values for the standard deviation, coefficient of variation, and margin of error at 2308.5, (-)0.7709%, and 2715.9, respectively. These indicate low variability in the differences among paired Baseline and LID results for each design storm.

- The calculated test statistic, tc lies to the left of the critical t value on the distribution. The null hypothesis, H03, that "there is no significant increase in Total Inflow Volume after rerouting runoff into Dean's Ditch and adding LID" is therefore rejected.
- The mean of the paired differences, μd, is less than zero, further supporting rejection of the null hypothesis.
- The alternative hypothesis, Ha3, that "there is a significant increase in Total Inflow Volume after rerouting runoff into Dean's Ditch and adding LID" is therefore accepted.

4.3.4.2.4 Time to Peak at Node OF1—Paired T-Test

The LID scenario shows a 20-minute Time to Peak compared to the Baseline scenario. Although the calculated test statistic, tc, could not be generated because a zero would be in the denominator, the mean of the paired differences, μ, is greater than zero, suggests that the null hypothesis, H07, that ""there is no significant delay in time to peak" should be rejected in favor of the alternative hypothesis, Ha7, that "there is a significant delay in Time to Peak".

4.3.4.3 Nash-Sutcliffe Efficiency Coefficient (NSE) Analysis at Node OF1

The Nash-Sutcliffe Efficiency Coefficient (NSE) is a normalized statistic adapted to this experiment to compare the similarity of the shapes of the Baseline and the LID Total Inflow (cfs) time series curves for Design Storm 1 only.

Table 4.17. Nash-Sutcliffe Efficiency Coefficient (NSE) to evaluate Baseline and LID scenario Total Inflow time series curve shape similarity at Node OF1, Dean's Ditch Vegetated Swale.

NSE Coefficient	NSE Interpretation	Statistically Significant Correlation Between Baseline and LID Curves?
-4.50	NSE<0	NO

The calculated NSE value is (-) 4.50. The negative NSE value suggests that there is a statistically insignificant correlation between the shape of the Baseline and LID Total Inflow time series curves. This further supports the alternative hypothesis that rerouting runoff into Dean's Ditch and adding LID did have a significant impact on the Total Inflow (cfs).

4.3.5 Node J47 Analysis – Lafitte Village Parking Lot Permeable Pavement and Bioretention Cell

The following analysis supports the Summary Analysis section with an in-depth review of statistical analysis at node J47.

Node J47 has several substantial changes from the Baseline to the LID scenario including the upstream Cove Parking Lot runoff being rerouted away from the Founders Road conduit and the formerly impervious Lafitte Village parking lot being converted to a pervious concrete parking lot and a large bioretention cell, both with substantial storage.

4.3.5.1 Precision of Results and Uncertainty at Node J47

At node J47, there is a significant reduction in Peak Flow, Mean Total Inflow, and Total Inflow Volume after adding LID features, suggesting that the LID features are effective, as shown in the table below.

Table 4.18. Node J47 statistical analysis of the Baseline and LID scenario model results for four 10-year, 24-hour design storms based on four different design depths.

Node: J47, Lafitte Village Parking Lot Permeable Pavement & Bioretention Cell

Parameter	**Uncertainty**		
PEAK FLOW, Qp (cfs)	**Baseline, µ1**	**LID, µ2**	**Percent Reduction from Baseline to LID**
Mean	10.203	9.4458	7.4138%
SD	0.069940	0.0052520	6.7712E-03
Coefficient of Variation	0.68552%	0.05560%	9.1332%
Margin of Error	0.082285	0.0061790	7.9663E-03
MEAN TOTAL INFLOW, Qmean (cfs)	**µ1**	**µ2**	
Mean	5.3205	4.5575	14.3%
SD	0.023671	0.023058	2.1928E-03
Coefficient of Variation	0.44491%	0.50593%	1.5291%
Margin of Error	0.027849	0.027128	2.5799E-03
TOTAL INFLOW VOLUME, V (ft3)	**µ1**	**µ2**	
Mean	419775	359575	14.3%
SD	1855.4	1857.2	2.2616E-03
Coefficient of Variation	0.44200%	0.51650%	1.5770%
Margin of Error	2182.9	2185.0	2.6608E-03
TIME TO PEAK (hh:mm)	**µ2***	**µ1***	
Mean	6:43	7:51	
SD	0:02	0:00	
Coefficient of Variation	0.7%	0.0%	
Margin of Error	0:03	0:00	

*Unlike the other parameters, for Time to Peak,

µ1 represents the LID, µ2 represents Baseline.

4.3.5.1.1 Peak Flow at Node J47—Precision of Results and Uncertainty

The Peak Flow percent reduction and precision analysis results are as follows:

- There is a 7% reduction in mean Peak Flow between the Baseline and LID scenarios.
- With a 95% confidence limit, at node J47, the mean Baseline Peak Flow is 10.203 ± 0.082 cfs and the mean LID Peak Flow is 9.4458 ± 0.0062 cfs, indicating a reduction in Peak Flow in the LID scenario.
- The percent reduction Peak Flow from the Baseline to the LID scenario is approximately 7.4%, suggesting that the LIDs are effective at reducing Peak Flow at node J47.

- The low standard deviation of results for the four design storms for the Baseline and LID scenarios, at 0.069940 and 0.0052520, respectively, indicate that the data points are close to the mean with little variation and are therefore precise.
- The low coefficient of variation of results for the four design storms for the Baseline and LID scenarios, at 0.68552% and 0.05560%, respectively, indicate that the results are reasonably precise.
- The low margin of error of results for the four design storms for the Baseline and LID scenarios, at 0.082285and 0.0061790, respectively, indicate confidence in the results.

4.3.5.1.2 Mean Total Inflow at Node J47—Precision of Results and Uncertainty

The Mean Total Inflow percent reduction and precision analysis results are as follows:

- There is a 14% reduction in mean Mean Total Inflow between the Baseline and LID scenarios.
- With a 95% confidence limit, at node J47, the mean Baseline Mean Total Inflow is 5.3205 ± 0.0278 cfs and the mean LID Mean Total Inflow is 4.5575 ± 0.0271cfs.
- The percent reduction in Mean Total Inflow from the Baseline to the LID scenario is approximately 14.3%, suggesting that the LID and rerouting the Cove parking lot runoff are effective at reducing Mean Total Inflow at node J47.
- The low standard deviation of results for the four design storms for the Baseline and LID scenarios, at 0.023671 and 0.023058, respectively, indicate that the data points are close to the mean with little variation and are therefore precise.
- The low coefficient of variation of results for the four design storms for the Baseline and LID scenarios, at 0.44491% and 0.50593%, respectively, indicate that the results are reasonably precise.
- The low margin of error of results for the four design storms for the Baseline and LID scenarios, at 0.027849 and 0.027128, respectively, suggest confidence in the results.

4.3.5.1.3 Total Inflow Volume at Node J47—Precision of Results and Uncertainty

The Total Inflow Volume percent reduction and precision analysis results are as follows:

- There is a 14% reduction in mean Total Inflow Volume between the Baseline and LID scenarios.
- With a 95% confidence limit, the mean Baseline Total Inflow Volume is 419775 ± 2182 ft3 and the mean LID Total Inflow Volume is 359575 ± 2185, showing a reduction from the Baseline to the LID scenarios.
- The percent reduction in Total Inflow Volume from the Baseline to the LID scenario is approximately 14.3%, indicating that the LID and rerouting the Cove parking lot runoff are effective measures to reduce Total Inflow Volume.
- The relatively low standard deviation of results for the four design storms for the Baseline and LID scenarios, at 1855.4 and 1857.2, respectively, indicate that the data points are close to the mean, with little variation, and are therefore precise.
- The low coefficient of variation of results for the four design storms for the Baseline and LID scenarios, at 0.44200% and 0.51650%, respectively, indicate that the results are reasonably precise.
- The relatively low margin of error of results for the four design storms for the Baseline and LID scenarios, at 2812.9 and 2185.0, respectively, suggest confidence in the results.

4.3.5.1.4 Time to Peak at Node J47—Precision of Results and Uncertainty

The Baseline four design storms produced slightly different Times to Peak, creating a mean Time to Peak of 6:43 ± 0:03. The four design storms for the LID scenario produced the same delayed Time to Peak, creating a mean Time to Peak of 7:51 ± 0:00.

4.3.5.2 Paired T-Test Analysis

The paired t-test compares the mean of the Baseline scenario results to the paired mean of the LID scenario results for each design storm. For example, the Baseline results for Design Storm 1 are paired and compared with the LID results for Design Storm 1.

Assuming a normal distribution with a 95% confidence limit, for the four design storms, the critical t-value, ta, selected from a table is 2.353. This critical t-value defines the boundary under the normal distribution where the null hypothesis, H0, is accepted or rejected, as shown in the table below. A calculated test statistic value, tc, for each parameter is compared to the critical t-value. If the value of the test statistic, tc, falls within the rejection region of the normal distribution curve, the null hypothesis, H0, is rejected in favor of the alternative hypothesis, Ha. At this node, all four parameters used a right-tailed t-test distribution curve, as shown in the table below.

Table 4.19. Node J47 paired t-test statistical analysis and the corresponding hypothesis conclusion.

Node: J47, Lafitte Village Parking Lot Permeable Pavement and Bioretention Cell

Parameter **Paired T-Test**

PEAK FLOW, Qp (cfs)	Paired Difference, μd = μ1 - μ2	H0	Ha	Critical t-value from table, ta	Calculated Test Statistic, tc	Normal Distribution Curve	Accept or Reject Null Hypothesis
Mean	0.75675	μd ≤ 0	μd > 0	2.353	20.413	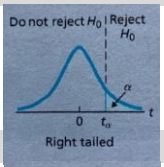	REJECT
SD	0.074146						
Coefficient of Variation	9.7979%		μ1 > μ2				
Margin of Error	0.087232						
MEAN TOTAL INFLOW, Qmean (cfs)							
Mean	0.76300	μd ≤ 0	μd > 0	2.353	124.60	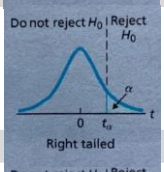	REJECT
SD	0.012247						
Coefficient of Variation	1.6052%		μ1 > μ2				
Margin of Error	0.014409						
TOTAL INFLOW VOLUME, V (ft3)							
Mean	60200	μd ≤ 0	μd > 0	2.353	122.46	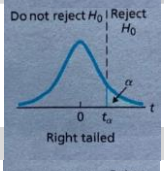	REJECT
SD	983.19						
Coefficient of Variation	1.6332%		μ1 > μ2				
Margin of Error	1156.7						
TIME TO PEAK (hh:mm)	**Mean Tp Delay, μd = μ1 - μ2**						
Mean	1:07	μd ≤ 0	μd > 0	2.353	46.765	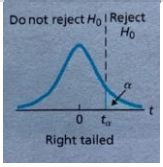	REJECT
SD	0:02						
Coefficient of Variation	4.2767%		μ1 < μ2*				
Margin of Error	0:03						

*Unlike the other parameters, for Time to Peak, μ1 represents the LID, μ2 represents Baseline.

4.3.5.2.1 Peak flow at Node J47—Paired T-Test

The Peak Flow paired t-test analysis results are as follows:

- The mean paired Peak Flow difference between the Baseline and LID scenarios at this node is 0.75675 ± 0.08723 cfs. This indicates that flow is only slightly reduced after adding LID and rerouting the Cove parking lot runoff at this node.
- The paired Peak Flow differences demonstrate low values for the standard deviation, and margin of error at 0.074146, and 0.087232, respectively. These indicate low variability in the differences among paired Baseline and LID results for each design storm. The coefficient of variation is higher than in other scenarios reported here, at 9.7979%, indicating a greater variation in the paired difference results for the four design storms.
- The calculated test statistic, tc lies to the right of the critical t value on the distribution. The null hypothesis, H04, that "there is no significant reduction in Peak Flow after adding LID" is therefore rejected.
- The mean of the paired differences, μd, is greater than zero, though only slightly, further supporting rejection of the null hypothesis.
- The alternative hypothesis, Ha4, that "there is significant reduction in Peak Flow after adding LID" is therefore accepted.

4.3.5.2.2 Mean Total Inflow at Node J47—Paired T-Test

The Mean Total Inflow paired t-test analysis results are as follows:

- The mean paired Mean Total Inflow difference between the Baseline and LID scenarios at this node is 0.76300 ± 0.01441 cfs, which is only a slight reduction from the Baseline to the LID scenario.
- The paired Mean Total Inflow differences demonstrate low values for the standard deviation, coefficient of variation, and margin of error at 0.012247, 1.6052%, and 0.014409, respectively. These indicate low variability in the differences among paired Baseline and LID results for each design storm.
- The calculated test statistic, tc lies to the right of the critical t value on the distribution. The null hypothesis, H05, that "there is no significant reduction in Mean Total Inflow after adding LID" is therefore rejected at node J47.
- The mean of the paired differences, μd, is greater than zero, further supporting rejection of the null hypothesis.
- The alternative hypothesis, Ha5, that "there is significant reduction in Total Inflow Volume after adding LID" is therefore accepted for node J47.

4.3.5.2.3 Total Inflow Volume at Node J47—Paired T-Test

The Total Inflow Volume paired t-test analysis results are as follows:

- The mean paired Total Inflow Volume difference between the Baseline and LID scenarios at this node is 60200 ± 1156 ft3.
- The paired Total Inflow Volume differences demonstrate relatively low values for the standard deviation, coefficient of variation, and margin of error at 983.19, 1.6332%, and 1156.7, respectively. These indicate low variability in the differences among paired Baseline and LID results for each design storm.

- The calculated test statistic, tc lies to the right of the critical t value on the distribution. The null hypothesis, H06, that "there is no significant reduction in Total Inflow Volume after adding LID" is therefore rejected at node J47.
- The mean of the paired differences, μd, is greater than zero, further supporting rejection of the null hypothesis.
- The alternative hypothesis, Ha6, that "there is significant reduction in Total Inflow Volume" is therefore accepted for node J47.

4.3.5.2.4 Time to Peak at Node J47—Paired T-Test

The Time to Peak paired t-test analysis results are as follows:

- The mean paired difference in Time to Peak between the Baseline and LID scenarios is 1:07 ± 0:03, showing a significant delay in time to peak.
- The calculated test statistic, tc lies to the right of the critical t value on the distribution. The null hypothesis, H07, that "there is no significant delay in Time to Peak after adding LID" is therefore rejected at node J47.
- The mean of the paired differences, μd, is greater than zero, further supporting rejection of the null hypothesis.
- The alternative hypothesis, Ha7, that "there is a significant delay in Time to Peak" is therefore accepted.

4.3.5.3 Nash-Sutcliffe Efficiency Coefficient (NSE) Analysis at Node J47

The Nash-Sutcliffe Efficiency Coefficient (NSE) is a normalized statistic adapted to this experiment to compare the similarity of the shapes of the Baseline and the LID Total Inflow (cfs) time series curves for Design Storm 1 only.

Table 4.20. Nash-Sutcliffe Efficiency Coefficient (NSE) to evaluate Baseline and LID scenario Total Inflow time series curve similarity for node J47, Lafitte Village Permeable Pavement and Bioretention Cell.

NSE Coefficient	NSE Interpretation	Statistically Significant Correlation Between Baseline and LID Curves?
0.86	NSE≈1	YES

The calculated NSE value is 0.86. This value was interpreted to approximate one (1), indicating that there is a statistically significant correlation between Baseline and LID curves. This means that the Baseline and LID Total Inflow time series curves are not different enough statistically to suggest that the LID were effective on changing the Total Inflow curve.

This NSE conclusion is informative of curve shape but does not provide sufficient statistical rigor to override the previous paired t-test conclusion that the LIDs do have effective impact on Total Inflow at this node, especially given the subjective thresholds for NSE tests.

4.4 Node OF1 Dean's Ditch Further Investigation

To investigate some of the anomalies described in this analysis, node OF1 Dean's Ditch is further investigated here as case study that may provide insights to results at other nodes.

Node OF1, Dean's Ditch had many simultaneous changes between the Baseline scenario and LID scenario, making the factors influencing the results difficult to isolate. To evaluate the impact of the Cove's LID feature storage on the Dean's Ditch results, an additional scenario called "Intermediate" was created. The Intermediate scenario is identical to the LID scenario except that the Cove parking lot is not a LID feature; it is the same original asphalt impervious surface as in the Baseline scenario. Therefore, the Intermediate scenario is identical to the LID scenario, with the exception of the following modifications:

- The permeable pavement LID Control was deleted from each Cove parking lot subcatchment. This step alone did not cause the Intermediate scenario's hydrograph to differ from the LID scenario hydrograph. This observation may indicate that there is an error with the permeable pavement and subsurface storage simulation.
- The depression storage over the Cove LID feature pervious area (DstorePerv), whose values were set to 22.4 inches in the LID scenario, were changed back to their Baseline scenario values. These are the same Baseline DstorePerv values imported from GIS, summarized in the table below. Reducing the DstorePerv values reduced the Cove LID feature storage capacity causing the Intermediate scenario's Peak Flow, Mean Total Inflow, and Total Inflow Volume values to increase substantially.
- The percent imperviousness (%Imperv) for each subcatchment was changed from their 5% LID scenario value back to the Baseline scenario values, as summarized in the table below.

The above modifications changed the Intermediate scenario's time to peak to five minutes earlier than the LID scenario, suggesting that the Cove parking lot storage adds at least a five-minute delay in Time to Peak.

Table 4.21. Intermediate and LID scenario depression storage and percent imperviousness at the Cove parking lot.

	DstorePerv (in)		% Imperviousness (%)	
Name	Intermediate Scenario	LID Scenario	Intermediate Scenarios	LID Scenario
S50_2	0.02	22.4	88	5
S66	0.01	22.4	95	5
S76_1	0.004	22.4	98	5
S76	0.001	22.4	100	5
S13_3	0.018	22.4	91	5
S108	0.028	22.4	80	5
S28	0.008	22.4	91	5
S75	0.017	22.4	82	5

The table below shows the results of the Intermediate scenario model run mean results compared to the LID scenario at node OF1 Dean's Ditch.

Table 4.22. Mean flow parameter results for the four design storms for the Intermediate and LID scenarios at node OF1 Dean's Ditch.

Parameter	Intermediate	LID
PEAK FLOW (cfs)	117.95	80.323
MEAN TOTAL INFLOW (cfs)	8.6845	6.5525
TOTAL INFLOW VOLUME (ft3)	685200	516975
TIME TO PEAK (hh:mm)	7:21	7:26

The table below shows the mean difference and percent change between scenarios.

Table 4.23. Difference and percent change calculations between Intermediate and LID scenario mean results at node OF1 Dean's Ditch.

Intermediate to LID Scenario Parameter	Difference	% Change
PEAK FLOW (cfs)	-37.63	-32%
MEAN TOTAL INFLOW (cfs)	-2.1320	-25%
TOTAL INFLOW VOLUME (ft3)	-168225	-25%

As the hydrograph on the following page and the table above corroborate, when the Cove parking lot LID storage is added, the mean Peak Flow reduces by 32% from the Intermediate scenario to the LID scenario; the mean Total Inflow and mean Total Inflow Volume are both reduced by 25%. The difference between the LID scenario and Intermediate scenario Total Inflow Volume is 168225 ft3, implying that the Cove parking lot LID feature contributes this a similar storage capacity. These results suggest that adding the Cove parking lot LID feature is indeed an effective measure for reducing runoff because of this storage volume contribution.

The following hydrographs illustrate the changes in Peak Flow and time to peak for the Intermediate and LID scenarios.

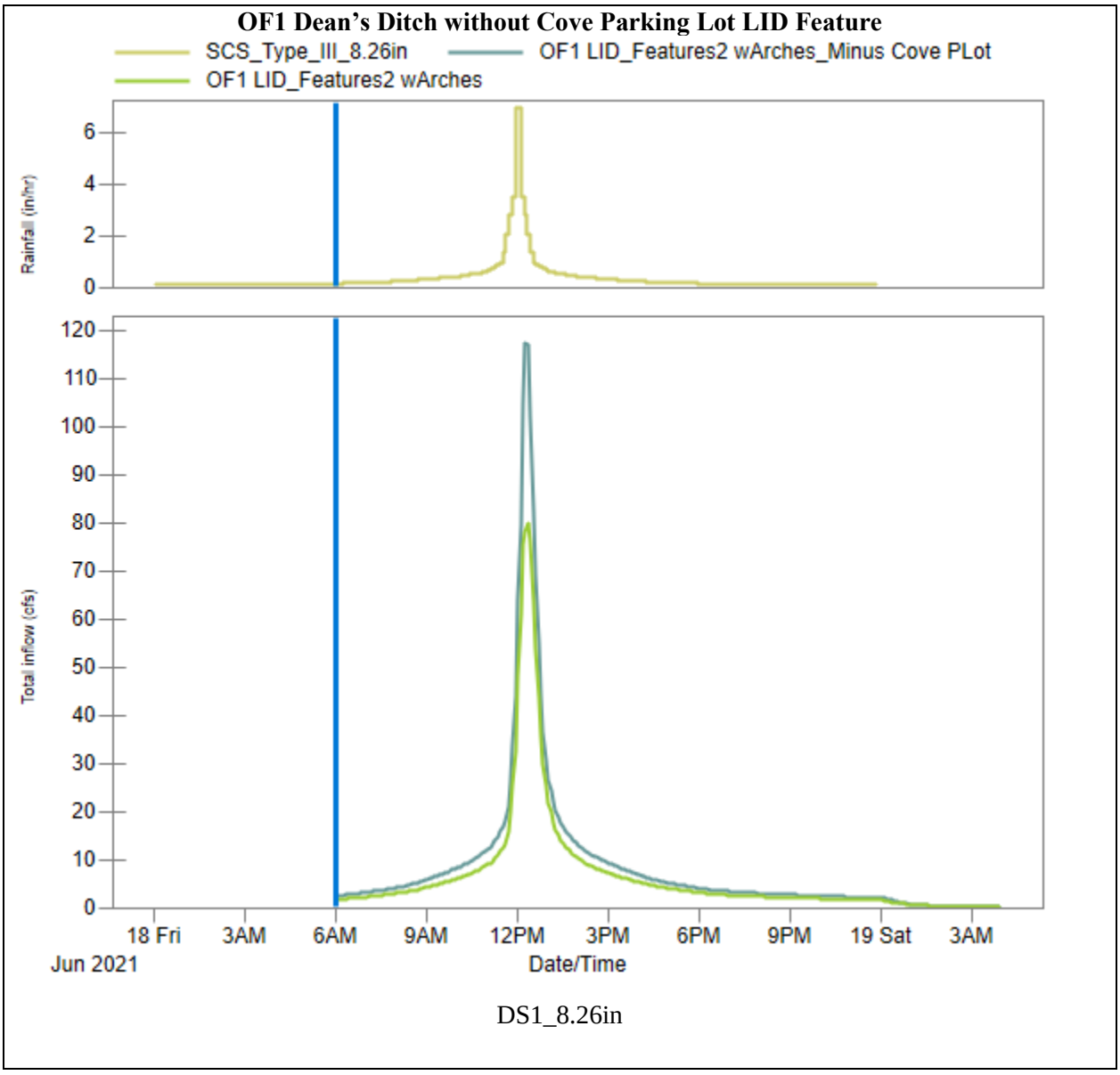

Figure 4.9. Node OF1 Intermediate and LID scenario hydrograph and hyetograph for Design Storm 1, a 10-year, 24-hour design storm with 8.26 inches of rainfall.

The following figure is a closeup of the same Design Storm 1 hydrograph, zoomed in to 11am to 2pm during the hypothetical design storm, which began at 4:54 am in the SWMM model. The closeup shows more clearly the slight delay in Time to Peak that the Cove LID feature storage adds in the LID scenario (7 hours 21 minutes) as compared to the Intermediate scenario without the Cove LID storage (7 hour 26 minutes).

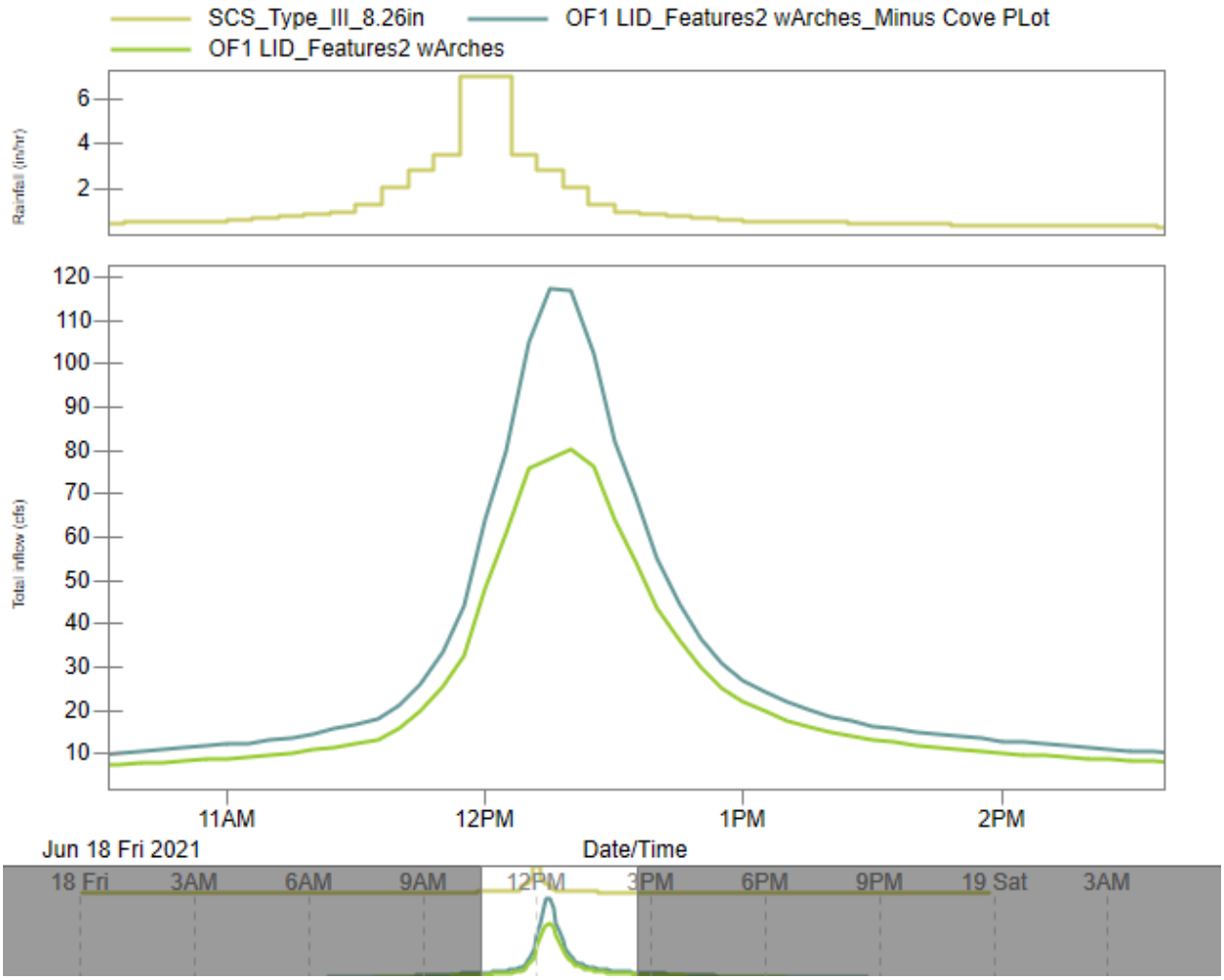

Figure 4.10. A closeup of node OF1 Intermediate and LID scenario hydrograph and hyetograph closeup for Design Storm 1, a 10-year, 24-hour design storm with 8.26 inches of rainfall.

5. CONCLUSIONS AND RECOMMENDATIONS

5.1 Summary of Research

Through this research, the three stated objectives were met: 1) to use GIS geoprocessing tools to more consistently calculate hydrologic attributes for 82 subcatchments, 2) to use GIS to more efficiently enter attributes into the SWMM model, and 3) to conduct a preliminary study to evaluate the effectiveness of low impact development (LID) features in a SWMM model of the University of New Orleans (UNO) as an exercise to apply the first two objectives.

In this study, a GIS pre-processing tool was developed to calculate hydrologic attributes for multiple subcatchments for import into the EPA SWMM5 model. Using ArcGIS Pro by Esri, 574 area-weighted subcatchment attributes were calculated including percent impervious surfaces, Manning's n for overland flow over impervious surfaces, Mannings's n for overland flow over pervious surfaces, depression storage on impervious surfaces, depression storage on pervious surfaces, and SCS curve numbers.

These GIS attributes were successfully imported into CHI's PCSWMM model. Thus, the area-weighted attributes for each subcatchment were more consistently determined and the attribute entry to SWMM was more efficient compared to manual attribute determination and entry methods.

Building on the UNO research team's original SWMM model under construction, a Modified Base Model was created in SWMM. Methods to create the Modified Base Model included deleting duplicate subcatchments, modifying select conduit geometry, adding missing conduits, connecting orphan nodes, and modifying node invert elevations to create a 0.1% slope in the drainage conduits.

Four 10-year, 24-hour design storms, each with different total rainfall amounts from four different weather stations near UNO, were used to evaluate the proposed LID features and generate uncertainty in the model results. The SWMM model Baseline and LID scenarios were each run with the four design storms.

Five hypothetical LID systems were designed as an exercise to test the preliminary SWMM model and identify SWMM nodes of interest for hydraulic analysis: the Dean's Ditch Vegetated Swale node OF1, the Cove Parking Lot Permeable Pavement node J504, the Administration Building Parking Lot Permeable Pavement node J34, and the Lafitte Village Parking Lot Permeable Pavement and Bioretention Cell, which both share node J47.

A preliminary study in SWMM was performed as an exercise to apply this thesis' objectives and evaluate the effectiveness of five hypothetical LID systems on UNO's campus using a dynamic, uncalibrated, SWMM model-in-progress provided by UNO researchers on 13 September 2021 (Cothren, 2021). This preliminary SWMM model is a building block towards the broader objectives in collaboration with the UNO Civil and Environmental Engineering Department to 1) model the university campus drainage and runoff with ongoing site developments in real-time, and 2) model UNO's runoff impacts on the Gentilly Resilience District (Cothren & Christo, 2021). The preliminary SWMM model created in this thesis is also a valuable, cost-effective and timely tool to perform preliminary evaluation of proposed stormwater and green infrastructure the 2021 "University of New Orleans Comprehensive Master Plan".

5.2 LID Modeling Conclusion

At each node of interest, the effectiveness of the LID at reducing Peak Flow, Mean Total Inflow, Total Inflow Volume, and delayed Time to Peak was tested using several statistical analyses for each experimental parameter. Statistical analysis evaluated the precision and uncertainty of results generated by the four design storms. The paired t-test statistically determined the effectiveness of the LID and determined if the null hypothesis should be accepted or rejected. The Nash-Sutcliffe efficiency coefficient (NSE) evaluated the similarities of the Baseline and LID curves to determine if there is a statistically significant difference between them. All trials showed low standard deviation, low coefficient of variation, and low margin of error values, proving the results for each trial to be precise with low uncertainty.

Based on the paired t-test analysis, the more rigorous of the statistical analyses performed in this study, only two null hypotheses were accepted: there was not a significantly delayed Time to Peak at either the Cove Permeable Pavement node J504 or at the Administration Building Permeable Pavement node J34.

All other experimental trials resulted in the acceptance of the alternative hypotheses. As hypothesized, the Dean's Ditch Vegetated Swale node OF1 experienced an increase in Peak Flow, Mean Total Inflow, and Total Inflow Volume after adding LID and Cove parking lot runoff into Dean's Ditch. As hypothesized, the Cove Permeable Pavement node J504, the Administration Building node J34, and

the Lafitte Village Permeable Pavement and Bioretention Cell node J47 experienced a significant reduction in Peak Flow, Mean Total Inflow, and Total Inflow Volume after adding the LID features. As hypothesized, the Dean's Ditch Vegetated Swale node OF1 and the Lafitte Village Permeable Pavement and Bioretention Cell node J47 experienced a significant delay in Time to Peak.

The Nash-Sutcliffe efficiency coefficient (NSE) analysis evaluated the similarity of the Baseline to LID total inflow time series curve shapes for Design Storm 1 only. Nodes J504 near the Cove, and node J34 near the Administration building, node J47 near Lafitte Village all had values that approximated one (1), indicating that the Baseline and LID curves are not statistically different in shape. Only node OF1 for Dean's Ditch had a negative NSE value, suggesting that the Baseline and LID curves are statistically different in shape. While this NSE analysis is informative of curve shape, it does not provide statical rigor to override the conclusions of the paired t-tests, especially given the subjective thresholds for the paired t-tests. NSE analysis also has disadvantages in that it weighs towards peak flow.

Node OF1 Dean's Ditch was investigated further to evaluate the Cove LID feature's storage contribution node OF1 results in SWMM. To perform this analysis, a new "Intermediate" scenario was created to compare the LID scenario against. To create the Intermediate scenario, the LID scenario was duplicated in SWMM, the permeable pavement LID Control was deleted from each Cove parking lot subcatchment, the depression storage was changed back to Baseline scenario values, and the percent imperviousness was changed back to Baseline scenario values. The LID scenario demonstrated a 32% reduction in Peak Flow and a 25% reduction in Mean Total Inflow and Total Inflow Volume compared to the Intermediate scenario, suggesting that the storage in the Cove permeable pavement LID feature is effective at reducing these flow results.

5.3 Recommendations

Future modelers should delete duplicate subcatchment layers before importing GIS attributes.

The GIS process can be automated by using ArcGIS Pro's Model Builder tools. Not only would this streamline the geoprocessing tasks and remove the manual "calculate fields" tasks, but adjustments could easily be made to the original surface attributes, allowing for real-time adjustments to subcatchment area-weighted attribute values as surfaces properties change over time. For example, the GIS and SWMM model could quickly be re-run after the Hynes School construction changes the Engineering Building pervious gravel parking lot to an impervious building roof surface.

Actual node invert elevations, conduit size, and flow directions are currently being inventoried in the field and entered into the UNO SWMM model for a more accurate representation of site conditions. UNO civil engineering researchers are continuously collecting and entering this data (Cothren, 2021). The node invert elevation calculation Excel worksheet created in this study is a tool which future researchers can use to adjust node invert elevations in the absence of field data to estimate node invert elevations.

Further work is needed to calibrate this SWMM model. This study should be repeated with the field data calibrated model. The Nash-Sutcliffe Efficiency coefficient (NSE) can be utilized in this calibration process.

In SWMM, future modelers should investigate why the decrease in Peak Flow, Mean Total Inflow, and Total Inflow Volume at node J504 near the Cove is not proportional to the increase in these parameters at node OF1 in Dean's Ditch considering the flow was rerouted from node J504 (Baseline scenario) to node OF1 (LID scenario).

Future modelers should also investigate why there is not a delayed Time to Peak at node J504 near the Cove and node J34 near the Administration Building parking lot since the pervious concrete with subsurface arch retention chambers provide substantial storage. The lack of delay in Time to Peak at nodes only impacted by permeable pavement LID features, including node J34 and node J504, may indicate that there is an error with the SWMM model's permeable pavement LID controls and storage.

The LID features designed in this study would need to be refined before installing. For example, future studies are needed to evaluate if Dean's Ditch outfall OF1 can handle the volume of water rerouted to it. The vegetated swale slope should be more precisely engineered to convey the peak flow while minimizing erosion.

Because UNO experiences flooding at 2–5-year storm events, future modelers should rerun the models with smaller storm events using a calibrated. Preliminary model runs of a 1-year, 15-minute storm still showed flooding at three nodes, even after the node invert elevations were adjusted to a 0.1% slope. Follow-up model runs in this model still reported flooding at nodes even with a 2-year, 6-hour storm.

6. REFERENCES

Advanced Drainage Systems (ADS). (2021) *Water Management Solutions, Detention, Infiltration. StormTech SC-160LP.* < https://www.adspipe.com/water-management-solutions/detention-infiltration/stormtech-sc160>

Bedient, P.B. & Huber, W.C. (2002). *Hydrology and Floodplain Analysis. Third* Edition. Prentice-Hall.

Chopra, M., Stuart, E., Hardin, M., Uju, I., Wanielista, M. (2011) *Pervious Pavements – Installation, Operations and Strength Part 1: Pervious Concrete Systems.* (FDOT Project Number BDK78). Work Performed for the Florida Department of Transportation. Stormwater Management Academy, University of Central Florida.
<https://nacto.org/docs/usdg/pervious_pavements_installation_operations_and_strength_chopra.pdf>

Computational Hydraulics International (CHI). (2021a). *Computational Methods.* < https://support.chiwater.com/77653/computational-methods>

Computational Hydraulics International (CHI). (2021b). *LID Control Editor* <https://support.chiwater.com/77680/lid-control-editor>

Computational Hydraulics International (CHI). (2021c). *LID Drain Coefficient* <https://support.chiwater.com/83629/estimating-the-lid-drain-coefficient>

Computational Hydraulics International (CHI). (2021d). *PCSWMM Overview.* < SWMM5 modeling with PCSWMM>

Computational Hydraulics International (CHI). (2021e). PCSWMM Professional 2D. (Version 7.4.3200) [Computer software].

Computational Hydraulics International (CHI). (2021f). *Soil Characteristics*. < https://support.chiwater.com/77766/soil-characteristics>

Computational Hydraulics International (CHI). (2021g). *Surface Runoff.* < https://support.chiwater.com/77726/surface-runoff>

ConcreteNZreadymix. (2018) *Technical Note 9: Pervious Concrete (2018).* [Pamphlet]. https://cdn.ymaws.com/concretenz.org.nz/resource/resmgr/docs/readymix/r_tech_note_9.pdf

Cothren, G.M. (2021). *UNOManualDelineate.pcz* PCSWMM File [Computer software model].

Cothren, G.M., Christo, D.C. (2021, August 11). *Developing a Low Impact Development System GIS for SWMM Modeling.* [Conference presentation]. 2021 EPA Region 6 Stormwater Conference, New Orleans, LA, United States.

Cothren, G. M., Spelman, D. (2021) Rational Method to PCSWMM: Matching Models to Situations. HydroLearn. <https://edx.hydrolearn.org/courses/course-v1:HydroLearn+HydroLearn406+2019_S2/about.>

Esri. (2021). ArcGIS Overview.< About ArcGIS | Mapping & Analytics Software and Services (esri.com)>

Huber, W.C., Cannon, L., and Stouder, M. (2006). *BMP Modeling Concepts and Simulation*. U.S. Environmental Protection Agency, Washington, DC, EPA/600/R-06/033.< https://cfpub.epa.gov/si/si_public_record_Report.cfm?Lab=NRMRL&dirEntryID=152387>

Hwang, J., Rhee, D., Seo, Y. (2017). *Implication of Directly Connected Impervious Areas to the Mitigation of Peak Flows in Urban Catchments*. Water, Volume 9 (696). http://doi.org/10.3390/w9090696

James, W., Rossman L., James W.R.C. (2003). *User's Guide to SWMM5, based on original USEPA SWMM documentation*. (13th Edition). CHI Press.< https://www.chiwater.com/Files/UsersGuideToSWMM5Edn13.pdf>

McCuen, R.; Johnson, P.; Ragan, R. 1996. *Highway hydrology. Hydraulic Design Series No. 2*. Pub. No. FHWA-SA-96-067. September. Washington, DC: U.S. Department of Transportation, Federal Highway Administration. [Online] <http://www.fhwa.dot.gov/bridge>

Minnesota Pollution Control Agency. (2012). *Minnesota Stormwater Manual, Pervious Concrete Cross Section*.< https://stormwater.pca.state.mn.us/index.php?title=File:Pervious_concrete_cross_section.jpg>

Nash, J. E.; Sutcliffe, J. V. (1970). "River flow forecasting through conceptual models part I — A discussion of principles". *Journal of Hydrology*. 10 (3): 282–290. Bibcode:1970JHyd...10..282N. doi:10.1016/0022-1694(70)90255-6.

National Oceanic and Atmospheric Administration (NOAA), National Weather Service, Office of Weather Prediction (OWP), Hydrometeorological Design Studies Center. (2017). *Precipitation Frequency Data Server (PFDS). NOAA Atlas 14 Precipitation Frequency Estimates.*< https://hdsc.nws.noaa.gov/hdsc/pfds/pfds_map_cont.html?bkmrk=la>

National Ready Mixed Concrete Association (NRMCA) (2011). *Pervious Pavement Engineering Properties*. Concrete Answers Series for Architects, Engineers and Developers. < https://www.perviouspavement.org/engineering.html>

Natural Resource Conservation (NRCS), United States Department of Agriculture (USDA). Conservation Engineering Division. (1986). *Urban Hydrology for Small Watersheds*. (TR-55).< https://www.nrcs.usda.gov/Internet/FSE_DOCUMENTS/stelprdb1044171.pdf>

Natural Resources Conservation Service (NRCS), U.S. Department of Agriculture (USDA). (January 2009). *Part 630 Hydrology National Engineering Handbook*. Chapter 7, Hydrologic Soil Groups and Chapter 16, Hydrographs. https://directives.sc.egov.usda.gov/OpenNonWebContent.aspx?content=22526.wba

Natural Resources Conservation Service (NRCS), U.S. Department of Agriculture (USDA).(2021). *Web Soil Survey*.[Interactive Map and Soils Data] <https://websoilsurvey.sc.egov.usda.gov/App/WebSoilSurvey.aspx>

Rincón, Guillermo. "Laboratory Statistics, Environmental Analysis." Environmental Engineering Laboratory, August 2018, University of New Orleans.

Rossman, L. AND W. Huber. *Storm Water Management Model Reference Manual Volume I, Hydrology*. U.S. EPA Office of Research and Development, Washington, DC, EPA/600/R-15/162A, 2015.

Rossman, L. AND W. Huber. *Storm Water Management Model Reference Manual Volume III – Water Quality*. U.S. EPA Office of Research and Development, Washington, DC, EPA/600/R-16/093, 2016. P 97.

Rossman, L. *Stormwater Management Model User's Manual Version 5.1*. U.S. EPA Office of Research and Development, Washington, DC, EPA/600/R-14/413b, 2015.

Sewerage and Water Board New Orleans, LA. (2020). *Drainage System Overview & Map Website*. < Stormwater - Drainage System Overview & Map - Sewerage & Water Board of New Orleans (swbno.org)>

StormTech, Inc. (2019) *SC-160LP, SC-310, SC-740 & DC-780 Design Manual, StormTech Chamber Systems for Stormwater Management*. < https://www.stormtech.com/download_files/pdf/SC160_SC310_SC740_DC780_Design_Manual_06-19.pdf>

The City of New Orleans (City of N.O.). Office of Resilience and Sustainability. (2018a). [Pamphlet]. *Gentilly Resilience District Fact Sheet*.< https://www.nola.gov/resilience-sustainability/resources/fact-sheets/gentilly-factsheet/>

The City of New Orleans (City of N.O.). (2018b). *Stormwater Code of the City of New Orleans*. <https://www.nola.gov/nola/media/One-Stop-Shop/Safety%20and%20Permits/27702-MCS.PDF>

The University of New Orleans (UNO). (2013). *The University of New Orleans 2020 Campus Master Plan.*

UNO Master Planning Committee, Trapolin-Peer Architects, VMDO Architects. (2021) *The University of New Orleans Comprehensive Master Plan.*

U.S. Army Corps of Engineers (USACE) Hydrologic Engineering Center. (2021) *HEC-HMS Technical Reference Manual, SCS Curve Number Loss Model.* < https://www.hec.usace.army.mil/confluence/hmsdocs/hmstrm/infiltration-and-runoff-volume/scs-curve-number-loss-model>

U.S. Environmental Protection Agency (EPA). (2021). *Storm Water Management Model (SWMM)* website. < https://www.epa.gov/water-research/storm-water-management-model-swmm>

U.S. Geological Survey (USGS). (2021). *The National Map: National Boundaries Dataset, 3DEP Elevation Program, Geographic Names Information System, National Hydrography Dataset, National Land Cover Database, National Structures Dataset, and National Transportation Dataset; USGS Global Ecosystems; U.S. Coastal Relief Model.* Powered by Esri. <https://apps.nationalmap.gov/viewer/>

U.S. Department of Transportation, Federal Highway Administration (1984). *Hydrology*. (FHWA-IP-84-15). Hydraulic Engineering Circular No.19. Research, Development and Technology. Turner-Fairbank Highway Research Center. <https://www.fhwa.dot.gov/engineering/hydraulics/pubs/hec/hec19.pdf>

Weiss, N. A. (2016*). Introductory Statistics, Second Custom Edition for the University of New Orleans*, Taken from *Introductory Statistics 10th Edition* by Neil A. Weiss (Pearson).

APPENDICES

Appendix A. GIS area-weighted attribute calculation results imported into SWMM.

Subcatchment Name	Imperv. (%)	N Imperv	N Perv	Dstore Imperv (in)	Dstore Perv (in)	Zero Imperv (%)	Curve Number
S101	60	0.006	0.096	0.022	0.08	16	92
S102	37	0.004	0.152	0.018	0.127	0	89
S105	66	0.007	0.081	0.03	0.068	5	93
S108	80	0.009	0.023	0.032	0.028	16	96
S112	28	0.003	0.173	0.004	0.144	21	88
S114	30	0.003	0.168	0.012	0.14	6	88
S115	40	0.004	0.145	0.011	0.12	18	90
S116	90	0.01	0.024	0.029	0.02	32	97
S117	61	0.007	0.064	0.03	0.063	1	94
S118	9	0.001	0.039	0	0.091	9	91
S119	0	0	0.024	0	0.09	0	91
S120	28	0.003	0.088	0	0.101	28	91
S121	2	0	0.065	0	0.11	2	90
S122	4	0	0.089	0.002	0.12	0	89
S124	77	0.008	0.056	0.037	0.046	3	95
S125	60	0.007	0.095	0.024	0.079	12	92
S127	37	0.004	0.211	0.012	0.126	14	89
S128	75	0.008	0.059	0.033	0.049	9	95
S129	89	0.01	0.027	0.035	0.022	19	96
S13_1	5	0.001	0.213	0.003	0.182	0	85
S13_2	23	0.002	0.064	0	0.093	23	91
S13_3	91	0.01	0.021	0.046	0.018	0	97
S130	32	0.004	0.163	0.016	0.136	0	88
S131	37	0.004	0.15	0.004	0.125	29	89
S132	61	0.007	0.092	0.013	0.077	35	93
S15_1	29	0.003	0.197	0.006	0.137	18	88
S15_2	29	0.003	0.197	0.006	0.137	18	88
S197_1	45	0.005	0.131	0.023	0.11	0	90
S247_2	44	0.004	0.134	0	0.112	43	90
S247_4	24	0.003	0.181	0.012	0.151	0	87
S27	71	0.008	0.064	0.033	0.056	4	94
S28	91	0.01	0.003	0.046	0.008	0	97
S32	25	0.01	0.1	0.05	0.05	25	80
S33	25	0.01	0.1	0.05	0.05	25	80
S34	25	0.01	0.1	0.05	0.05	25	80

(Table continued)

(Table continued from previous page)

S34_1	25	0.01	0.1	0.05	0.05	25	80
S34_2	25	0.01	0.1	0.05	0.05	25	80
S34_3	25	0.01	0.1	0.05	0.05	25	80
S34_4	25	0.01	0.1	0.05	0.05	25	80
S34_5	25	0.01	0.1	0.05	0.05	25	80
S34_7	25	0.01	0.1	0.05	0.05	25	80
S35	25	0.01	0.1	0.05	0.05	25	80
S37	25	0.003	0.241	0.012	0.151	0	87
S38	68	0.008	0.078	0.022	0.065	24	93
S39	54	0.006	0.101	0.026	0.087	3	92
S4	48	0.005	0.124	0.013	0.103	23	91
S42	27	0.003	0.174	0.007	0.145	14	88
S43	62	0.007	0.092	0.02	0.077	22	93
S44	38	0.004	0.148	0.019	0.124	0	89
S45	43	0.005	0.138	0.021	0.115	0	90
S46	62	0.007	0.09	0.031	0.075	0	93
S48	47	0.005	0.127	0.01	0.106	26	91
S49	0	0	0.24	0	0.2	0	84
S50_2	88	0.01	0.024	0.044	0.02	0	97
S51	45	0.005	0.132	0.012	0.11	21	90
S52	76	0.008	0.052	0.024	0.045	27	95
S53	23	0.003	0.184	0.012	0.153	0	87
S54	87	0.01	0.03	0.044	0.025	0	96
S55	55	0.006	0.109	0.026	0.091	3	92
S57	94	0.01	0.015	0.047	0.012	0	97
S59	44	0.005	0.051	0.019	0.07	5	93
S60	74	0.008	0.063	0.023	0.053	27	94
S61	35	0.004	0.156	0.017	0.13	1	89
S62	57	0.006	0.102	0.02	0.085	17	92
S63	0	0	0.06	0	0.109	0	90
S64	16	0.002	0.061	0	0.096	16	91
S65	14	0.001	0.055	0	0.095	13	91
S66	95	0.01	0.013	0.047	0.01	0	97
S67	41	0.004	0.141	0.009	0.118	24	90
S69	41	0.005	0.118	0.016	0.106	9	90
S70	55	0.006	0.114	0.021	0.082	13	92
S71	54	0.006	0.109	0.02	0.091	14	92
S72	29	0.003	0.195	0.006	0.141	18	88

(Table continued)

(Table continued from previous page)

S73	13	0.001	0.279	0.004	0.167	6	86
S74	64	0.007	0.085	0.022	0.071	21	93
S75	82	0.009	0.007	0.041	0.017	0	97
S76	100	0.011	0.001	0.05	0.001	0	98
S76_1	98	0.011	0.005	0.049	0.004	0	98
S77	65	0.007	0.086	0.023	0.07	19	93
S78	62	0.006	0.096	0.013	0.076	35	93
S80	38	0.004	0.148	0.019	0.124	0	89
S82	29	0.003	0.197	0.006	0.137	18	88
S83	64	0.007	0.082	0.007	0.07	50	93
S84	43	0.005	0.137	0.015	0.114	12	90
S85	92	0.01	0.018	0.046	0.015	0	97
S86	55	0.006	0.107	0.01	0.09	35	92
S87	83	0.009	0.041	0.032	0.034	20	96
S88	55	0.006	0.109	0.022	0.091	11	92
S89	50	0.005	0.121	0.023	0.101	4	91
S90	57	0.006	0.104	0.015	0.087	26	92
S91	47	0.005	0.12	0.019	0.101	10	91
S92	11	0.001	0.204	0	0.173	11	86
S94	70	0.008	0.072	0.022	0.06	25	94
S97	55	0.006	0.12	0.027	0.083	0	92
S999	25	0.01	0.1	0.05	0.05	25	85

Appendix B. LID areas.

Node	LID Control	Subcatchment Name	LID Area (ft2)	Total Areas
OF1 Dean's Ditch	Vegetative Swale	S247_2	1,393.4	
		S4	11,334.4	
		S43	1,673.5	
		S13_1	4,357.4	
		S13_2	18,856.6	
		S122	10,139.6	
		S27	8,673.5	
		S197_1	1,877.0	58,305.4
J504 Cove Parking Lot	Permeable Pavement	S50_2	34,939.7	
		S66	14,921.8	
		S76_1	13,703.7	
		S76	8,891.1	
		S13_3	8,671.6	
		S108	30,060.5	
		S28	63,658.3	
		S75	39,891.2	214,737.9
J34 Admin Building Parking Lot	Permeable Pavement	S77	58,396.7	58,396.7
J47 Lafitte Village Parking Lot	Permeable Pavement	S117	4,410.2	
		S118	22,016.8	
		S64	20,688.8	
		S63	4,824.3	
		S65	17,841.9	
		S120	8,390.5	
		S119	8,984.7	87,157.2
J47 Lafitte Village	Bioretention Cell	S65	19,108.3	19,108.3

Appendix C1. SWMM node invert elevation calculations starting from an assumed invert elevation of (-) 8-feet at node OF11. Actual node invert elevations can be entered in blue cells to recalculate invert elevations.

Location	Node d/s	Conduit	Conduit Length	Slope	Original Invert Elevation (ft)	Calculated Invert Elevation (ft)
Founders Road					**(Model as Received)**	
	Outfall OF11				0	-8.00
	J122	C128	27.981	0.001	0	-7.97
	J73	C112	74.109	0.001	0	-7.90
	J72	C65	246.311	0.001	0	-7.65
	J69	C63	262.65	0.001	0	-7.39
	J62	C62	272.136	0.001	0	-7.12
	J61	C58	34.264	0.001	0	-7.08
	J499	C130	36.351	0.001	-4.028	-7.05
	J47	C68	53.835	0.001	-2.963	-6.99
	J35	C47	28.158	0.001	0	-6.96
	J44	C199	269.357	0.001	-1.264	-6.69
	J78	C198	135.717	0.001	0	-6.56
	J43	C197	79.414	0.001	-0.656	-6.48
	J240	C196_2	224.661	0.001	-0.575	-6.26
	J42	C196_1	192.679	0.001	-0.505	-6.06
	J41	C195	163.612	0.001	-1.192	-5.90
	J40	C194	197.98	0.001	-0.008	-5.70
	J39	C244	116.502	0.001	-0.091	-5.58
	J504	C223	184.556	0.001	0.412	-5.40
	J38	C133	97.153	0.001	0.566	-5.30
	J477	C132	71.193	0.001	0.965	-5.23
	J231	C131	38.867	0.001	0	-5.19
	J26	C24	92.725	0.001	1.281	-5.10
	J230	C221	107.968	0.001	0	-4.99
	J520	C136	75.438	0.001	1.823	-4.92
	J13	C134	103.597	0.001	2.586	-4.81
	J275	C219	202.081	0.001	2.696	-4.61
	J227	C218	217.523	0.001	0	-4.39

Appendix C2. SWMM node invert elevation calculations starting from an assumed invert elevation of (-) 8-feet at node OF11. Actual node invert elevations can be entered in blue cells to recalculate invert elevations.

Location	Node d/s	Conduit	Conduit Length	Slope	Original Invert Elevation (ft)	Calculated Invert Elevation (ft)
Dean's Ditch Upper Reach						
	J13	C104	71.007	0.001	0	-4.81
	J4	C99	88.292	0.001	0	-4.72
	J3	C67	90.975	0.001	0	-4.63
	J2	C59	132.568	0.001	0	-4.50
	J1	C193	53.031	0.001	0	-4.45
	J77	C192	119.817	0.001	0	-4.33
	J71	C191	36.4	0.001	0	-4.29
	J70	C190	116.0	0.001	0	-4.26
	J68	C174	101.8	0.001	0	-4.14
	J67	C164	88.1	0.001	0	-4.04
	J66	C140	163.4	0.001	0	-3.95
	J65	C139	216.7	0.001	0	-3.79
	J32	C135	158.9	0.001	0	-3.57
	J16	C129	445.7	0.001	0	-3.41
	J12	C126	73.5	0.001	0	-2.96
	J11	C124	534.5	0.001	0	-2.89
	J110	C123	309.3	0.001	0	-2.36
	J9				0	-2.05
Math Building						
	J520	C234	27.915	0.001		-4.92
	J232	C232	268.032	0.001	0	-4.89
	J15	C230	260.82	0.001	2.315	-4.62
	J17	C228	254.29	0.001	2.998	-4.36
	J19	C226	263.251	0.001	3.654	-4.11
	J21				4.444	-3.85

Appendix C3. SWMM node invert elevation calculations starting from an assumed invert elevation of (-) 8-feet at node OF11. Actual node invert elevations can be entered in blue cells to recalculate invert elevations.

Location	Node d/s	Conduit	Conduit Length	Slope	Original Invert Elevation (ft)	Calculated Invert Elevation (ft)
Cove Parking Lot						
	J230	C230	170.786	0.001	0	-4.99
	J7	C239	86.436	0.001	0	-4.82
	J6	C238	84.299	0.001	0	-4.73
	J5				0	-4.65
	J504	C246	88.24	0.001	0.412	-5.40
	J237	C245	201.152	0.001	0	-5.31
	J236				0	-5.11
	J79	C200	285.358	0.001	0	-5.00
	J80	C201	618.34	0.001	0	-4.71
	J226	C203_1	34.48	0.001	0	-4.10
	J229	C203_2	117.9	0.001	0	-4.06
	OF1				0	-3.94
Lafitte Village Parking Lot						
	J43	C60	133.556	0.001	-0.656	-6.48
	J447	C55	51.446	0.001	-1.238	-6.35
	J55	C54	168.08	0.001	-1.051	-6.29
	J58				0.33	-6.13
	J44	C251	80.7	0.001	-1.264	-6.69
	J51	C250	49.5	0.001	-1.492	-6.61
	J52	C249	53.0	0.001	-1.707	-6.56
	J53				-1.45	-6.51
	J47	C204	79.4	0.001		-6.99
	J48	C253	52.6	0.001	-1.878	-6.91
	J49	C252	52.0	0.001	-1.862	-6.86
	J50				-1.745	-6.81

Appendix C4. SWMM node invert elevation calculations starting from an assumed invert elevation of (-) 8-feet at node OF11.

Location	Node d/s	Conduit	Conduit Length	Slope	Original Invert Elevation (ft)	Calculated Invert Elevation (ft)
To Admin Building						
	J122	C111	107.9	0.001	0	-7.97
	J85	C66	24.3	0.001	0	-7.86
	J219	C81	670.2	0.001	-4.412	-7.84
	J528	C70	152.4	0.001	-3.687	-7.17
	J74	C64	563.3	0.001	0	-7.02
	J36	C37	305.0	0.001	0	-6.45
	J118	C33	428.3	0.001	2.715	-6.15
	J34				0	-5.72
	J528	C80	373.3	0.001		-7.17
	J491	C79	201.0	0.001	-2.892	-6.80
	J436				-2.865	-6.60
	J85	C88	264.236	0.001		-7.86
	J84	C87	1093.182	0.001	0	-7.60
	J83	C84	15.087	0.001	0	-6.50
	J76	C83	284.335	0.001	0	-6.49
	J75	C82	162.977	0.001	0	-6.20
	J135	C77	107.692	0.001	-2.043	-6.04
	J134	C76	116.72	0.001	0	-5.93
	J133	C75	90.945	0.001	0.184	-5.82
	J132	C74	395.479	0.001	0	-5.72
	J131	C73	199.275	0.001	1.544	-5.33
	J130	C71	227.301	0.001	3.267	-5.13
	J129	C30	152.859	0.001	0	-4.90
	J117	C19	137.74	0.001	4.371	-4.75
	J496				3.661	-4.61
	J129	C41	408.875	0.001		-4.9
	J505				3.976	-4.49

Appendix D. Junctions and conduits added and deleted in the LID scenario as compared to the Baseline scenario.

Added	Junction	Conduit	Notes
	J499	C130	Added new conduit C130 between J61 and J499 bc J499 had no outlet wasn't connected
Deleted			
	J77	C193	deleted
	J53	C249	deleted
	J50	C252	deleted
	J49	C253	deleted
	J58	C54	deleted
	J55	C55	deleted
	J77	C193	deleted
	J1	C59	deleted
	J2	C67	deleted
	J3	C99	deleted
	J4	C104	deleted
	J5	C238	deleted
	J6	C239	deleted
	J77	C20	deleted
	J236	C245	deleted
	J237	C246	deleted
	J8		deleted

Appendix E. SWMM attribute default values.

Attribute	Value	Unit
Imperv	25	%
Nimperv	0.01	nondim
Nperv	0.1	nondim
DSImperv	0.05	nondim
Dsperv	0.05	nondim
%Zeroimperv	25	%

Appendix F. NOAA Atlas 14 PDS-based precipitation frequency estimate table with 90% confidence intervals (in inches) (NOAA, 2017). Design storm 1 example.

PDS-based precipitation frequency estimates with 90% confidence intervals (in inches)[1]

Duration	Average recurrence interval (years)									
	1	2	5	10	25	50	100	200	500	1000
5-min	0.547 (0.439-0.692)	0.623 (0.499-0.789)	0.752 (0.601-0.954)	0.863 (0.686-1.10)	1.02 (0.788-1.34)	1.15 (0.865-1.53)	1.28 (0.932-1.74)	1.42 (0.990-1.97)	1.61 (1.08-2.28)	1.76 (1.15-2.52)
10-min	0.801 (0.643-1.01)	0.912 (0.731-1.16)	1.10 (0.880-1.40)	1.26 (1.00-1.61)	1.50 (1.15-1.97)	1.68 (1.27-2.23)	1.88 (1.36-2.54)	2.08 (1.45-2.88)	2.35 (1.58-3.34)	2.57 (1.68-3.69)
15-min	0.977 (0.784-1.24)	1.11 (0.892-1.41)	1.34 (1.07-1.70)	1.54 (1.22-1.96)	1.83 (1.41-2.40)	2.05 (1.55-2.73)	2.29 (1.66-3.10)	2.53 (1.77-3.51)	2.87 (1.93-4.08)	3.14 (2.05-4.50)
30-min	1.49 (1.19-1.88)	1.71 (1.37-2.17)	2.09 (1.67-2.65)	2.40 (1.91-3.06)	2.86 (2.20-3.75)	3.22 (2.42-4.27)	3.59 (2.61-4.86)	3.97 (2.77-5.51)	4.50 (3.02-6.38)	4.90 (3.20-7.04)
60-min	2.03 (1.63-2.57)	2.32 (1.86-2.94)	2.85 (2.27-3.61)	3.33 (2.64-4.24)	4.06 (3.16-5.40)	4.69 (3.55-6.28)	5.36 (3.92-7.33)	6.10 (4.27-8.52)	7.14 (4.81-10.2)	7.99 (5.22-11.5)
2-hr	2.58 (2.08-3.24)	2.93 (2.36-3.69)	3.61 (2.90-4.54)	4.25 (3.40-5.38)	5.27 (4.14-7.00)	6.16 (4.70-8.23)	7.13 (5.26-9.73)	8.22 (5.81-11.5)	9.79 (6.65-13.9)	11.1 (7.29-15.8)
3-hr	2.92 (2.36-3.66)	3.31 (2.67-4.14)	4.08 (3.29-5.12)	4.85 (3.89-6.11)	6.12 (4.85-8.16)	7.25 (5.57-9.71)	8.52 (6.32-11.6)	9.95 (7.08-13.9)	12.1 (8.24-17.2)	13.8 (9.13-19.6)
6-hr	3.50 (2.85-4.35)	3.97 (3.22-4.93)	4.93 (3.99-6.14)	5.92 (4.77-7.40)	7.57 (6.05-10.1)	9.06 (7.02-12.1)	10.8 (8.04-14.6)	12.7 (9.09-17.6)	15.5 (10.7-22.0)	17.9 (11.9-25.3)
12-hr	4.06 (3.32-5.01)	4.66 (3.80-5.75)	5.85 (4.76-7.24)	7.03 (5.70-8.74)	8.96 (7.18-11.8)	10.7 (8.30-14.1)	12.6 (9.46-17.0)	14.8 (10.6-20.3)	17.9 (12.4-25.2)	20.6 (13.8-28.8)
24-hr	4.62 (3.80-5.66)	5.41 (4.44-6.63)	6.88 (5.63-8.45)	8.26 (6.73-10.2)	10.4 (8.35-13.5)	12.3 (9.58-16.0)	14.3 (10.8-19.1)	16.6 (12.0-22.6)	19.8 (13.8-27.6)	22.5 (15.2-31.4)
2-day	5.23 (4.32-6.36)	6.19 (5.11-7.54)	7.93 (6.52-9.68)	9.52 (7.79-11.7)	11.9 (9.57-15.3)	14.0 (10.9-18.0)	16.2 (12.2-21.3)	18.5 (13.5-25.0)	21.9 (15.4-30.2)	24.7 (16.8-34.2)
3-day	5.62 (4.66-6.81)	6.60 (5.46-8.00)	8.38 (6.92-10.2)	10.0 (8.24-12.2)	12.6 (10.1-16.1)	14.7 (11.6-19.0)	17.1 (13.0-22.4)	19.6 (14.3-26.3)	23.2 (16.4-31.9)	26.2 (17.9-36.1)
4-day	5.96 (4.95-7.20)	6.94 (5.75-8.39)	8.74 (7.23-10.6)	10.4 (8.58-12.7)	13.0 (10.6-16.6)	15.3 (12.0-19.6)	17.7 (13.5-23.2)	20.4 (15.0-27.3)	24.2 (17.2-33.2)	27.4 (18.8-37.7)
7-day	6.92 (5.77-8.31)	7.94 (6.62-9.55)	9.84 (8.18-11.9)	11.6 (9.62-14.1)	14.4 (11.7-18.3)	16.8 (13.3-21.5)	19.4 (14.9-25.4)	22.3 (16.5-29.8)	26.5 (18.9-36.1)	29.9 (20.7-40.9)
10-day	7.84 (6.56-9.39)	8.95 (7.48-10.7)	11.0 (9.15-13.2)	12.9 (10.7-15.5)	15.8 (12.9-19.9)	18.3 (14.5-23.2)	21.0 (16.1-27.2)	23.9 (17.7-31.7)	28.1 (20.1-38.2)	31.6 (21.9-43.1)
20-day	10.6 (8.92-12.6)	12.0 (10.1-14.3)	14.5 (12.1-17.3)	16.7 (13.9-19.9)	19.9 (16.2-24.6)	22.5 (17.9-28.1)	25.2 (19.4-32.2)	28.1 (20.9-36.8)	32.2 (23.1-43.1)	35.4 (24.8-47.9)
30-day	12.9 (10.9-15.3)	14.6 (12.3-17.3)	17.4 (14.6-20.7)	19.8 (16.6-23.6)	23.2 (18.9-28.5)	25.9 (20.7-32.2)	28.7 (22.2-36.4)	31.6 (23.5-41.0)	35.5 (25.5-47.2)	38.5 (27.1-51.9)
45-day	15.7 (13.3-18.5)	17.7 (15.0-20.9)	21.0 (17.7-24.8)	23.7 (19.9-28.1)	27.4 (22.3-33.3)	30.3 (24.2-37.3)	33.1 (25.7-41.7)	36.0 (26.9-46.4)	39.8 (28.7-52.6)	42.7 (30.1-57.3)
60-day	18.0 (15.3-21.2)	20.3 (17.2-23.9)	24.0 (20.2-28.2)	26.9 (22.6-31.9)	30.9 (25.2-37.4)	33.9 (27.1-41.6)	36.9 (28.6-46.2)	39.8 (29.8-51.2)	43.7 (31.6-57.5)	46.5 (32.9-62.2)

[1] Precipitation frequency (PF) estimates in this table are based on frequency analysis of partial duration series (PDS).

Numbers in parenthesis are PF estimates at lower and upper bounds of the 90% confidence interval. The probability that precipitation frequency estimates (for a given duration and average recurrence interval) will be greater than the upper bound (or less than the lower bound) is 5%. Estimates at upper bounds are not checked against probable maximum precipitation (PMP) estimates and may be higher than currently valid PMP values.

Please refer to NOAA Atlas 14 document for more information.

VITA

Demetria Christo earned her B.S. in Ecology and Evolutionary Biology from Tulane University in 2006. Following Hurricane Katrina in 2005, Demetria studied Biology at the University of Virginia. Demetria worked for eight summers in fisheries science at the Virginia Institute of Marine Science 2001 to 2006.

Demetria founded, owned and operated EcoUrban, LLC, a landscape architecture design-build and maintenance firm in New Orleans, LA in 2007-2019, which specialized in over $3Million of stormwater management projects and green infrastructure including low impact development features (LID) such as bioswales, cisterns, and native plants.

Demetria became a Licensed Landscape Contractor and Horticulturalist in Louisiana in 2007, a Certified Green Infrastructure Professional in 2015, a Licensed Landscape Architect in 2019, and earned her Coastal Engineering Certificate in 2021.

Demetria joined the University of New Orleans (UNO) civil engineering department in Fall 2018, where she served as a Teaching Assistant and Lab Manager in the Environmental Engineering lab until December 2020. Demetria also taught the Hydraulic Engineering lab for one semester.

Demetria currently works in the Flood Risk Management section of the U.S. Army Corps of Engineers Regional and Environmental Planning Division, South (RPEDS).